Biogenic self-healing mortar

Material development and experimental evaluation

Tziviloglou, Eirini

DOI
10.4233/uuid:d52fe8b2-8076-4a80-84ad-9030633a39fd

Publication date
2018

Document Version
Final published version

Citation (APA)
Tziviloglou, E. (2018). *Biogenic self-healing mortar: Material development and experimental evaluation*. [Dissertation (TU Delft), Delft University of Technology]. https://doi.org/10.4233/uuid:d52fe8b2-8076-4a80-84ad-9030633a39fd

Important note
To cite this publication, please use the final published version (if applicable).
Please check the document version above.

BIOGENIC SELF-HEALING MORTAR

Material development and experimental evaluation

Dissertation

for the purpose of obtaining the degree of doctor
at Delft University of Technology
by the authority Rector Magnificus, prof. Prof.dr.ir. T.H.J.J. van der Hagen,
chair of the Board of Doctorates
to be defended publicly on
Wednesday 26 September 2018 at 10:00 o' clock

by

Eirini TZIVILOGLOU
Master of Science in Civil Engineering, Delft University of Technology
born in Athens, Greece

This dissertation has been approved by the promotors.

Composition of the doctoral committee:

Rector Magnificus	chairman
Prof. dr. ir. E. Schlangen	Delft University of Technology, promotor
Dr. H. M. Jonkers	Delft University of Technology, promotor

Independent members

Prof. dr. ir. K. van Breugel	Delft University of Technology
Prof. dr. ir. D. A. Hordijk	Delft University of Technology
Prof. dr. ir. N. De Belie	University of Ghent, Belgium
Prof. dr. C. Grosse	Technical University of Munich, Germany
Dr. V. A. C. Wiktor	Cugla B.V., Netherlands

Printed by: OPSI

Cover by: Pantelis Nikoforos

ISBN: 978-94-6366-064-8

An electronic copy of this dissertation is available at

http://repository.tudelft.nl/.

Στους δικούς μου

Acknowledgements

The years I spent as a PhD student at Delft University of Technology was a remarkable experience for me in professional, as well as, in personal level. I consider myself very lucky that I was involved in HEALCON, a European collaborative project whose participants came from seven European countries. It was a great pleasure for me not only to communicate and work with experts in the field of concrete science, but also to have the opportunity to travel and get to know a little bit of those countries. I would like to acknowledge the financial support of European Union Seventh Framework Programme (FP7/2007-2013) under grant agreement No 309451 (HEALCON) that allowed me to complete my doctoral studies in Delft University of Technology.

I will always be grateful to my promotor, professor Erik Schlangen, who trusted me and gave me the chance to start this PhD project. I truly appreciate his advice and guidance during the experimental and result interpretation processes. I should also not ignore the fact that he was always available, supportive and patient for discussions with or without technical context, even though the queue outside of his office was getting longer and longer!

I would like to thank my co-promotor, Dr. Henk Jonkers, who let me in the magnificent world of bacteria and microbiology. He is a great man for persuading the crude civil engineers to work with those small creatures! I am thankful for his advice and support even during moments that I thought my research problems would be unsolvable.

The committee members are very appreciated for allowing me to defend my thesis.

I would also like to acknowledge the precious help I received from the Microlab technicians; Ger Nagtegaal, Arjan Thijssen and Maiko van Leeuwen. Ger was always sharing his practical experience and was giving me bright experimental set-up solutions. Without Arjan's assistance, the valuable bacterial traces could not have been found. I will never forget how joyful he made our long-ESEM days with Dutch lessons, which I have still put on hold. Maiko was a great support with the large castings, particularly during a period of my life that my mobility was somewhat limited. His enthusiasm, eagerness to help and kindness will be always appreciated.

A special thanks to my colleague, supervisor but most of all friend Virginie Wiktor. She was always there, willing to help, give advice, guidance, inspiration and courage to continue even when the days were not particularly sunny. Words cannot express my gratitude for the support she provided me throughout those four years.

To all the Microlab friends, thank you for the joyful moments, the constructive discussions and shared experiences! Branko, Mladena, Natalie, Lourdes, Marija, Stefan, Claudia, Jiayi, Martin and Xu Ma. Special thanks to the Bio-team members: Lupita, Renee, Balqis, Damian, Senot, Yask and Zichao, for the numerous fruitful conversations regarding the 'bacteria-world' but mostly many other topics! To Xiaowei, Yibing, Haolinag and Hua for sharing the same office, but also enlightening me about Chinese customs, tradition and culture.

Thanks, to all my dear 'outside-university' friends, who were always curious for the progress of my research and full of truly awkward questions!

My sincere gratitude to my family in Greece, who has been always supportive and was giving me extra courage to keep going, even if we were so many kilometres apart. Thank you for believing in my potential!

A special thanks to Cleopatra, for taking care of the most precious thing in the world during my last months as PhD student.

Finally, to Kostas and Amalia. Kosta, thank you for being partly the reason to come in the Netherlands and start this whole adventurous experience. During this five-years-journey, we learned together a lot, but most of all we learned how to support, understand and love each other at critical moments. Nowadays, I still feel that we are having fun the same way we did back in our first year of our master studies. My little Amalia, thank you for choosing us, for the most happy and unforgettable moments that we have shared so far and for giving me the strongest motivation of all!

Contents

List of Symbols

Roman

A	[mm^2]	area of the crack on the bottom section of the specimen
A_1	[g]	constant
A_2	[g/h]	constant
d_{cr}	[mm]	crack depth used in the computer simulation
F_2	[kN]	peak load value of the first unloading cycle (before healing treatment)
F_3	[kN]	peak load value of the second loading cycle (after healing treatment)
H	[mm]	height of prismatic specimen
I	[g]	cumulative amount of absorbed water
l_x	[mm]	model size along the x-direction
l_y	[mm]	model size along the y-direction
$\overline{m}_h$	[g]	average mass of water that has passed (during crack permeability test) through the healed cracks of the three specimens in 5 minutes
$\overline{m}_{n\text{-}h}$	[g]	average mass of water that has passed (during crack permeability test) through the unhealed cracks of the three specimens in 5 minutes
R	[-]	relative respiration rate
RH	[-]	relative humidity
R_S	[-]	recovery of flexural strength
R_{WA}	[-]	recovery of absorption resistance
R_{WT}	[-]	recovery of water-tightness
S	[$g/h^{0.5}$]	sorptivity of the material
$\overline{SC}_{healed}$	[$g/h^{0.5}$]	sorption coefficient of healed samples
$\overline{SC}_{non\text{-}cracked}$	[$g/h^{0.5}$]	sorption coefficient of non-cracked samples
$\overline{SC}_{non\text{-}healed}$	[$g/h^{0.5}$]	sorption coefficient of non-healed samples
T	[h]	time
V_{cr}	[mm^3]	crack volume
V_{cp}	[mm^3]	volume of the cracked particles
V_{sp}	[mm^3]	volume of the healing product
V_L	[mm^3]	initial crack volume
V_i	[mm^3]	volume after a healing certain healing time

w	[mm]	crack width
$\bar{w}$	[mm]	average crack width calculated using microscopy

Greek

α_m	[%]	crack sealing percentage calculated using microscopy
α_s	[%]	crack sealing percentage calculated using computer simulation
β	[-]	amount of healing product formed for each unit of volume of LWA
γ	[-]	mass of healing agent inside the unit mass of the LWA
κ	[µM/min]	oxygen consumption rate
κ_a	[µM /min]	slope of the autogenous respiration curve
κ_c	[µM /min]	slope of the curve from bacteria respiration in a certain compound
ΔG	[kJ/mole]	standard Gibbs free energy

List of Abbreviations

$Ca(HCOO)_2$	calcium formate
$Ca(NO_3)_2$	calcium nitrate
$Ca(OH)_2$	calcium hydroxide, portlandite
Ca^{2+}	calcium ion
CaA	calcium acetate
$CaC_4H_6O_4$	calcium acetate
$CaC_6H_{10}O_6$	calcium lactate
$CaCO_3$	calcium carbonate
CaL	calcium lactate
CO_3^{2-}	carbonate ion
CO_2	carbon dioxide
DE	diatomaceous earth
ECC	engineered cementitious composites
EDS	energy dispersive x-ray spectrometer
ESEM	environmental scanning electron microscopy
FT-IR	Fourier-transform infrared spectrometry
HCO_3^-	bicarbonate ion
LVDT	linear variable differential transducers
LWA	lightweight aggregates
MICP	microbial induced calcium carbonate precipitation
MIP	mercury intrusion porosimetry
$NaC_6H_{11}O_7$	sodium gluconate
NaG	sodium gluconate
NO_2^-	nitrite ion
NO_3^-	nitrate ion
NU	Northumbria University
PVA	polyvinyl alcohol
REF, CTRL, BAC	mortar mixtures that are studied in the thesis
RRT	round robin test
SAP	superabsorbent polymers
SC	sorption coefficient
SEM	scanning electron microscopy
TU Delft	Delft University of Technology
UBath	Bath university
UGhent	Ghent University
WP	work package
YE	yeast extract

1

General introduction

The chapter introduces the background and the motivation for conducting this research. General information regarding the concept of self-healing in cementitious materials with emphasis on the biogenic self-healing mortar is also given. The chapter continues with a short description of the collaborative research programme that this thesis contributed to and it finishes with the presentation of the research objectives and a summary of the thesis chapters.

1.1 BACKGROUND

Cracking is an unavoidable characteristic of concrete that originates from its brittle nature and it is a sign that the tensile strength has been locally exceeded. However, it can highly influence the durability of the material and affect the functionality and the life span of a structure [1], since aggressive substances can penetrate through the crack network and degrade either the matrix or the embedded reinforcement. Design codes indicate maximum allowable crack widths based on empirical studies [2]. Specifically, Eurocode 2 recommends that the maximum crack width should be up to 0.4 mm for mild and up to 0.2 mm for more aggressive exposure classes, to minimize the risk of reinforcement corrosion.

Once cracks have exceeded the advised limits, common practise dictates instant repair in order to prevent the initiation or the further propagation of the damage. Yet, conventional repair practices can raise several issues related to:

- the lack of compatibility between the repair and the concrete substrate,
- the high direct and indirect costs, due economic losses from traffic jams and associated loss of productivity [3],
- the inability to access the structure locations that need maintenance and
- the non-environmental friendly nature of the currently available repair systems [4].

Concrete, like all cement-based materials, has the intrinsic autogenous “ability” to seal micro-cracks (up to 0.2 mm) due to prolonged hydration, carbonation of matrix etc. [5-7]. The relatively recently introduced “self-healing concrete” tries to enhance this natural property of concrete. The technology targets on the closure of micro-cracks through different “autonomous” self-healing systems. By this means, the inner part of the structure is protected and the danger of reinforcement corrosion is minimized. Many self-healing concepts have been developed in the last 20 years, using several types of healing agents [8]. Among those systems, the most popular concepts are those which target:

- the limitation of the crack width by incorporating fibres [9-11],
- the expansion of the cement matrix when in contact with water by using hydrogels [12-13],
- the filling of the crack by introduction of a healing agent incorporated during mixing or casting of concrete [14-19] and
- the combination of the previous systems [20-23].

One of the most studied concepts is the biogenic self-healing concrete. The biogenic healing agents usually contain bacteria and organic compounds acting as bacterial nutrients or 'feed'. The healing agent is incorporated in concrete during mixing. After hardening and upon cracking, the bacteria are activated by the water inflowing the crack, resulting in the production of inorganic minerals (often calcium carbonate), which ultimately fill the open cracks. Consequently, crack sealing is improved and the structure is less susceptible to leakage and deleterious liquids and gasses.

The use of biogenic healing agent has three advantageous points over the other similar technologies. These are the use of less synthetic compounds, compared to the polymeric agents, the potential to be used repeatedly and the long shelf life of the compounds, which is translated to prolonged functionality. Consequently, the concept of biogenic self-healing concrete is oriented towards increasing sustainability and reducing the total cost-of-ownership of the concrete structures.

The current research project described in this thesis focuses on the development of biogenic mortar with lightweight aggregates, acting as carriers of the healing agent. Previous research on the specific self-healing system has revealed promising results regarding its healing efficiency, when the mortar samples were exposed to certain conditions for a specific period. In fact, it was proven that the maximum healable crack width was more than doubled after the inclusion of the biogenic healing agent in the mortar [16]. However, there are some additional aspects, related to the material development and the experimental methodology, which needed further investigation such as:

- the possibility to use another organic compound as bacterial feed,
- the possibility to increase the amount of healing agent in the lightweight aggregates,
- the exposure to more realistic healing (environmental) conditions and for shorter periods and
- the development of a test methodology that could evaluate the functionality of the self-healing system in a rather scientifically sound but also simple way.

For structures such as tunnels or water retaining reservoirs liquid tightness is necessary to sustain the health of the structure. Hence, these structures could benefit from the application of a material with enhanced crack sealing behaviour that can prevent durability problems related to micro-cracking. Lightweight biogenic self-healing mortar is designed to provide reduced crack permeability, in areas of a structure where a lightweight element or an external lightweight layer is needed.

1.2 HEALCON: THE CONCRETE WHICH REPAIRS ITSELF

This thesis contributed to a collaborative European (Seventh Framework Programme) research programme on Nanosciences, Nanotechnologies, Materials and new Production technologies. The project, entitled "HEALCON: the concrete which repairs itself", started in January 2013 and it was completed in December 2016. The consortium of the research project consisted of three universities, two research institutes and seven industrial partners from seven European countries. The overall objective of the project was to design, develop, test, apply and evaluate self-healing methods for concrete structures. In addition, HEALCON contained eleven work packages (WP) assigned to partners with extensive experience on the subject of each WP (Figure 1.1). TU Delft participated in the development of biogenic healing agents (WP2) and lead WP4 and WP5 which dealt with the evaluation of self-healing at laboratory scale and the modelling of self-healing, respectively.

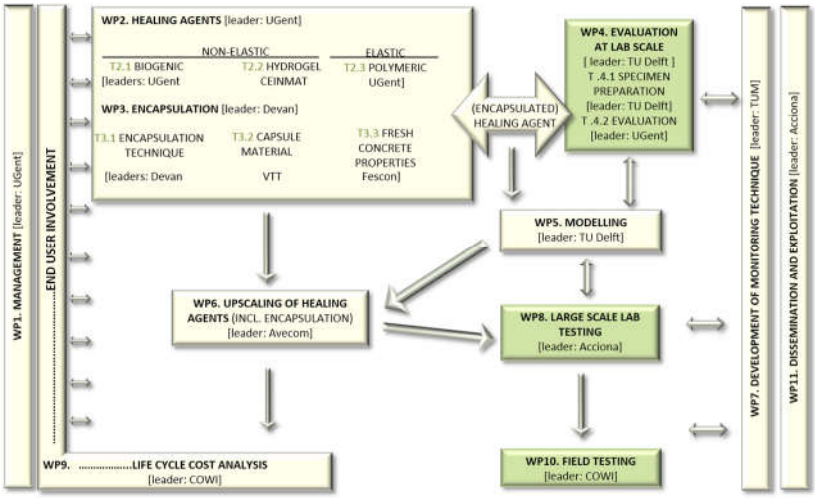

Figure 1.1 Work packages (WP) within the HEALCON project and their interdependencies [24].

1.3 RESEARCH OBJECTIVE

The main goal of this research project was to develop and investigate the mechanical and the crack sealing behaviour of biogenic self-healing mortar, which has been designed to enhance the water-tightness after cracking and exposure to certain conditions. Furthermore, the research focused on developing an experimental methodology for quantifying and evaluating the recovery of crack sealing at laboratory scale.

1.4 OUTLINE OF THE THESIS

The thesis is composed of seven chapters organized as presented in Figure 1.2. The first chapter describes briefly the concept and the background of biogenic self-healing mortar that is covered in this thesis.

Chapter 2 contains a literature survey on the biogenic self-healing cementitious materials as well as on the testing methods that have been developed to examine the healing efficiency at laboratory-scale.

Chapter 3 deals with the development of the biogenic healing agent. Different organic precursors are considered as possible bacterial nutrient. The physical properties of the expanded clay particles, which are used as carriers of the healing agent, are investigated as well. Finally, the chapter examines possible methods to optimize incorporation of the biogenic healing agent in the expanded clay particles.

Chapter 4 presents the mixture design of the biogenic self-healing mortar and investigates the influence of the healing agent on the fresh- and hardened-state properties of the mortar through laboratory tests. In addition, the chapter studies the crack sealing, the recovery of flexural strength and stiffness and the presence of bacterial activity in biogenic self-healing mortar.

Towards standardization of an experimental methodology to evaluate self-healing at laboratory scale, chapter 5 assesses and presents results obtained by a round robin test within the framework of RILEM/TC 253 MCI (Micro-organisms-Cementitious Materials Interactions). The experimental methodology comprises of standard mechanical tests on mortars and additional tests to quantify crack sealing through water flow and capillary water absorption.

Chapter 6 investigates the sealing performance of the biogenic self-healing mortar through experimental and computational approaches. Image processing and crack permeability test results are compared with results obtained by computer simulations.

Chapter 7 summarizes the conclusions of this research project and presents some recommendations for future research.

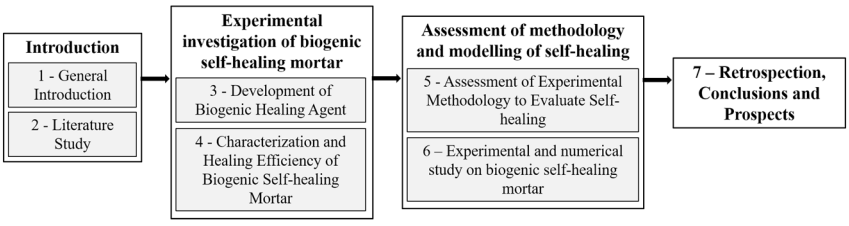

Figure 1.2 Outline of the thesis.

REFERENCES

[1] Schlangen, E. and Joseph, C., *Self-Healing Processes in Concrete*. in *Self-Healing Materials*, Eds. 2009, Wiley-VCH Verlag GmbH & Co. KGaA : Weinheim, Germany. p. 141-182.

[2] Pacheco, J., Šavija, B., Schlangen, E., and Polder, R.B., *Assessment of cracks in reinforced concrete by means of electrical resistance and image analysis.* Construction and Building Materials, 2014. 65: p. 417-426.

[3] van Breugel, K., *Is there a market for self-healing cement-based materials?* 2007. In: 1st International Conference on Self-Healing Materials. Noordwijk aan Zee, the Netherlands.

[4] Sierra-Beltran, M.G., Jonkers, H.M., and Schlangen, E., *Characterization of sustainable bio-based mortar for concrete repair.* Construction and Building Materials, 2014. 67: p. 344-352.

[5] Hearn, N., *Self-sealing, autogenous healing and continued hydration: What is the difference?* Materials and Structures 1998. 31(8): p. 563-567.

[6] Edvardsen, C., *Water Permeability and Autogenous Healing of Cracks In Concrete.* ACI materials journal, 1999. 96(4): p. 448-454.

[7] ter Heide, N., Crack healing in hydrating concrete. 2005. MSc Thesis, Delft University of Technology,

[8] de Rooij, M., Van Tittelboom, K., De Belie, N., and Schlangen, E., *Self-healing phenomena in cement-based materials : state-of-the-art-report of RILEM Technical Committee 221-SHC*. RILEM state of the art reports; v. 11. 2013, Dordrecht, The Netherlands: Springer.

[9] Li, V.C., Lim, Y.M., and Chan, Y.-W., *Feasibility study of a passive smart self-healing cementitious composite.* Composites Part B: Engineering, 1998. 29(6): p. 819-827.

[10] Yang, Y., Lepech, M.D., Yang, E.H., and Li, V.C., *Autogenous healing of engineered cementitious composites under wet-dry cycles.* Cement and Concrete Research, 2009. 39(5): p. 382-390.

[11] Tziviloglou, E., Self-healing in ECC materials with low content of different microfibers and micro-particles. 2009. MSc, Delft University of Technology, Delft.

[12] Kim, J.S. and Schlangen, E., *Self-healing in ECC stimulated by SAP under flexural cyclic load* 2011. In: 3rd International Conference on Self-Healing Materials. Bath, UK.

[13] Snoeck, D., Dewanckele, J., Cnudde, V., and De Belie, N., *X-ray computed microtomography to study autogenous healing of cementitious materials promoted by superabsorbent polymers.* Cement and Concrete Composites, 2016. 65: p. 83-93.

[14] Dry, C.M., *Three designs for the internal release of sealants, adhesives, and waterproofing chemicals into concrete to reduce permeability.* Cement and Concrete Research, 2000. 30(12): p. 1969-1977.

[15] Mihashi, H., Kaneko, Y., Nishiwaki, T., and Otsuka, K., *Fundamental study on development of intelligent concrete characterized by self-healing capability for strength.* Transactions of the Japan Concrete Institute, 2000. 22: p. 441-450.

[16] Wiktor, V. and Jonkers, H.M., *Quantification of crack-healing in novel bacteria-based self-healing concrete.* Cement and Concrete Composites, 2011. 33(7): p. 763-770.

[17] Van Tittelboom, K., De Belie, N., Van Loo, D., and Jacobs, P., *Self-healing efficiency of cementitious materials containing tubular capsules filled with healing agent.* Cement and Concrete Composites, 2011. 33(4): p. 497-505.

[18] Sangadji, S. and Schlangen, E., *Mimicking Bone Healing Process to Self Repair Concrete Structure Novel Approach Using Porous Network Concrete.* Procedia Engineering, 2013. 54: p. 315-326.

[19] Mors, R.M. and Jonkers, H.M., Reduction of water permeation through cracks in mortar by addition of bacteria based healing agent. 2015. In: 5th international conference on self-healing materials. Durham, North Carolina, USA.

[20] Snoeck, D., Van Tittelboom, K., Steuperaert, S., Dubruel, P., and De Belie, N., *Self-healing cementitious materials by the combination of microfibres and superabsorbent polymers.* Journal of Intelligent Material Systems and Structures, 2014. 25(1): p. 13-24.

[21] Wang, J.Y., Snoeck, D., Van Vlierberghe, S., Verstraete, W., and De Belie, N., *Application of hydrogel encapsulated carbonate precipitating bacteria for approaching a realistic self-healing in concrete.* Construction and Building Materials, 2014. 68: p. 110-119.

[22] Sangadji, S., Porous Network Concrete : a bio-inspired building component to make concrete structures self-healing. 2015. PhD Thesis, Delft University of Technology,

[23] Sierra Beltran, M.G., Jonkers, H.M., Mors, R.M., and Mera-Ortiz, W., *Field application of self-healing concrete with natural fibres as linings for irrigation canals in Ecuador*. 2015. In: 5th international conference on self-healing materials. Durham, North Carolina, USA.

[24] De Belie, N., *HEALCON – Self-healing concrete to create durable and sustainable concrete structures.* 2013. In: 4th International conference in self-healing materials (ICSHM 2013). Ghent, Belgium.

2

Literature study

The chapter starts by explaining the terms autogenous and autonomous healing. Further on, a description of three self-healing strategies in cementitious materials is given. The concept of each strategy and potential benefits and limitations of the systems are also presented. Moreover, the chapter reviews the biogenic self-healing systems which have been or are being investigated by several research groups. Three metabolic pathways which result in calcium carbonate production are described; namely, the enzymatic hydrolysis of urea, the aerobic oxidation of organic carbon and the anaerobic oxidation of organic carbon. Finally, the chapter closes with the presentation of the most common evaluation methods to investigate self-healing at laboratory scale.

Parts of this chapter have been published in the book "Advances in Polymer Sciences", in the chapter "Bio-Based Self-Healing Concrete: From Research to Field Application", Springer International, 2016 [1].

2.1 AUTOGENOUS AND AUTONOMOUS HEALING

2.1.1 AUTOGENOUS HEALING

The term *autogenous* originates from the Greek word *autogenís* (αὐτογενής < αὐτός (Eng. self) + γίγνομαι (Eng. become)) and it is used to describe something that is natural, spontaneous and self-created. Lately, in the concrete publication record there are several reports that define the term "autogenous healing". Neville [2], described autogenous healing as "the closure of the fine cracks under moist conditions, without tangential displacement". Schlangen and Josef [3] referred to the autonomic property of a cementitious material as "the innate ability to self-repair". In 2009 [4] the Japanese technical committee TC-075B defined autogenous healing as "a natural process of filling or sealing cracks without any external operations and works". Furthermore, the definition that RILEM TC-221 [5] gave for the autogenic healing was "the self-healing process when the recovery process uses materials components that could otherwise also be present when not specifically designed for self-healing".

The autogenous healing ability of concrete was first reported by the French Academy of Science in 1836. Numerous studies since then have followed [6-9]. Autogenous healing upon contact with water is primarily attributed to three processes:

- swelling of the cement matrix,
- hydration of unhydrated cement particles and
- precipitation of calcium carbonate [6-10]

The most significant of these processes is the precipitation of calcium carbonate ($CaCO_3$), which is formed as a result of carbon dioxide (CO_2) reacting with calcium hydroxide ($Ca(OH)_2$) (Equation 2.1).

$$\boldsymbol{CO_2 + Ca(OH)_2 \rightarrow CaCO_3 + H_2O} \quad (2.1)$$

Precipitation occurrence depends on the amount of calcium hydroxide present and the solubility product of calcium carbonate, which in turn depends on the temperature, the ionic strength, the composition, the pH and carbon dioxide partial pressure of water in the crack [6] Primarily, the amount of precipitates and hence crack healing potential depends on the amount of calcium- and carbonate ions available in the cracks.

2.1.2 AUTONOMOUS HEALING

In the past, autogenous healing in cementitious materials was commonly addressed as self-healing. Several studies from the 1970's and until the early 2000's were using both the terms "self-healing" [8, 11-14] and "autogenous

healing" [6, 7, 15-17], yet they were implying the same thing. After the mid 2000's, the use of the phrase "autogenous healing" became more popular when someone wanted to refer to the natural ability of concrete to seal micro-cracks. The reason behind it was the scientific progress on the topic. After the publication of White et. al [18], who introduced the "autonomic healing" concept for polymer composites, progressively more studies were focused on developing cementitious materials that would be able to close micro-cracks by incorporating the so-called "healing agents". The focus of the researchers deviated from studying the natural autogenic concrete property, to rather creating new, "smart" and self-repairing cementitious materials. Thereafter, it came practice discriminating self-healing from autogenous healing.

The roots of the term autonomous are also found in the Greek language and come from the word autónomos (αὐτόνομος < αὐτός (Eng. self) + νόμος (Eng. regulation)), which means self-regulated. The word is used to describe something, which does not depend on someone/something else to be functional. In 2007, Josef et al. [19] brought the phrase "autonomous healing" in cementitious materials. The phrase refers to the ability of the material to close cracks, and yet recover functionality, by a self-activated system. There are various definitions also for autonomic healing. In 2009, Schlangen and Josef [3] defined autonomic healing property as "the self-healing capability due to the release of encapsulated resins or glues as a result of cracking from the onset of damage". Moreover, the Japanese technical committee TC-075B [4] explained the same term as "the involuntary healing of cracks that are provided by admixtures". A later definition given by RILEM TC-221 [5] referred to autonomic healing as "the recovery process which uses materials components that would otherwise not be found in the material (engineered additions)".

2.1.3 SELF-HEALING STRATEGIES

Scientists for more than two decades have worked on various autonomous healing concepts in cementitious materials. Several classifications could be found regarding:

- the nature of the materials that are used,
- the recovery property that they target,
- the mechanism of healing etc.

In this chapter, the various self-healing systems will be presented based on the mechanism of healing; namely, by limiting the crack width via the use of fibres, by promoting autogenous healing through the use of superabsorbent polymers (SAP) and by release of encapsulated healing agents (Figure 2.1).

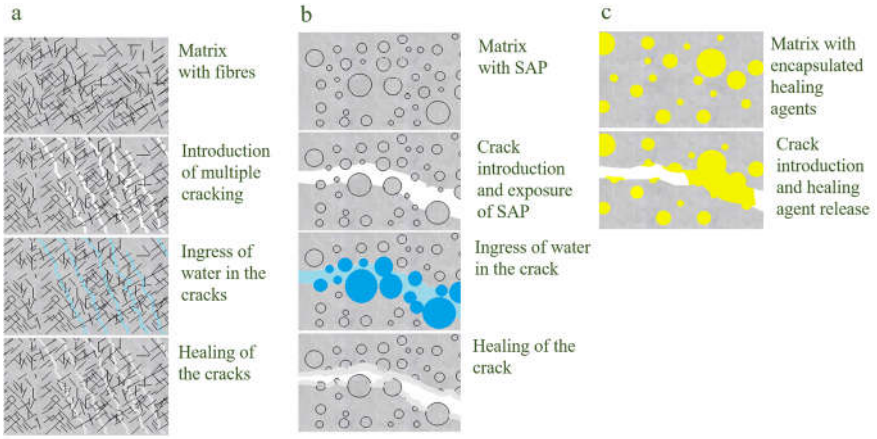

2

Figure 2.1 Self-healing strategies according to the mechanism of healing: a. limiting the crack width with the use of fibres, b. improving autogenous healing by incorporation of SAP and c. releasing of encapsulated healing agent in the crack.

Limiting the crack width

Limiting the crack width to enhance autogenous healing is often achieved by the addition of fibres in the cementitious matrix. Engineered Cementitious Composites (ECC) is a material, which was designed to possess self-controlled crack width that does not depend on steel reinforcement or structural dimensions [20]. Instead, the polyvinyl alcohol (PVA) fibres used in ECC are tailored [21] to be embedded in the cement matrix to give ductility and create small micro-cracks that work in favour of the healing process. Various studies have investigated the self-healing efficiency of ECC materials [22-29]. The results reveal that after loading, either through direct tension or bending, multiple micro-cracks are created on the surface of the specimens. After exposure to humid environment the cracks are filled (Figure 2.2) with an autogenous healing product that is often calcium-based (calcium carbonate or calcium hydroxide [24, 25, 28 29]).

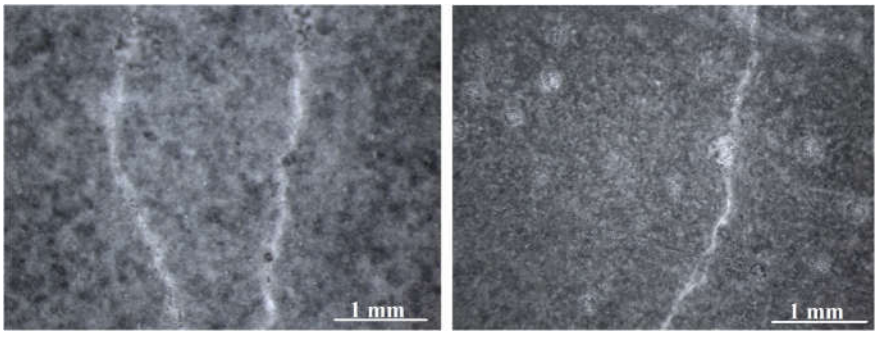

Figure 2.2 Closed cracks after 28 days of water immersion [24].

The healing is often functionally related to reduced water permeability [23,26,27] as well as recovery of mechanical properties such as flexural strength and stiffness [22,26,28]. Enhanced self-healing capacity has been observed by other studies that have substituted the PVA fibres with different types of synthetic, metal or hybridized natural fibres (with steel fibres) to achieve crack bridging [30-33].

The method of restricting the crack width, to promote autogenous healing, via fibre reinforcement adds extra ductility to the originally brittle material. However, there are some issues that need to be taken in consideration such as:

- the difficulty in casting, due to clustering of fibres,
- the viability of the fibres. The fibres should be able to survive the high alkaline cement environment without being damaged,
- the physical properties of the fibres, such as tensile strength and elasticity modulus and
- the bonding: the physical/chemical properties of the interface between the cement matrix and the fibres.

Therefore, the fibres should be carefully selected to fulfil the target of restricting the crack width without negatively affecting the properties of the cementitious material.

Crack blockage by means of superabsorbent polymers

SAP have been traditionally used for their ability to absorb water in high amounts (up to several hundred times of their own weight [34]). Chemically speaking, SAP are hydrophilic cross-linked polymers that swell upon contact with water or aqueous solutions resulting in the formation of a hydrogel [34]. SAP have been used for internal curing of concrete and more specifically for the mitigation of autogenous shrinkage [35,36]. SAP are added in dry state in the wet mixture and they start to take in mixing water. Therefore, water-filled pockets are created. During cement hydration, the relative humidity (RH) drops and the water contained in the hydrogels is released. The released water can then be used for further hydration and reduction of the autogenous shrinkage [37].

Furthermore, SAP have been also used to promote autogenous healing by adopting the following mechanism, as described by Lee et al. [38]. During mixing, the SAP absorb water and swell, while during cement hydration, they release water and shrink, creating pores in the hardened cement paste. The pores can be characterized as defects or flaws of the paste and thus can be initiation or propagation crack locations. When moisture ingresses through the crack, the SAP will swell significantly. The swollen SAP can then seal the crack and slow down or even prevent further penetration of water. Except from the physical blocking,

the swollen SAP can protect the material by promoting autogenous healing inside the cracks. This mechanism can contribute in retaining the water-tightness of cracked cementitious materials. Dejonghe et al. [39], Snoeck et al. [40] and Gruyaert et al. [41] showed visual closure of cracks when they were stored in an environment with adequate humidity.

As it is mentioned above, the water that is absorbed by SAP during mixing causes the formation of macro pores in the hardened paste. As a result, the cementitious material with incorporated SAP particles tends to show reduced strength [35, 42-44] in comparison with the same material without SAP. To overcome this disadvantage, scientists suggested two alternative solutions; to provide a coating around SAP particles [45,46] or to introduce pH-sensitive SAP particles [43,44,47]. The coating is ruptured at the moment of crack formation; therefore, the SAP and the matrix do not interact before this moment and the swelling reaction happens only after crack formation. Moreover, the pH-sensitive SAP allow the swelling when the pH drops from approximately 13 (concrete environment) to below 9-10 (crack surface environment).

Although this system of voids facilitates the crack propagation and it may enhance the freeze-thaw resistance, the presence of macropores can also decrease the compressive strength of the material, which should be considered during the designing process of a structure.

Crack blockage by release of encapsulated healing agent

One of the most popular concepts among the self-healing strategies in cementitious materials originates from nature and tries to mimic the healing system of the animals (artery-blood). Proportionally, in cementitious materials the tube or capsule (artery) carries the healing agent (blood). The system in cementitious materials is either externally- or self-triggered upon cracking (injury). Further, the crack is blocked by the release of the healing agent and therefore the material is protected from the ingress of deleterious liquids or gasses. Experimental studies have discussed and demonstrated the feasibility of the specific self-healing concept.

The first and the most important consideration is that the capsules should be compatible with the cementitious matrix but also adequately resistant and brittle, so that they can withstand the mixing process and they will break only upon crack formation. Glass capsules have been used by several researchers [48-56]. All studies underline the advantage of the glass material which is the ability to sense the crack, immediately break and release the healing agent. In most cases, where the filling material is enough for the resulting crack width, the healing is successful and (partial) recovery of functionality is achieved. However, there are several concerns regarding the glass as capsule material. In fact, Li et al. [48] raised the

issues of placing, of economics and of shelf-life of the capsules when embedded in large scale conventional concrete structures. Thao et al. [50] for the protection of the capsules during mixing suggested to coat them with a 6.5 mm thick mortar layer. Van Tittelboom et al. [52] mentioned that the incorporation of glass in the cementitious matrix might also result in unwanted alkali-silica reaction. In addition, Van Tittelboom et al. [52] and Feiteira et al. [55] drew the attention to the fact that the capsules should be pre-placed in the moulds for the laboratory experiments, something that is inconvenient for larger-scale castings. In another study, Gilabert et al. [57] underlined the importance of the strong bond between the glass capsule and the cementitious matrix in order to avoid debonding, which can lead to the failure of the release of the healing agent into the crack.

As an alternative for the glass Van Tittelboom et al. [52] used ceramic capsules. These capsules showed similar brittleness (as glass) without endangering the durability of the cementitious material (alkali-silica reaction). Furthermore, it was shown that ceramic capsules exhibit a higher bond to the cementitious matrix and could release the embedded healing agent in an enhanced way. A few studies [58,59] suggested the use of natural fibres as carriers of healing agents in cementitious materials. However, they also addressed the significance of some practical issues, such as the insufficient tensile strength of some fibres that can break even upon formation of very small crack widths and the production of a coating that keeps the repair agent in the fibre during mixing.

Besides the use of glass capsules another type of material that is often used to encapsulate various types of healing agents is lightweight aggregates (LWA). LWA have been traditionally used to reduce the dead weight of the structures and as a medium for internal curing of the cementitious materials, which mitigates the early age autogenous shrinkage and micro-cracking [60]. The essential characteristic of the LWA is their high porosity, which makes them weaker than the normal weight aggregates. Therefore, they can act as crack attraction points, when embedded in the cementitious matrix. Additionally, as capsules, LWA can carry the healing agent in their pores and protect it during mixing and setting stage. At a later phase, the crack will meet the aggregate and will separate it into two parts. Upon aggregate breakage, the healing agent will be exposed and released in the crack. Several studies concerning self-healing cementitious materials used synthetic aggregates [61-64], which are produced by thermal treatment of the materials, such as clay, resulting in expanded porous particles. The impregnation of the healing material in the LWA can be succeeded either by simply soaking them in the healing agent solution [63, 65-69] or by vacuum application [61, 62, 64, 70]. In comparison to glass capsules, the LWA as healing agent carriers provide:

- similar weak point/ crack attraction behaviour,

- stronger bonding with the cementitious matrix, due to their rough external surface and
- improved viability during wet mixing.

On the other hand, the incorporation of LWA in the cementitious matrix is accompanied by decreased compressive strength, due to replacement of normal weight aggregates with a weaker and porous material. Further, another issue that needs to be considered, in view of using LWA as healing agent carriers, is the possibility of leakage of the healing agent into the cementitious matrix. The network of the pores allows the healing agent to be embedded in the particles. Yet, through the same network the healing agent can be leached in the matrix, depending on the connectivity and the size distribution of the pores. The leakage of the healing agent from the LWA will be further discussed in chapter 3.

An alternative approach in encapsulation of healing agents is the use of polymeric capsules to avoid all the undesirable effects of the glass, ceramic, natural and LWA. Some examples of polymeric capsules used as healing agent reservoirs are made of: wax [71], gelatine [72], polyurethane [73], melamine [74], polylactic acid [75] and alginate [76,77]. The above-mentioned studies confirm the ability of those capsules to survive the concrete mixing. However, further research should also investigate whether these materials:

- are brittle enough to break immediately upon crack formation,
- create a strong bond with the cementitious matrix so that the crack intersects the capsule and does not circumvent it and
- can withstand the high alkalinity of the cementitious matrix.

The nature of the inner part of the capsules; i.e. the healing agent, is equally important as the shell of the capsule. Therefore, numerous studies focused on the development of different healing agents. Three are the most distinct categories of healing agent materials; namely, the synthetic polymeric, the inorganic and the biogenic healing agents. The first two categories are described in this section, while the last one will be extensively discussed in section 2.2.

When the subject of self-healing in cementitious materials was initially introduced, the healing agents were synonymous with polymeric materials. Single-component polymeric healing agents have been widely studied [14, 48, 50, 51, 78]. However, these healing agents cannot act completely autonomously, as stated by Dry et al. [79], since they either need special curing treatment before or after their release from the capsules or might be prematurely activated (before cracking). Thus, multi-component polymeric healing agents were suggested in several studies [14, 53, 55, 72, 80-82]. The multi-component polymeric healing agents offer an extra autonomy to the system, compared to single-component ones,

since they do not need special curing conditions to flow and harden. Yet, there are still some aspects to be considered, such as:

- the premature activation,
- the shelf-life of the agent,
- the viscosity of the agent,
- the chemical interaction with the cementitious matrix and
- the shrinkage of the filling material after polymerization.

The healing capacity of inorganic healing agents in concrete has been studied also by several researchers. The advantage of these agents, compared to polymeric agents, is that they exhibit better compatibility with the (inorganic) cementitious matrix. Encapsulated inorganic healing agent such as calcium hydroxide, after cracking, reacts with the carbon dioxide present in the crack and forms limestone crystals [72, 83]. Another inorganic healing agent that has been often used is sodium silicate [14, 84-87], which reacts with the calcium hydroxide present in the cementitious matrix to form calcium-silicate-hydrate gel and fill the crack. Other inorganic compounds such as sodium monofluorophosphate [63], calcium nitrate [88] and expansive minerals (reactive magnesium, bentonite and quicklime) [56] have been also used to promote self-healing in cementitious materials.

Although the healing efficiency of the described encapsulated healing agents has been proven, the use of biogenic healing agents has gained ground the last years, due to their environmental friendly compounds, their potential to bridge cracks larger than 0.4 mm also in aged concrete (months to years rather than days), their potential to be used repeatedly, and their long shelf life, which is translated to prolonged functionality. Consequently, the concept of biogenic self-healing concrete, which is described in the following section, is oriented towards increasing sustainability and reducing total cost of ownership of concrete structures.

2.2 BIOGENIC SELF-HEALING SYSTEMS IN CEMENTITIOUS MATERIALS

In the past decade, several research groups world-wide addressed the durability related problem of micro-crack formation in traditional concrete by developing bacteria-based self-healing concrete and repair systems [89]. Early age crack formation in concrete is known to occur due to temperature effects and shrinkage of the setting concrete as well as due to loading of steel reinforced structures. While micro-crack formation does not pose an immediate threat to strength and

integrity of the structure, it does typically lead to water-tightness and durability problems particularly in wet or moist environments.

Limestone and other types of mineral formation in concrete can be beneficial and durable, as these are concrete compatible materials. Filling up i.e. sealing of cracks makes concrete watertight and at the same time protects the embedded steel reinforcement from detrimental compounds such as chlorides and other corrosion stimulating ions which otherwise migrate rapidly through micro-cracks. One of the main targets of applying bacteria which stimulate limestone deposition is therefore the recovery of decreasing functional concrete properties such as water-tightness or strength. Self-healing of concrete therefore relates to the regain of a certain functional property that might be in addition to water-tightness and strength also porosity or aesthetics. To enhance the autogenous healing capacity of concrete, a specific healing agent in form of encapsulated bacteria and required nutrients and mineral precursor compounds or chemicals are added to the concrete mixture.

Several specific species of bacteria are known to precipitate calcium carbonate and other inorganic types of minerals in the direct vicinity of the cells. This process, however, is strongly dependent on environmental conditions. It can therefore be stated that bacteria, by employing specific metabolic pathways, change environmental conditions in such a way that precipitation of inorganic minerals is increased. The designation of “limestone-producing bacteria” in relation to a functional trait is therefore strictly speaking largely incorrect, as metabolically driven limestone precipitation by bacteria is always due to a specific combination of metabolic pathway, activity and physico-chemical environmental conditions. A specific bacterium can thus be 'limestone-producing' in one environment but not in another.

The potential application of limestone deposition enhanced by bacteria for improving durability aspects of concrete has been investigated using specific types of bacteria employing different metabolic pathways. A common characteristic of the various bacterial metabolic pathways is that they result in super saturation of calcium carbonate in solution, resulting in precipitation of calcium carbonate. While bacteria usually only change environmental calcium ion concentration to a minor extent, several metabolic pathways strongly affect the environmental concentration of carbonate ions and thereby also the saturation state of calcium carbonate in solution. Typical bacterial metabolic pathways that increase the carbonate ion concentration and related calcium carbonate saturation in solution are hydrolysis of urea, oxidation of organic compounds using oxygen under aerobic conditions or oxidation of organic compounds using nitrate under anaerobic conditions. This part reviews the biogenic self-healing systems which have been or are being investigated by several research groups.

2.2.1 ENZYMATIC HYDROLYSIS OF UREA

Enzymatic hydrolysis of urea is a process that results in formation of carbonate ions, and as such increases the potential of calcium carbonate precipitation due to the increase of the calcium- and carbonate ion concentration product. The biogenic, urease-driven, reaction rate of urea hydrolysis is approximately 1014 times faster than the chemical (non-urease driven) rate [90]. Equation 2.2 shows the overall reaction of enzymatic urea hydrolysis:

$$\boldsymbol{CO(NH_2)_2 + 2H_2O \rightarrow 2NH_4^+ + CO_3^{2-}} \quad (2.2)$$

The amount of calcium carbonate formed due to the reaction of available calcium ions with produced carbonate ions is directly dependent on the amount of urea decomposed during the process of urea hydrolysis. Urease active bacteria can be used to increase autogenous healing rates of concrete due to the potentially enhanced rate of calcium carbonate formation. To obtain truly autonomous healing of concrete, both bacteria and nutrients required for bacteria-driven calcium carbonate formation should be introduced to the concrete mixture. Therefore, spore-forming bacteria instead of vegetative cells are selected, as only the former can survive the direct incorporation in the concrete matrix. Spores can stay dormant inside concrete and become activated upon concrete cracking if water, oxygen, nutrients are present, and other environmental conditions such as temperature and pH are at values compatible with their metabolic capacity. Wang et al. used *Bacillus sphaericus*, an alkali-resistant spore-forming ureolytic strain initially applied for consolidation of building materials [74].

Ghent University studies revealed that the concentration of bacteria should be higher than 10^6 cells/mL to obtain a considerable amount of calcium carbonate precipitation. Apart from bacterial numbers, also concentrations of urea and calcium ions (Ca^{2+}) greatly influence the yield of $CaCO_3$ precipitation. Theoretically, ureolytic bacteria can continue hydrolysing urea if the urease enzyme remains active. Recommended concentrations of both urea and calcium source were 0.5 M [91]. Wang and colleagues also found that yeast extract (≥ 2g/L) is an essential nutrient as it stimulates germination of spores, a requirement for urease driven formation of calcium carbonate. As working with pure cultures is relatively expensive, a more economical way of producing ureolytic bacterial suspensions was developed at Ghent University. A new selective process named CERUP (Cyclic Enriched Ureolytic Powder) to obtain an ureolytic microbial community was developed [92]. It was estimated that the production cost of CERUP was about 40 times lower than that of pure cultures [93].

Encapsulation of bacteria is considered of crucial importance in a bacteria-based self-healing system, as mechanical forces during concrete mixing can damage the bacterial spores. Sorption of bacterial cells onto diatomaceous earth (DE) provided

a protective effect for bacteria in high pH cement slurry [94]. Furthermore, DE had no negative effect on the mechanical properties of mortar and may even show pozzolanic activity. The concept of impermeable microcapsules containing bacterial spores was patented [95]. The capsules change properties from humid to dry state, allowing them to withstand forces during concrete mixing, but break upon cracking [96]. Another idea for encapsulation was elaborated by use of the hydrogels as carriers. Hydrogels act not only as protective carriers for bacterial spores during mixing and hydration, but also as water reservoir for spore germination and bacterial activity when cracking occurs. In normal humidity conditions, hydrogels can absorb moisture and retain it for bacterial use, which is beneficial for a realistic self-healing. Wang et al. [97] observed substantial and fast crack closure: a crack of 0.5 mm was completely closed within 1~2 weeks (Figure 2.3). However, a drastic strength loss (as high as 50%) occurred after the addition of the bio-hydrogels, which indicated incompatibility between the hydrogels and concrete matrix. Regarding this, more compatible hydrogels have been developed [43], as well as modified alginate based ones [76].

Besides bacteria, the nutrients and the deposition agents (urea and calcium source) are also essential elements for biogenic precipitation and should therefore also be incorporated into concrete in advance. Latter compounds, however, do not necessarily need to be encapsulated and therefore were added directly to the concrete mixture. In subsequent studies, it was found that although urea and calcium source have no negative effect on the strength development of concrete, yeast extract and other organic compounds did.

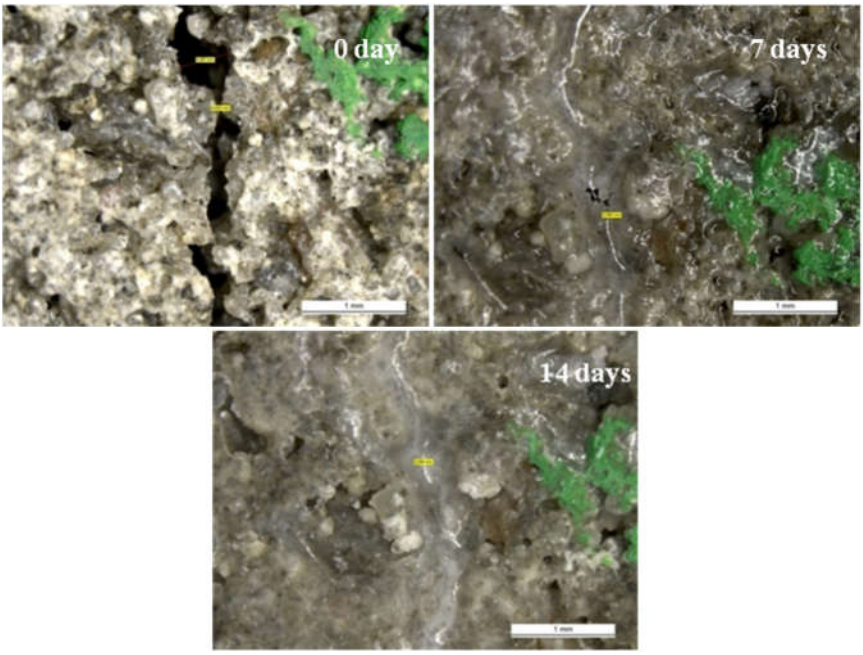

Figure 2.3 Crack closure process in the specimen with hydrogels encapsulated Bacillus sphaericus spores (The initial widest part: 507 µm)[97].

2.2.2 OXIDATION OF ORGANIC CARBON

Expanded Clay Particles System

Biological calcium carbonate precipitation and carbon dioxide production can also occur during the degradation of organic compounds, where bacteria act as catalyst. This bio-chemical reaction is the principle of biogenic healing in concrete, via organic carbon oxidation. Jonkers at al. [98,99] introduced the concept of filling the concrete cracks with $CaCO_3$ via metabolic conversion of calcium lactate, as an alternative mechanism to the urease-based system investigated in previous studies. However, it was observed that the bacterial spores (*Bacillus cohnii*) could apparently not survive the mixing forces and the high alkalinity of the fresh cement matrix when added directly (unprotected) to the concrete mixture [93]. Furthermore, the direct addition of organic bio-mineral precursor compounds to the concrete mixture could result in undesirable effects in setting and compressive strength of concrete. It was therefore suggested, to immobilize and protect the bacterial spores and the organic compounds in expanded clay particles [61].

Wiktor and Jonkers [62] investigated the efficiency of the specific healing agent incorporated into LWA (Liapor 1/4 mm, GmbH Germany). For protection and immobilization during concrete mixing, the healing agent components were dissolved in water and subsequently impregnated via vacuum application into

LWA. The healing agent solution contained spores from *Bacillus alkalinitrilicus* (10^{11} spores/L), calcium lactate (80 g/L) and yeast extract (1 g/L). It was found that the sealing of the cracks could be attributed primarily to the direct $CaCO_3$ precipitation through metabolic conversion of calcium lactate (Equation 2.3) and secondarily to the reaction of the metabolically produced CO_2 molecules with $Ca(OH)_2$ minerals present in the concrete matrix as product of cement hydration, leading to additional $CaCO_3$ precipitation (Equation 2.4).

$$\boldsymbol{CaC_6H_{10}O_6 + 6\,O_2 \rightarrow CaCO_3 + 5\,CO_2 + 5\,H_2O} \quad (2.3)$$

$$\boldsymbol{5CO_2 + 5Ca(OH)_2 \rightarrow 5CaCO_3 + 5H_2O} \quad (2.4)$$

Moreover, the stereomicroscopic observations showed crack-healing of up to 0.46 mm-wide cracks in biogenic mortar, while in non-biogenic mortar the healing occurred in up to 0.18 mm-wide cracks, after 100 days submersion in water. In addition, this study introduced an innovative experimental technique to prove the bacterial activity in the mortar specimens, namely, the oxygen consumption tests. The findings of the stereomicroscopic investigation were supported by oxygen profile measurements that were conducted in water-submerged specimens, that they indeed revealed that only biogenic specimens consumed O_2.

After the proven success of the concept and the promising results that were produced by previous studies, more researchers were interested in studying self-healing in cementitious materials via organic carbon oxidation. Sierra-Beltran et al. [65] incorporated the specific healing agent in strain-hardening cement-based composite (SHCC) used as repair system for concrete. They examined the mechanical properties, the self-healing capacity and the bonding behaviour of the cementitious material. The results showed that a SHCC type material with biogenic healing agent fulfilled the requirements of compressive and bonding strength for a structural repair material. The biogenic SHCC showed reduced delamination (almost 4 times less) from the concrete substrate and a similar recovery of both flexural strength and deflection capacity compared to the non-biogenic SHCC.

In another study, Stuckrath et al. [100] studied the healing behaviour of mortar with biogenic healing agent embedded in LWA (expanded clay particles with diameter between 1.18 mm and 4.75 mm). Through image analysis, they found that the median of crack healing at 100 days of water incubation was over 58% for all specimens with healing agent, whereas for specimens without self-healing agents such median was under 38% (cracks widths between 0.08 mm and 0.22 mm were considered in the analysis). Xu and Yao [101] also investigated the precipitation of $CaCO_3$ in cracked fibre-reinforced mortar specimens by incorporating bacteria and calcium-based nutrients (calcium lactate and calcium

glutamate) in the mortar matrix. They concluded that recovery of flexural strength after healing proved to be slightly enhanced for the biogenic specimens compared to the control specimens. In fact, the healing and recovery ratios of flexural strength and modulus of the two-component self-healing mortar were higher than that of control series by a factor of 2.

In a later study Tziviloglou et al. [64] built further on the study of Wiktor and Jonkers [56] by investigating the mechanical behaviour of mortar with biogenic healing agent, the crack permeability after cracking, the effect of healing treatment (wet-dry cycles), as well as the crack sealing. The test results revealed that compressive strength of mortar specimens containing the biogenic system was considerably reduced (Figure 2.4a), due to replacement of normal weight sand by LWA (Liapor 1/4 mm, GmbH Germany). Despite the lower strength performance, the biogenic mortar exhibited a significantly improved crack sealing performance (investigated by crack water flow tests) when exposed to wet-dry cycles, compared to mortars without healing agent (Figure 2.4b).

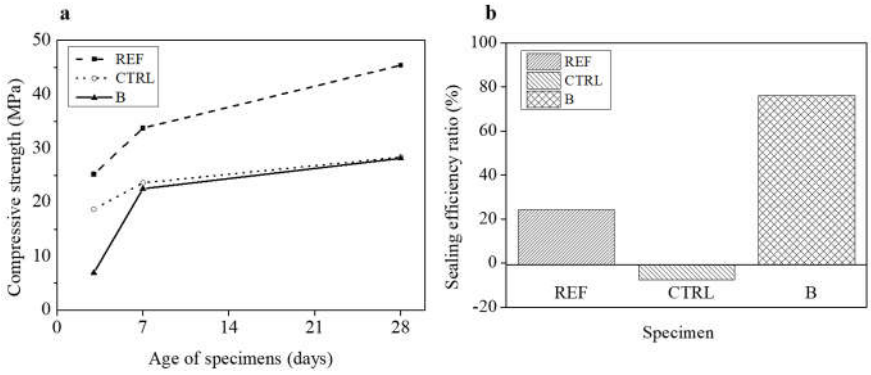

Figure 2.4 a. Compressive strength for REF (no healing agent and normal weight aggregates), CTRL (no healing agent and lightweight aggregates), and B (biogenic healing agent and lightweight aggregates) specimens, b. Average sealing efficiency ratio for REF, CTRL, and B specimens [1].

Paine et al. [69] conducted laboratory experiments to demonstrate the viability of self-healing concrete with biogenic healing agent consisting of spores from *Bacillus pseudofirmus*, calcium acetate and yeast extract incorporated into non-hydrated cement-coated LWA (perlite particles). The results revealed that neither the consistency nor setting was affected by the addition of the loaded perlite into the concrete mixture. Moreover, compressive tests on 28-days-old specimens revealed normal compressive strength values for the specimens with the biogenic healing agent. The visual inspection after cracking showed uniform distribution and splitting of the perlite. Thus, it was concluded that in practice cracking would lead to release of the self-healing agents.

Compressed powder System

Where proof of concept was shown for healing agent components contained in LWA, the application range may be limited due to their influence (decrease in compressive strength) in the mixture design. To extend the applicability, a step was taken to reduce the added volume of healing agent by increasing the efficient healing agent component content in particles. For this reason, scalability of production was an important factor to consider. A way of producing scalable particles almost fully consisting of active ingredients is by roller compacting powders to sheets, with subsequent milling to flakes in the size range of the sand fraction (1- 4 mm) [102]. Challenging, however, was to retain particle integrity during the wet mixing stage of mortar or concrete production to prevent premature disintegration of particles in the mixture. Therefore, a coating material was applied (Figure 2.5) [103-105]. To retain equal active healing agent content in the mortar or concrete mixture, the addition of particles went from 30% by volume for LWA [64] to 1% for the proposed flakes.

Figure 2.5 a. Roller compaction of powders, b. Coating of particles, c. Uncoated powders and d. Coated powders [1].

Important characteristics of healing agent containing flakes are survivability during the mixing stage, limited influence on mortar or concrete hardening properties, nutrient availability in time and enabling regain of crack water-

tightness as functionality [106]. Negligible influence on fresh mixture consistency was seen from flow tests, but some delay in strength development indicated interaction of healing agent particles and cementitious matrix. From 7 days of hardening, the influence on strength development became negligible.

To monitor bacterial activation and nutrient conversion, mortar slices with exposed healing agent flakes were immersed in water in a closed vial or stirred open system to measure decrease in oxygen concentration, as evidence for bacterial metabolic activity. Externally visible progressive mineral formation in a water immersed cracked mortar specimen (at the age of 28 days) indicated crack closure. More important than visual mineral formation was to confirm functionality regain, for which water-tightness tests were performed. Half cube mortar specimens were split to a crack width above the autogenous healing capacity (> 400 µm). It was found that for specimens with similar crack widths significantly higher recovery of water-tightness was found in mortar containing healing agent flakes (Figure 2.6).

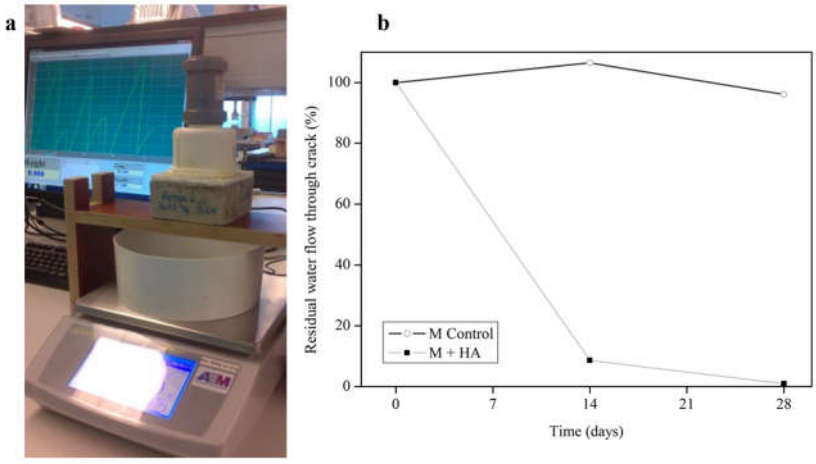

Figure 2.6 a. Set-up used to evaluate water-tightness on cracked mortar slices, b. Residual water flow through crack at various water curing times; M = control mortar, M+HA = mortar with healing agent flakes [1].

2.2.3 ANOXIC OXIDATION OF ORGANIC CARBON

Microbial urea hydrolysis and aerobic oxidation of organic carbon processes require oxygen to initiate germination of bacterial spores and urease production and to keep the microbial activity, respectively. Due to the poor solubility of oxygen in water (~ 9 mg/L) and its related deficiency in the deeper parts of the crack, healing efficiency through either of the processes is mostly inhibited with depth. Moreover, aerobic oxidation of organic carbon is known for its relatively low $CaCO_3$ yield [107] and urea hydrolysis is well known for its ammonia

production which is detrimental for the environment in higher concentrations [108,109]. These issues already prompted the attention to alternative pathways in several applications of microbial induced $CaCO_3$ precipitation (MICP). Anoxic oxidation of organic carbon is possible through consumption of nitrate (NO_3^-) or nitrite (NO_2^-) ions, functioning instead of oxygen as an electron acceptor and does via the denitrification pathway not produce any toxic by-products. The process is called denitrification and has been proposed for soil consolidation and Ca^{2+} removal from industrial wastewater [107,110, 111]. Due to its highly negative standard Gibbs free energy (ΔG^o) (Eq. 5), denitrification can be expected to dominate in the presence of NO_3^- and organic carbon under oxygen limited conditions and generates in addition to nitrogen gas (N_2), carbonate (CO_3^{2-}) and bicarbonate (HCO_3^-) ions which are necessary for $CaCO_3$ precipitation (Equation 2.5).

$$5HCOO^- + 2NO_3{}^- \leftrightarrow N_2 + 3HCO_3^- + 2CO_3{}^{2-} + H_2O$$
$$\Delta G° = -1153 \frac{kJ}{mole} \quad (2.5)$$

MICP studies aiming for sand and soil consolidation through nitrate reduction (denitrification) revealed that $CaCO_3$ precipitation rates achieved through NO_3^- reduction were rather low during in situ application [107, 111, 112]. Indeed, under optimum conditions, MICP rates achieved through denitrification are 100 to 1000 times lower than those achieved through ureolysis [111]. Yet, the concrete environment is far from the optimum conditions. Apart from its alkaline state, in concrete cracks, oxygen and nutrients are limited which are the main factors affecting germination and growth rate of the used bacteria. $CaCO_3$ precipitation rate mainly depends on the initial bacteria concentration, their growth rate and specific metabolic activity of each bacterium in the relevant environment. Therefore, the condition in concrete cracks favours denitrifying bacteria rather than aerobic bacterial strains. Bacteria that can grow on NO_3^- under oxygen limited conditions could supersede the MICP rate and self-healing performance of the aerobic bacteria provided that nitrate is available.

Anoxic oxidation of carbon sources as a self-healing mechanism requires three main components:

- an organic carbon source,
- NOx (NO_3^- and/or NO_2^-) as an electron acceptor and
- proper denitrifying bacteria.

There are already certain concrete admixtures, such as calcium formate ($Ca(HCOO)_2$) and calcium nitrate ($Ca(NO_3)_2$), which can serve as carbon source and electron acceptor, respectively. Calcium formate is used as set accelerator (0.5

to 4% w/w cement) and calcium nitrate is used as strength enhancer or anti-freeze admixture (0.2 to 4% w/w cement) in concrete [113,114]. Using this information, at Ghent University, microbial strains that can grow on these concrete admixtures were selected and investigated for MICP [111]. Among the selected strains, *Diaphorobacter nitroreducens*, a NO_3^- reducing vegetative bacterial strain, appeared to grow on formate and nitrate salts with a higher growth rate than NO_3^- reducing *Bacillus* species (Figure 2.7).

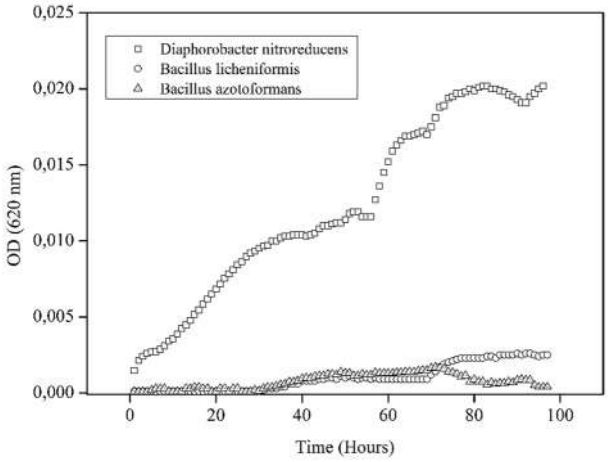

Figure 2.7 Difference in growth of different NO_3^- reducing species under minimal nutrient conditions lacking yeast extract and trace elements [1].

The difference in growth performances was attributed to the absence of yeast extract which is an essential nutrient for germination of *Bacillus* spores. The ability to grow in the absence of trace elements and nutrients such as vitamins and yeast extract makes *Diaphorobacter nitroreducens* advantageous over other currently studied strains. Furthermore, a $CaCO_3$ precipitation yield of 7 g $CaCO_3$/g NO_3-$N.d^{-1}$ could be achieved which is distinctive among the reported MICP studies [111]. In addition, survival experiments showed that *Diaphorobacter nitroreducens* can survive at pH 13 with the aid of protective carriers [115]. Prior to addition in mortar, bacterial cells (0.5% w/w cement) were incorporated in either diatomaceous earth, expanded clay particles or granular activated carbon (5% w/w cement), acting as protective carriers. In a recent study [116], various types of commercially available protective carriers and nutrients were investigated for their influence on mortar setting and strength properties. The results indicated that expanded clay particles or granular activated carbon particles could be successfully used as protective carriers for vegetative bacterial strains without significantly changing the setting and strength properties of mortar.

In another recent study [117], the self-healing performance of mortar specimens containing *Diaphorobacter nitroreducens* was investigated. Bacterial cells (0.5% w/w cement) were loaded into 0.5 – 2 mm expanded clay particles (5% w/w cement) and added to the mortar during mixing. As nutrient source, concrete admixtures $Ca(HCOO)_2$ (2% w/w cement) and $Ca(NO_3)_2$ (3% w/w cement) were dissolved in water and added during mixing. 28-days-old reinforced mortar specimens (30 mm x 30 mm x 360 mm) were subjected to direct tensile load, applied to the reinforcement (reinforcement diameter = 6 mm, reinforcement length = 660 mm) and multiple cracks (crack width range 100 - 500 μm) were achieved. Upon crack formation, mortar prisms were immersed in tap water for 28 days. Self-healing performance of the mortars was evaluated through analysis of stereomicroscopic pictures and water absorption tests. The results revealed that after 28 days of healing treatment specimens with bacteria could completely close the cracks up to 350 μm and they absorbed 51% less water than the reference specimens in the first 24 hours.

The bio-based self-healing agents described above use various bacterial strains that follow different metabolic pathways, yet, in all systems the final healing product that fills the cracks is limestone. Bacteria strains that are selected can survive in the alkaline concrete environment. To obtain maximum protection during concrete mixing and to yield the highest survival potential for many years, encapsulation of the healing agent is of great importance, although it might affect the mechanical properties of the material. From economical point of view, it is essential to optimize the amount of bacteria and nutrients necessary for efficient self-healing of concrete cracks. Therefore, various combinations of bacterial healing agents and nutrients should be tested in concrete and optimized based on the needs for the specific application.

2.3 EVALUATION OF SELF-HEALING IN CEMENTITIOUS MATERIALS AT LAB-SCALE

The state-of-the-art report by RILEM TC/221 [5] defines self-healing as “any process by the material itself involving the recovery and hence improvement of a performance after an earlier action that had reduced the performance of the material”. The term performance, though, is not one-dimensional, contrariwise, it includes various properties of the material, such as mechanical properties, durability and aesthetic appearance (Figure 2.8). Therefore, it is logical to investigate first the loss and then the recovery of those properties, to evaluate the self-healing efficiency of a cementitious material. Depending on the nature of the healing agent, the material might regain (partially or fully) one or more properties. The study of self-healing capacity then can be divided into tests which examine the mechanical recovery, the resistance against physical and chemical actions and crack closure. While some of the tests that are used to study self-healing are

qualitative, in most cases the researchers try to quantify the efficiency of the incorporated healing agent. Below are presented some of the most common methods that are used for this purpose.

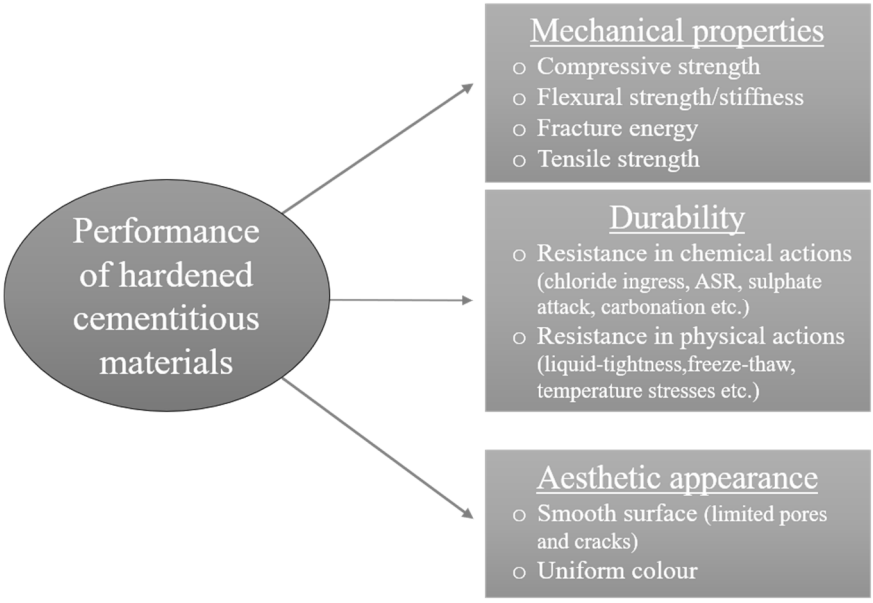

Figure 2.8 Performance requirements for hardened cementitious materials.

The most popular and simple method to evaluate healing efficiency has mostly been the investigation of the recovery of mechanical properties through mechanical testing. The principle lies in determining the value of a mechanical property of a specimen after it has been damaged and then after the end of the healing process. Bending tests can create cracks with controllable widths, therefore, in most cases flexural strength and/or stiffness recovery have been investigated [19, 24-26, 28, 48, 51, 52, 55, 65, 67, 70,73, 78, 80, 88, 118-121]. Considerably less studies have examined the recovery of compressive strength [80] and fracture energy [57, 122, 123]. The mechanical tests are rather straightforward, simple and can quantify the enhanced property of cementitious materials after healing.

Durability problems in concrete structures are often caused by ingress of deleterious substances through the network of cracks. Consequently, the crack closure, which is inextricably related to liquid tightness, has been also studied by methodologies that produce either quantitative or qualitative results. Optical microscopy is one of the most popular ways to ascertain, at least at a primary level, the occurrence and the amount of healing [27, 28, 33, 38, 62, 64, 70, 81, 88, 97, 124, 125]. The cracks are observed on specimens after damage introduction and

after healing. Through optical microscopy it is possible to study the morphology of the cracks and the filling material (healing product). In addition, optical microscopy combined with image analysis can give a quantitative indication for the extent of healing.

Scanning Electron Microscopy (SEM) or Environmental Scanning Electron Microscopy (ESEM) are used to observe the morphology of the cracks, but also the crystalline formations obtained during the healing period [27, 33, 48, 54, 56, 62-65, 88, 121, 124]. Additionally, X-ray tomography has been used to visualize the crack healing along the crack length [40, 52, 126]. Although this method allows the 3-dimensional representation of the crack, there are some limitations related to the small size of samples, the picture noise due to the presence of reinforcement, the difficulty to distinguish the cement from the healing product phases etc. For the identification of the scraped products from the crack surfaces Energy Dispersive X-ray spectrometry (EDS) [62, 63, 65, 88, 121, 124] and Fourier-Transform Infrared (FT-IR) analyses are often used [54, 56, 62, 70, 77, 127]. However, the restricted detection limit of some substances, or the presence of water can cause inaccuracy in the obtained results.

The crack closure investigation through microscopy gives limited results regarding recovery of the liquid tightness after healing. In other words, microscopy can indicate whether the crack has been adequately filled by the healing product, at least on the outer surface. However, by using only this tool it cannot be confirmed whether the material has regained its functionality, in this case water-tightness. Thus, tests that are examining the possibility of liquids to penetrate the crack are often performed to verify the efficiency of the healing agent. Crack permeability tests via water flow [6, 8, 23, 28, 41, 52, 64, 77, 81, 96, 128], water absorption tests [27, 54-56, 63, 70, 96] and air permeability tests [80] on pre-cracked and on healed specimens can quantify the extent of healing and the recovery of liquid tightness.

Other evaluation methods which include non-destructive techniques have also been used to determine the recovery of mechanical properties. Non-destructive testing (NDT) can evaluate the damage in concrete but also monitor the release of healing agents and the loss/recovery of the material properties. The NDT methods that are often used for monitoring of self-healing (either at laboratory or field scale) are ultrasonic measurements [129-131], acoustic emission [130-134], vibration analysis [130-131], resonance frequency [13, 26, 135] and several other techniques.

The main discussion issue regarding the self-healing assessment methods is the reliability of the results. The reliability concerns the possibility to obtain consistent and reproducible results through a certain evaluation methodology. Some

methodologies are based on or adapted from standardized tests on cementitious materials which can partially ensure consistency and repeatability of the results. However, since the self-healing technology in cementitious materials is relatively new there is lack of standardized testing procedures to evaluate healing efficiency. Moreover, the assessment methods cannot be applied to all kinds of self-healing systems and even if they are, the quality of the results may differ substantially. Hence, it is of great importance to know the nature of the healing mechanism, the healing product and which techniques could be possibly applied to obtain rather consistent results.

REFERENCES

[1] Tziviloglou, E., Van Tittelboom, K., Palin, D., Wang, J., Sierra-Beltrán, M.G., Erşan, Y.Ç., Mors, R., Wiktor, V., Jonkers, H.M., Schlangen, E., and De Belie, N., *Bio-Based Self-Healing Concrete: From Research to Field Application*. in *Self-healing Materials*, Eds. Hager, M.D., van der Zwaag, S., and Schubert, U.S. 2016, Springer International Publishing: Cham. p. 345-385.

[2] Neville, A., *Properties of concrete*. Fourth Edition. 1997, London: Longman Group Limited.

[3] Schlangen, E. and Joseph, C., *Self-Healing Processes in Concrete*. in *Self-Healing Materials: Fundamentals, Design Strategies, and Applications*, Eds. Gosh, S.K. 2009, Wiley-VCH Verlag GmbH & Co. KGaA : Weinheim, Germany. p. 141-182.

[4] Igarashi, S., Kunieda, M., and Nishiwaki, T., *Research activity of JCI technical committee TC-075B: Autogenous healing in cementitious materials*. 2009. In: 4th International Conference on Construction Materials: Performance, Innovation and Structural Implications, (ConMat'09). Nagoya, Japan.

[5] de Rooij, M., Van Tittelboom, K., De Belie, N., and Schlangen, E., *Self-healing phenomena in cement-based materials : state-of-the-art-report of RILEM Technical Committee 221-SHC*. RILEM state of the art reports; v. 11. 2013, Dordrecht, The Netherlands: Springer.

[6] Edvardsen, C., *Water Permeability and Autogenous Healing of Cracks In Concrete.* ACI materials journal, 1999. 96(4): p. 448-454.

[7] Neville, A., *Autogenous healing-a concrete miracle?* Concrete International, 2002. 24: p. 76-82.

[8] Reinhardt, H.W. and Jooss, M., *Permeability and self-healing of cracked concrete as a function of temperature and crack width.* Cement and Concrete Research, 2003. 33(7): p. 981-985.

[9] Li, V.C. and Yang, E.-H., *Self Healing in Concrete Materials*. in *Self Healing Materials: An Alternative Approach to 20 Centuries of Materials Science*, Eds. van der Zwaag, S. 2007, Springer Netherlands: Dordrecht. p. 161-193.

[10] Mihashi, H. and Nishiwaki, T., *Development of engineered self-healing and self-repairing concrete-state-of-the-art report.* Journal of Advanced Concrete Technology, 2012. 10(5): p. 170-184.

[11] Ivanov, F.M. and Polyakov, B.I., *Self-healing and durability of hydraulic concrete.* Hydrotechnical Construction, 1974. 8(9): p. 844-849.

[12] Jacobsen, S., Marchand, J., and Hornain, H., *Sem observations of the microstructure of frost deteriorated and self-healed concretes.* Cement and Concrete Research, 1995. 25(8): p. 1781-1790.

[13] Jacobsen, S. and Sellevold, E.J., *Self healing of high strength concrete after deterioration by freeze/thaw.* Cement and Concrete Research, 1996. 26(1): p. 55-62.

[14] Mihashi, H., Kaneko, Y., Nishiwaki, T., and Otsuka, K., *Fundamental study on development of intelligent concrete characterized by self-healing capability for strength.* Transactions of the Japan Concrete Institute, 2000. 22: p. 441-450.

[15] Gray, R.J., *Autogenous healing of fibre/matrix interfacial bond in fibre-reinforced mortar.* Cement and Concrete Research, 1984. 14(3): p. 315-317.

[16] Clear, C., *The effects of autogenous healing upon the leakage of wqater through cracks in concrete*, in *Cement and Concrete Association*. 1985.

[17] Hearn, N., *Self-sealing, autogenous healing and continued hydration: What is the difference?* Materials and Structures 1998. 31(8): p. 563-567.

[18] White, S.R., Sottos, N.R., Geubelle, P.H., Moore, J.S., Kessler, M.R., Sriram, S.R., Brown, E.N., and Viswanathan, S., *Autonomic healing of polymer composites.* Nature, 2001. 409(6822): p. 794-797.

[19] Joseph, C., Jefferson, A.D., and Cantoni, M.B., *Issues related to the autonomic healing of cementitious materials*. 2007. In: 1st International Conference on Self-healing Materials. Noordwijk aan Zee, The Nethrlands.

[20] Li, V.C., *On engineered cementitious composites (ECC)- A review of material and its applications.* Journal of Advanced Concrete Technology, 2003. 1(3): p. 215-230.

[21] Li, V.C., Wu, C., Wang, S., Ogawa, A., and Saito, T., *Interface tailoring for strain-hardening PVA-ECC.* ACI materials journal, 2002. 99(5): p. 463-472.

[22] Şahmaran, M. and Li, V.C., *De-icing salt scaling resistance of mechanically loaded engineered cementitious composites.* Cement and Concrete Research, 2007. 37(7): p. 1035-1046.

[23] Lepech, M.D. and Li, V.C., *Water permeability of engineered cementitious composites.* Cement and Concrete Composites, 2009. 31(10): p. 744-753.

[24] Tziviloglou, E., Self-healing in ECC materials with low content of different microfibers and micro-particles. 2009. MSc, Delft University of Technology, Delft.

[25] Antonopoulou, S., Self healing in ECC materials with high con-tent of different microfibers and micro particles. 2009. MSc,

[26] Yang, Y., Lepech, M.D., Yang, E.H., and Li, V.C., *Autogenous healing of engineered cementitious composites under wet-dry cycles.* Cement and Concrete Research, 2009. 39(5): p. 382-390.

[27] Zhang, Z., Qian, S., and Ma, H., *Investigating mechanical properties and self-healing behavior of micro-cracked ECC with different volume of fly ash.* Construction and Building Materials, 2014. 52: p. 17-23.

[28] Ma, H., Qian, S., and Zhang, Z., *Effect of self-healing on water permeability and mechanical property of Medium-Early-Strength Engineered Cementitious Composites.* Construction and Building Materials, 2014. 68: p. 92-101.

[29] Zhu, Y., Zhang, Z.C., Yao, Y., and Guan, X.M., *Analysis of Crack Microstructure, Self-Healing Products, and Degree of Self-Healing in Engineered Cementitious Composites.* Journal of Materials in Civil Engineering, 2016. 28(6).

[30] Homma, D., Mihashi, H., and Nishiwaki, T., *Self-healing capability of fibre reinforced cementitious composites.* Journal of Advanced Concrete Technology, 2009. 7(2): p. 217-228.

[31] Nishiwaki, T., Koda, M., Yamada, M., Mihashi, H., and Kikuta, T., *Experimental study on self-healing capability of FRCC using different types of synthetic fibers.* Journal of Advanced Concrete Technology, 2012. 10: p. 195-206.

[32] Ferrara, L., Ferreira, S.R., Krelani, V., Silva, F., and Filho, R.D.T., *Effect of natural fibres on the self-healing capacity of high performace fibre reinforced cementitious composites*. 2014. In: 3rd International RILEM Conference on Strain Hardening Cemementitious Composites. Dordrecht, The Netherlands.

[33] Krelani, V., Self-healing capacity of cementitious composites. 2015. PhD Thesis, Politecnico di Milano,

[34] Mechtcherine, V. and Reinhardt, H.W., *Application of super absorbent polymers (SAP) in concrete construction : State-of-the-Art report prepared by Technical Committee 225-SAP*. 2012, Springer: Dordrecht, The Netherlands.

[35] Jensen, O.M. and Hansen, P.F., *Water-entrained cement-based materials: I. Principles and theoretical background.* Cement and Concrete Research, 2001. 31(4): p. 647-654.

[36] Jensen, O.M. and Hansen, P.F., *Water-entrained cement-based materials: II. Experimental observations.* Cement and Concrete Research, 2002. 32(6): p. 973-978.

[37] Craeye, B.B.B., *Experimental evaluation of mitigation of autogenous shrinkage by means of a vertical dilatometer for concrete*. 2006. In: International RILEM Conference on Volume Changes of Hardening

Concrete: Testing and Mitigation. Jensen, O.M., Lura, P., and Kovler, K. Lyngby, Denmark.

[38] Lee, H.X.D., Wong, H.S., and NR, B., *Potential of superabsorbent polymer for self-sealing cracks in concrete.* Composites Part B: Engineering, 2010. 29(6): p. 819-827.

[39] Dejonghe, P., De Belie, N., Steuperaert, S., Snoeck, D., and Dubruel, P., *The behaviour of suberabsorbing polymers as a sealing agent in concrete: absorption kinetics, degradation and water permeability*. 2011. In: 3rd International conference in self-healing materials (ICSHM 2011). Bath, UK.

[40] Snoeck, D., Dewanckele, J., Cnudde, V., and De Belie, N., *X-ray computed microtomography to study autogenous healing of cementitious materials promoted by superabsorbent polymers.* Cement and Concrete Composites, 2016. 65: p. 83-93.

[41] Gruyaert, E., Debbaut, B., Snoeck, D., De Belie, N., Diaz, P., Arizo, A., Tziviloglou, E., and Schlangen, E., *Self-healing mortar with pH-sensitive superabsorbent polymers: Testing of the sealing efficiency by water flow tests.* Smart Materials and Structures, 2016. 25(8).

[42] Klemm, A.J. and Sikora, K.S., *The effect of Superabsorbent Polymers (SAP) on microstructure and mechanical properties of fly ash cementitious mortars.* Construction and Building Materials, 2013. 49(Supplement C): p. 134-143.

[43] Mignon, A., Graulus, G., Snoeck, D., Martins, J., De Belie, N., Dubruel, P., and Van Vlierberghe, S., *pH-sensitive super absorbent polymers : a potential candidate material for self-healing concrete.* Journal of Materials Science, 2015. 50(2): p. 970-979.

[44] Gruyaert, E., Debbaut, B., Snoeck, D., Díaz, P., Arizo, A., Tziviloglou, E., Schlangen, E., and De Belie, N., *Self-healing mortar with pH-sensitive superabsorbent polymers: testing of the sealing efficiency by water flow tests.* Smart Materials and Structures, 2016. 25(8).

[45] Liu, H., Bu, Y., Sanjayan, J.G., Nazari, A., and Shen, Z., *The application of coated superabsorbent polymer in well cement for plugging the microcrack.* Construction and Building Materials, 2016. 104(Supplement C): p. 72-84.

[46] Gruyaert, E., Debbaut, B., Kaasgaard, M., Erndahl Sørensen, H., Pelto, J., Branco, V., Malm, F., Grosse, C., Price, E., Krüger, M., and De Belie, N., *Evaluation of the performance of self-healing concrete at small and large scale under laboratory conditions*. 2017. In: 14th International Conference on Durability of Building Materials and Components. De Schutter, G., et al. Ghent, Belgium.

[47] Díaz-Gómez M.P., Arizo-Leon A., and A.M., L.-B., *Smart hydrogels with pH sensitiveness for self-healing concrete*. 2016. In: HEALCON Conference. Delft, The Netherlands.

[48] Li, V.C., Lim, Y.M., and Chan, Y.-W., *Feasibility study of a passive smart self-healing cementitious composite.* Composites Part B: Engineering, 1998. 29(6): p. 819-827.

[49] Dry, C.M., *Three designs for the internal release of sealants, adhesives, and waterproofing chemicals into concrete to reduce permeability.* Cement and Concrete Research, 2000. 30(12): p. 1969-1977.

[50] Thao, T.D.P., Johnson, T.J.S., Tong, Q.S., and Dai, P.S., *Implementation of self-healing in concrete – Proof of concept.* The IES Journal Part A: Civil & Structural Engineering, 2009. 2(2): p. 116-125.

[51] Joseph, C., Jefferson, A.D., Isaacs, B., Lark, R.J., and Gardner, D.R., *Experimental investigation of adhesive-based self-healing of cementitious materials.* Magazine of Concrete Research, 2010. 62(11): p. 831-843.

[52] Van Tittelboom, K., De Belie, N., Van Loo, D., and Jacobs, P., *Self-healing efficiency of cementitious materials containing tubular capsules filled with healing agent.* Cement and Concrete Composites, 2011. 33(4): p. 497-505.

[53] Escobar, M.M., Vago, S., and Vázquez, A., *Self-healing mortars based on hollow glass tubes and epoxy–amine systems.* Composites Part B: Engineering, 2013. 55: p. 203-207.

[54] Kanellopoulos, A., Qureshi, T.S., and Al-Tabbaa, A., *Glass encapsulated minerals for self-healing in cement based composites.* Construction and Building Materials, 2015. 98: p. 780-791.

[55] Feiteira, J., Gruyaert, E., and De Belie, N., *Self-healing of moving cracks in concrete by means of encapsulated polymer precursors.* Construction and Building Materials, 2016. 102, Part 1: p. 671-678.

[56] Qureshi, T.S., Kanellopoulos, A., and Al-Tabbaa, A., *Encapsulation of expansive powder minerals within a concentric glass capsule system for self-healing concrete.* Construction and Building Materials, 2016. 121: p. 629-643.

[57] Gilabert, F.A., Van Tittelboom, K., Tsangouri, E., Van Hemelrijck, D., De Belie, N., and Van Paepegem, W., *Determination of strength and debonding energy of a glass-concrete interface for encapsulation-based self-healing concrete.* Cement and Concrete Composites, 2016.

[58] Dry, C., *Smart materials which sense, acivate nad repair damage; hollow porous fibres in composites release chamical from fibres for self-healing, damage prevention and/or dynamic control*. 1992. In: 1st European conference on smart structures and materials. Glasgow, Scotland.

[59] de Rooij, M.R., Qian, S., Liu, H., and Ward, W.F., *Using natural wood fibers to self heal concrete*. in *Concrete repair*, Eds. 2009, CRC Press : Boca Raton, Florida, 2009. p. 123-124.

[60] Lura, P., Autogenous deformation and internal curing of concrete. 2003. PhD Thesis, Delft University of Technology, Delft, The Netherlands.

[61] Jonkers, H.M., *Bacteria-based self-healing concrete.* HERON 2011. 56(1/2): p. 1-12.

[62] Wiktor, V. and Jonkers, H.M., *Quantification of crack-healing in novel bacteria-based self-healing concrete.* Cement and Concrete Composites, 2011. 33(7): p. 763-770.

[63] Sisomphon, K., Copuroglu, O., and Fraaij, A., *Application of encapsulated lightweight aggregate impregnated with sodium monofluorophosphate as a self-healing agent in blast furnace slag mortar* HERON, 2011. 56(1): p. 13-32.

[64] Tziviloglou, E., Wiktor, V., Jonkers, H.M., and Schlangen, E., *Bacteria-based self-healing concrete to increase liquid tightness of cracks.* Construction and Building Materials, 2016. 122: p. 118-125.

[65] Sierra-Beltran, M.G., Jonkers, H.M., and Schlangen, E., *Characterization of sustainable bio-based mortar for concrete repair.* Construction and Building Materials, 2014. 67: p. 344-352.

[66] Sierra-Beltran, M.G., Jonkers, H.M., Mors, R.M., and Mera-Ortiz, W., *Field application of self-healing concrete with natural fibres as linings for irrigation canals in Ecuador*. 2015. In: 5th international conference on self-healing materials. Durham, North Carolina, USA.

[67] Şahmaran, M., Yildirim, G., Ozbay, E., Ahmed, K., and Lachemi, M., *Self-healing ability of cementitious composites: effect of addition of pre-soaked expanded perlite.* Magazine of Concrete Research, 2014. 66(8): p. 409-419.

[68] Khaliq, W. and Ehsan, M.B., *Crack healing in concrete using various bio influenced self-healing techniques.* Construction and Building Materials, 2016. 102, Part 1: p. 349-357.

[69] Paine, K., Alazhari, M., Sharma, T., Cooper, R., and Health, A., *Design and performance of bacteria-based self-healing Concrete*. 2016. In: 9th International Concrete Conference 2016. Jones, M.R., et al. Dundee.

[70] Alghamri, R., Kanellopoulos, A., and Al-Tabbaa, A., *Impregnation and encapsulation of lightweight aggregates for self-healing concrete.* Construction and Building Materials, 2016. 124: p. 910-921.

[71] Mihashi, H., Nishiwaki, T., Kaneko, Y., and Nishiyama, N., *Development of smart concretes*. 2002. In: 1st FIB congress. Osaka, Japan.

[72] Cailleux, E. and Pollet, V., *Investigations on the development of self-healing properties in protective coatings for concrete and repair mortars*. 2009. In: 2nd International Conference on Self Healing Materials. Chicago, USA.

[73] Pelletier, M., Self-healing concrete with a microencapsulated healing agent. 2011. Master Thesis, University of Rhode Island,

[74] Wang, J., Self-healing concrete by means of immobilized carbonate precipitating bacteria. 2013. PhD thesis, Ghent University,

[75] Hilloulin, B., Van Tittelboom, K., Gruyaert, E., De Belie, N., and Loukili, A., *Design of polymeric capsules for self-healing concrete.* Cement and Concrete Composites, 2015. 55: p. 298-307.

[76] Wang, J., Mignon, A., Snoeck, D., Wiktor, V., Van Vliergerghe, S., Boon, N., and De Belie, N., *Application of modified-alginate encapsulated carbonate producing bacteria in concrete: a promising strategy for crack self-healing.* Frontiers in Microbiology, 2015. 6: p. 1088.

[77] Palin, D., Wiktor, V., and Jonkers, H.M., *A bacteria-based bead for possible self-healing marine concrete applications.* Smart Materials and Structures, 2016. 25: p. 084008.

[78] Dry, C., *Matrix cracking repair and filling using active and passive modes for smart timed release of chemicals from fibers into cement matrices.* Smart Materials and Structures, 1994. 3(2): p. 118.

[79] Dry, C. and McMillan, W., *Three-part methylmethacrylate adhesive system as an internal delivery system for smart responsive concrete.* Smart Materials and Structures, 1996. 5(3): p. 297.

[80] Yang, Z., Hollar, J., He, X., and Shi, X., *A self-healing cementitious composite using oil core/silica gel shell microcapsules.* Cement and Concrete Composites, 2011. 33(4): p. 506-512.

[81] Van Tittelboom, K., Adesanya, K., Dubruel, P., Van Puyvelde, P., and De Belie, N., *Methyl methacrylate as a healing agent for self-healing cementitious materials.* Smart Materials and Structures, 2011. 20(12): p. 125016.

[82] Perez, G., Gaitero, J.J., Erkizia, E., Jimenez, I., and Guerrero, A., *Characterisation of cement pastes with innovative self-healing system based in epoxy-amine adhesive.* Cement and Concrete Composites, 2015. 60: p. 55-64.

[83] Huang, H., Ye, G., and Shui, Z., *Feasibility of self-healing in cementitious materials – By using capsules or a vascular system?* Construction and Building Materials, 2014. 63: p. 108-118.

[84] Pelletier, M., Brown, R., Shukla, A., and Bose, A., *Self-healing concrete with a microencapsulated healing agent.* 2010.

[85] Huang, H. and Ye, G., *Application of sodium silicate solution as self-healing agent in cementitious materials*. 2011. In: International Conference on Advances in Construction Materials through Science and Engineering. Hong Kong, China.

[86] Formia, A., Terranova, S., Antonaci, P., Pugno, M.N., and Tulliani, M.J., *Setup of Extruded Cementitious Hollow Tubes as Containing/Releasing Devices in Self-Healing Systems.* Materials, 2015. 8(4).

[87] Giannaros, P., Kanellopoulos, A., and Al-Tabbaa, A., *Sealing of cracks in cement using microencapsulated sodium silicate.* Smart Materials and Structures, 2016. 25(8): p. 084005.

[88] Arce, G., Hassan, M., Mohammad, L., and Rupnow, T., *Characterization of Self-Healing Processes Induced by Calcium Nitrate Microcapsules in Cement Mortar.* Journal of Materialas in Civil Engineering, 2017. 29(1).

[89] *Proceedings of the 5th International conference In self-healing materials*. In: 2015. Durham, North Carolina, USA.

[90] Benini, S., Gessa, C., and Ciurli, S., *Bacillus pasteurii urease: A heteropolymeric enzyme with a binuclear nickel active site.* Soil Biology and Biochemistry, 1996. 28: p. 819-821.

[91] Wang, J., Van Tittelboom, K., De Belie, N., and Verstraete, W., *Potential of applying bacteria to heal cracks in concrete*. 2010. In: 2nd international conference on sustainable construction materials and technologies. Ancona, Italy.

[92] Silva, F., Up-scaling the production of bacteria for self-healing concrete application. 2015. PhD thesis, Ghent University, Belgium,

[93] Silva, F., De Belie, N., Boon, N., and Verstraete, W., *Production of non-axenic ureolytic spores for self-healing concrete applications.* Construction and Building Materials, 2015. 93: p. 1034-1041.

[94] Wang, J., De Belie, N., and Verstraete, W., *Diatomaceous earth as a protective vehicle for bacteria applied for self-healing concrete.* Journal of Industrial Microbiology and Biotechnology, 2012. 39: p. 567–577.

[95] De Belie, N., Wang, J., and Soens, H., Microcapsules and concrete containing the same. 2013. UK Patent application. 1303690.0.

[96] Wang, J., Soens, H., Verstraete, W., and De Belie, N., *Self-healing concrete by use of microencapsulated bacterial spores.* Cement and concrete research 2014. 56: p. 139-152.

[97] Wang, J.Y., Snoeck, D., Van Vlierberghe, S., Verstraete, W., and De Belie, N., *Application of hydrogel encapsulated carbonate precipitating bacteria for approaching a realistic self-healing in concrete.* Construction and Building Materials, 2014. 68: p. 110-119.

[98] Jonkers, H.M., *Self Healing Concrete: A Biological Approach*. in *Self Healing Materials: An Alternative Approach to 20 Centuries of Materials*

Science, Eds. van der Zwaag, S. 2007, Springer Netherlands: Dordrecht. p. 195-204.

[99] Jonkers, H.M., Thijssen, A., Copuroglu, O., and Schlangen, E., *Application of bacteria as self-healing agent for the development of sustainable concrete*. 2008. In: 1st International BioGeoCivil Conference. Delft, The Netherlands.

[100] Stuckrath, C., Serpell, R., Valenzuela, L.M., and Lopez, M., *Quantification of chemical and biological calcium carbonate precipitation: Performance of self-healing in reinforced mortar containing chemical admixtures.* Cement and Concrete Composites, 2014. 50: p. 10-15.

[101] Xu, J. and Yao, W., *Multiscale mechanical quantification of self-healing concrete incorporating non-ureolytic bacteria-based healing agent.* Cement and Concrete Research, 2014. 64: p. 1-10.

[102] Jonkers, H.M. and Mors, R.M., *Full scale application of bacteria-based self-healing concrete for repair purposes*. 2012. In: 3rd International Conference on Concrete Repair, Rehabilitation and Retrofitting. Cape Town, South Africa.

[103] Francisconi, J., Bacteria-based self-healing mortar through embedded compressed particles 2013. MSc Thesis, University of Bologna, Italy and Delft University of Technology, The Netherlands,

[104] de Koster, S.A., Mors, R.M., Jonkers, H.M., Meesters, G.M.H., and van Ommen, J.R., *Geopolymer coating of bacteria-containing granules for use in self-healing concrete.* Procedia Engineering, 2015. 102: p. 475-484.

[105] Lawant, S.A.G., Mors, R.M., Jonkers, H.M., Meesters, G.M.H., and Nugteren, h.w., *Developing a geopolymer based coating for use in self-healing concrete. Paper presented at geopolymers – an ECI conference, 24-29 May 2015,Schloss Hernnstein, Hernnstein, Austria*. 2015. In: ECI conference. Schloss Hernnstein, Austria.

[106] Mors, R.M. and Jonkers, H.M., *Reduction of water permeation through cracks in mortar by addition of bacteria based healing agent*. 2015. In: 5th international conference on self-healing materials. Durham, North Carolina, USA.

[107] van Paassen, L.A., Daza, C.M., Staal, M., Sorokin, D.Y., van der Zon, W., and van Loosdrecht, M.C.M., *Potential soil reinforcement by biological denitrification.* Ecological Engineering, 2010. 36(2): p. 168-175.

[108] Randall, D.J. and Tsui, T.K.N., *Ammonia toxicity in fish.* Marine Pollution Bulletin, 2002. 45(1–12): p. 17-23.

[109] Hammes, F., Boon, N., de Villiers, J., Verstraete, W., and Siciliano, S.D., *Strain-Specific Ureolytic Microbial Calcium Carbonate Precipitation.* Applied and Environmental Microbiology, 2003. 69(8): p. 4901-4909.

[110] Karatas, I., Microbiological Improvement of the Physical Properties of Soil. 2008. PhD Thesis, Arizona State University, USA,

[111] Erşan, Y.Ç., Belie, N.d., and Boon, N., *Microbially induced CaCO3 precipitation through denitrification: An optimization study in minimal nutrient environment.* Biochemical Engineering Journal, 2015. 101: p. 108-118.

[112] Van Der Star, W.R.L., Taher, E., Harkes, M.P., Blauw, M., Van Loosdrecht, M.C.M., and Van Paassen, L.A., *Use of waste streams and microbes for in situ transformation of sand into sandstone*. 2009. In: International symposium on Ground Improvement Technologies and Case Histories. Singapore.

[113] Ramachandran, V.S., *Concrete Admixtures Handbook*. 2nd edition. 1996: Elsevier.

[114] Justnes, H., *Calcium nitrate as a multifunctional concrete admixture*. 1999. In: international RILEM Conference on the role of admixtures in high performance concrete. Mexico.

[115] Ersan, Y.C. and De Belie, N., *Resilient denitrifiers wink at microbial self-healing concrete.* International Journal of Environmental Engineering, 2015. 2(1): p. 28-32.

[116] Ersan, Y.C., Silva, F., Boon, N., Verstraete, W., and de Belie, N., *Screening of bacteria and concrete compatible protection materials.* Construction and Building Materials, 2015. 88: p. 196-203.

[117] Ersan, Y.C., Boon, N., and De Belie, N., *Microbial Self-Healing Concrete: Denitrification as an Enhanced and Environment-Friendly Approach*. 2015. In: 5th International Conference on Self-healing Materials. Durham, North Carolina, USA.

[118] Dry, C., Corsaw, M., and Bayer, E., *A comparison of internal self-repair with resin injection in repair of concrete.* Journal of Adhesion Science and Technology, 2003. 17(1): p. 79-89.

[119] Homma, D., Mihashi, H., and Nishiwaki, T., *Self-healing capabiliy of fibre reinforced cememntitious composites.* Journal of Advanced Concrete Technology, 2009. 7(2): p. 217-228.

[120] Kim, J.S. and Schlangen, E., *Self-healing in ECC stimulated by SAP under flexural cyclic load* 2011. In: 3rd International Conference on Self-Healing Materials. Bath, UK.

[121] Chen, H., Qian, C., and Huang, H., *Self-healing cementitious materials based on bacteria and nutrients immobilized respectively.* Construction and Building Materials, 2016. 126: p. 297-303.

[122] Joseph, C., Experimental and numerical study of the fracture and self-healing of cementitious materials. 2008. PhD Thesis, Cardiff University, UK,

[123] Tsangouri, E., Van Tittelboom, K., Hillewaere, X.K.D., Van Hemelrijck, D., De Belie, N., and Du Prez, F.E., *Investigation of the fracture cracking behavior of self-healing systems by use of optical and acoustic experimental methods*. 2013. In: 4th International Conference on Self-Healing Materials. De Belie, N., et al. Ghent, Belgium.

[124] Palin, D., Wiktor, V., and Jonkers, H.M., *Autogenous healing of marine exposed concrete: Characterization and quantification through visual crack closure.* Cement and Concrete Research, 2015. 73: p. 17-24.

[125] Li, V.C. and Herbert, N., *Robust Self-Healing Concrete for Sustainable Infrastructure.* Journal of advanced concrete technology, 2012. 10: p. 207-218.

[126] Wang, J., Dewanckele, J., Cnudde, V., Van Vlierberghe, S., Verstraete, W., and De Belie, N., *X-ray computed tomography proof of bacterial-based self-healing in concrete.* Cement and Concrete Composites, 2014. 53: p. 289-304.

[127] Huang, H., Ye, G., and Damidot, D., *Characterization and quantification of self-healing behaviors of microcracks due to further hydration in cement paste.* Cement and Concrete Research, 2013. 52: p. 71-81.

[128] Mors, R.M. and Jonkers, H.M., *Feasibility of lactate derivative based agent as additive for concrete for regain of crack water tightness by bacterial metabolism.* Industrial Crops and Products.

[129] In, C.-W., Holland, R.B., Kim, J.-Y., Kurtis, K.E., Kahn, L.F., and Jacobs, L.J., *Monitoring and evaluation of self-healing in concrete using diffuse ultrasound.* NDT & E International, 2013. 57: p. 36-44.

[130] Malm, F. and Grosse, C.U., *Efficiency of self-healing agents for cementitious materials characterized by NDT*. 2016. In: 19th World Conference on Non-Destructive Testing. Munich, Germany.

[131] Gruyaert, E., Feiteira, J., Nele De, B., Malm, F., Nahm, M., Grosse, C.U., and Tziviloglou, E., *Non-destructive testing techniques to evaluate the healing efficiency of self-healing concrete at lab-scale*. 2016. In: Emerging Technologies in Non-Destructive Testing VI. Aggelis, D.G., et al. Leiden, The Netherlands.

[132] Granger, S., Loukili, A., Pijaudier-Cabot, G., and Chanvillard, G., *Experimental characterization of the self-healing of cracks in an ultra high performance cementitious material: Mechanical tests and acoustic emission analysis.* Cement and Concrete Research, 2007. 37(4): p. 519-527.

[133] Feiteira, J., Tsangouri, E., Gruyaert, E., Lors, C., Louis, G., and De Belie, N., *Monitoring crack movement in polymer-based self-healing concrete through digital image correlation, acoustic emission analysis and SEM in-situ loading.* Materials & Design, 2017. 115: p. 238-246.

[134] Van Tittelboom, K., De Belie, N., Lehmann, F., and Grosse, C.U., *Acoustic emission analysis for the quantification of autonomous crack healing in concrete.* Construction and Building Materials, 2012. 28(1): p. 333-341.

[135] Yildirim, G., Aras, G.H., Banyhussan, Q.S., Şahmaran, M., and Lachemi, M., *Estimating the self-healing capability of cementitious composites through non-destructive electrical-based monitoring.* NDT & E International, 2015. 76: p. 26-37.

3

Development of biogenic healing agent

Biogenic self-healing cementitious materials target on the closure of micro-cracks with precipitated inorganic minerals originating from bacterial metabolic activity. Dormant bacterial spores and organic mineral precursor compounds constitute the biogenic healing agent used in this research. The current chapter focuses on the investigation of the most appropriate organic carbon source to be used as component of the biogenic healing agent. The selection is made among three different organic compounds, namely, calcium lactate, calcium acetate and sodium gluconate. The experimental methodology was based on continuous and non-continuous oxygen consumption measurements of washed bacterial cultures and on compressive strength tests on mortar cubes. The investigation revealed a preference for calcium lactate and acetate, but an indifferent behaviour for sodium gluconate. In addition, the compressive strength on mortar cubes with different amounts of either calcium lactate or acetate was not or it was positively affected when the organic compounds were dissolved in the mixing water.

Previous studies on the specific biogenic healing agent indicated that encapsulation was needed to maintain the functionality of the system when embedded in the cementitious matrix. Porous expanded clay particles were used as carriers of the healing agent. The absorption capacity and the total porosity of the lightweight aggregates was investigated through water absorption and Mercury Intrusion Porosimetry tests. The inclusion of the healing agent in the porous aggregates was also studied. Finally, the functionality of the aggregates-healing agent system in presence of water and in relatively high pH conditions was also examined via monitoring of oxygen concentration.

Parts of this chapter have been published: a. in the journal paper entitled "Selection of nutrient used in biogenic healing agent for cementitious materials", in the Frontiers in Materials, 2017 [1] and b. in the conference paper "Preparation and optimization of bio-based and light weight aggregate-based healing agent for application in concrete", in ICSHM 2015, held in Durham, NC, USA [2].

3.1 INTRODUCTION

The technology of biogenic self-healing cementitious materials targets on the closure of micro-cracks through bacterial metabolic activity. In case that the bacteria included in the healing agent follow the metabolic pathway of oxidation of organic carbon, the precipitates that are formed in the crack are products of a biochemical reaction between organic carbon (often calcium-based) and oxygen, where bacteria act as catalysts.

During microbially induced calcium carbonate precipitation, organisms are able to secrete one or more metabolic products (CO_3^{2-}) that react with ions (Ca^{2+}) in the environment resulting in the subsequent precipitation of minerals [3]. Although there are several bacterial species that are known to produce $CaCO_3$ not all of them can be functional in the high alkaline cementitious environment. Jonkers et al. [4] incorporated spores from *Bacillus cohnii*, calcium lactate (CaL) and yeast extract (YE) in concrete. CaL is the organic carbon source, which acts as nutrient for the bacteria, while YE helps the bacterial spores to germinate and grow. CaL was selected as bacterial nutrient, since it did not affect significantly the compressive strength of the concrete. The compounds of the healing agent were added directly in the mixture. In the same study, they observed loss of viability of the bacterial spores embedded in the concrete matrix. The fact was attributed to the continuous reduction of the matrix pore sizes. The larger pores diameters present in 3-days- and 7-days-old concrete tend to wane in the older concrete (28-days-old). Therefore, the spores, whose diameter ranges between 0.8-1.0 μm, contained initially in the larger pores become crushed as the cement hydration proceeded. To overcome this problem, they suggested that the spores should be encapsulated. In a later study [5], and while the spores were encapsulated together with their nutrients in lightweight aggregates (LWA), it was proven that bacterial spore viability increased from two to more than six months. In addition, the results of the crack permeability tests revealed that the specimens with the biogenic healing agent showed 100% crack sealing after healing treatment, while the reference specimens recovered only 33% of the lost water-tightness.

Later, Wiktor and Jonkers [6] examined the same self-healing system with *Bacillus alkalinitrilicus*. The LWA were impregnated twice under vacuum with a CaL - (80 g/l), and YE- (1 g/l) solution, followed by another impregnation with the bacterial spore suspension. After each impregnation treatment, the LWA were dried at 37 °C until a constant weight was succeeded. The study monitored the crack closure through optical microscopy and evaluated the crack width changes. They found that after 40 days of water submersion the maximum healable crack width (460 μm) was more than doubled for the biogenic specimens. Furthermore, the oxygen consumption profiles supported that the increased mineral

precipitation found in the biogenic specimens was due to the bacterial metabolic activity.

The preliminary results obtained by both studies [5, 6] revealed the great potential in applying the biogenic healing agent for self-healing concrete. However, several aspects such as the possibilities to use another organic compound as bacterial nutrient and the to increase the amount of healing agent in the LWA needed to be carefully considered in the further research. As a following up study, the current chapter focuses on the investigation of:

- the most appropriate organic carbon source to be used as component of the healing agent,
- the absorption capacity of the LWA,
- the most appropriate available method to incorporate the healing agent into the LWA and
- the functionality of the biogenic healing agent system (bacteria spores, nutrients and LWA).

In this chapter, bacterial spores obtained from three different isolates from the genus *Bacillus* are packed in concrete together with YE and a calcium-based organic carbon source, all embedded in LWA. The oxidation of the organic carbon source produces carbon dioxide (CO_2) and $CaCO_3$ as presented in Equations 3.1, 3.2 and 3.3 for the case of calcium lactate ($CaC_6H_{10}O_6$) [6] calcium acetate ($CaC_4H_6O_4$) and sodium gluconate ($NaC_6H_{11}O_7$) respectively.

$$\boldsymbol{CaC_6H_{10}O_6 + 6\,O_2 \rightarrow CaCO_3 + 5\,CO_2 + 5\,H_2O} \quad (3.6)$$

$$\boldsymbol{CaC_4H_6O_4 + 4\,O_2 \rightarrow CaCO_3 + 3\,CO_2 + 3\,H_2O} \quad (3.7)$$

$$\boldsymbol{NaC_6H_{11}O_7 + 5.5\,O_2 \rightarrow 0.5\,Na_2CO_3 + 5.5\,CO_2 + 5.5\,H_2O} \quad (3.8)$$

The reason to investigate the possibility to use another organic nutrient stems from the fact that CaL has rather low solubility in water (3,4 - 6,0 g/100 g) at 20 °C [7] compared to other organic compounds that can be also used as bacterial nutrient in the biogenic healing agent. Calcium acetate (CaA) and sodium gluconate (NaG) were chosen to be tested because they are also suitable nutrient sources for the applied bacterial strains, economical and commercially available in bulk amounts. In addition, these organic compounds have a water solubility of 34,7 g/100 g [8] and 57,4 g/100 g [9] respectively.

The experimental methodology that was used for the nutrient selection process was based on continuous and non-continuous oxygen consumption measurements and compressive strength tests on mortar cubes. In addition, for the

characterization of the LWA, physical properties of the LWA such as absorption capacity and porosity were also investigated. Finally, the functionality of the healing agent system was examined through continuous oxygen consumption measurements to confirm the ability of the healing agent to activate when in favourable environmental conditions.

3.2 MATERIALS AND METHODS

3.2.1 SELECTION OF NUTRIENT FOR BACTERIA

Preparation of bacterial cultures

Three alkali-resistant bacterial isolates related to the genus *Bacillus* were previously obtained from enrichment cultures inoculated with sediment derived from the alkaline natural lakes Playa (Aragon, Spain), Kulunda (Siberia, Russia), and Wadi Natrun (Egypt) and tentatively named Iso-01, Iso-06 and Iso-10 respectively. Phylogenetic analysis based on partial 16S rRNA gene sequence analysis revealed that isolate Iso-01 was most closely related to the scientifically described alkaliphilic species *Bacillus cohnii* (>99% sequence homology), and isolates Iso-06 and Iso-10 to *Bacillus alkalinitrilicus* (both > 98% sequence homology).

Isolates are routinely cultured in alkaline medium with the following composition per litre of demineralized water: 0.375g KNO_3, 0.2g NH_4Cl, 0,02g KH_2PO_4, 0.225g $CaCl_2.2H_2O$, 0.2g KCl, 0.2g $MgCl_2.6H_2O$, sodium sesqui carbonate/bicarbonate buffer (0.42g $NaHCO_3$ and 0.53g Na_2CO_3), 1g YE, 1ml trace element solution SL-12B and an additional organic carbon source (either lactate 1g/L, acetate 0.8g/L, or gluconate 2g/L). The pH of the medium was 9.8. The cultivation was done aerobically by incubation of cultures in cotton wool stoppered Erlenmeyer flasks on a shaking table at 150 rpm.

For experimental assays (oxygen consumption measurements) cultures were pre-grown as described above followed by centrifugation and resuspension of the cell pellet in 0.1M sesqui buffer amended with one of the specific substrates under investigation (CaL, CaA and NaG) at a final concentration of 0.1M.

Continuous oxygen consumption measurements

Almost an hour after the preparation of the washed bacterial suspensions, oxygen consumption measurements took place in order to evaluate the preference of each isolate to a certain organic compound. The measurements were conducted in transparent glass flasks, which contained a sensor spot (SP-PSt3, PreSens - Precision Sensing GmbH) glued on the inner part of their wall, as it is depicted in Figure 3.1.

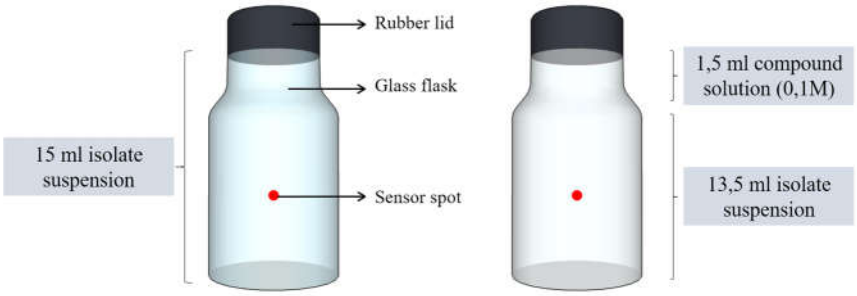

Figure 3.1 Glass flasks with oxygen sensor spots attached to the inner wall of the flasks.

The volume capacity of the flasks was 15 ml. The flasks were either filled only with the cell suspension (Iso-01, Iso-06 or Iso-10) or with 13,5 ml cell suspension and 1,5 ml compound solution (CaL, CaA or NaG) of 0,1 M. The oxygen concentration (in µM) inside the sealed flask was measured with a battery powered Fibox 4 oxygen meter (PreSens - Precision Sensing GmbH). A polymer optical fibre (POF) connected to the oxygen meter was used to transfer excitation light to the sensor and the sensor response back to the meter. The POF enabled non-invasive and non-destructive measurements to be made in the sealed flask from outside through its transparent wall. Frequent measurements were taken every 5 minutes. Each experiment lasted approximately from 30 until 100 minutes, depending on the oxygen consumption rate of each isolate. A typical graph obtained after the completion of the test is presented in Figure 3.2. From the graph, it was possible to calculate the slope of each curve in µM/min as shown in Figure 3.2. The slope of each curve (oxygen consumption rate, κ) was the base of comparison for this set of experiments.

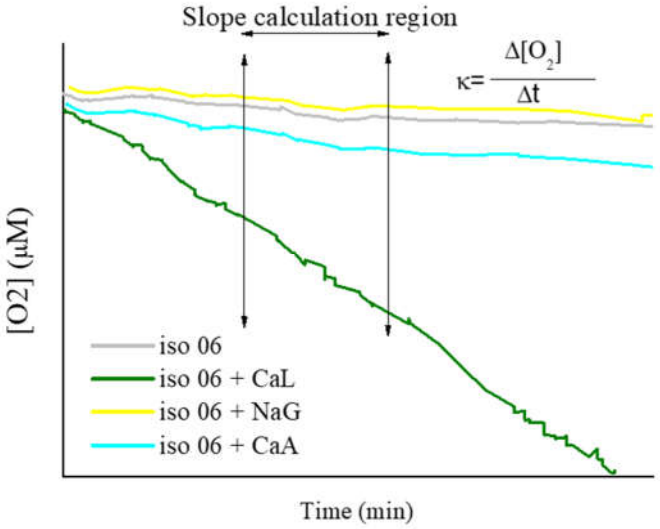

Figure 3.2. Typical graph obtained by the oxygen consumption assay. Four different curves are presented; the curve of autogenous respiration of vegetative cells (Iso-06), the curve of vegetative cells respiring in CaL- (Iso-06 + CaL), the curve of vegetative cells respiring in CaA- (Iso-06 + CaA) and the curve of vegetative cells respiring in NaG solution (Iso-06 + NaG).

Biolog test

Isolates Iso-01, Iso-06 and Iso-10 were prior to further experimental testing characterized with respect to aerobically metabolizable substrates. Therefore commercial 96-wells Biolog plates were used, which feature a specific organic compound in each of 95 wells leaving the last well as blank. Each of the 0.2 ml volume wells were filled with 0.18 ml washed cell suspension and incubated aseptically at room temperature (20 ±2 °C). After 48 hours of incubation, the oxygen concentration in each of the wells was measured by inserting an oxygen micro-sensor (Fibre optic oxygen sensor, PreSens - Precision Sensing GmbH) halfway into the liquid. Decrease of oxygen concentration relative to the control well (not containing any organic substrate) was indicative for the metabolizability of the specific organic substrate by the specific isolate.

Compressive strength tests on mortar cubes

The healing agent (bacteria spores, organic compound and YE) under investigation is loaded into LWA (Liapor 1/4 mm, Liapor GmbH Germany) followed by mixing with the fresh mortar paste. For the loading procedure of LWA, the healing agent compounds were dissolved in water and then via impregnation under vacuum the healing agent was incorporated into the LWA. Following the impregnation, the LWA were dried for approximately for 5–6 days

in the laboratory, until a constant weight was obtained. After drying, it was conservatively estimated, by weighing the bulk LWA amount, that the initial dry weight of the LWA approximated increased by 10%. It was, therefore, needed to examine how the compressive strength would be affected by a possible leakage of the healing agent (from the LWA into the matrix) during mixing and setting of the mortar. As a result, compressive strength tests on mortar cubes (40 mm x 40 mm x 40 mm) were conducted according to EN 1015-11 at the age of 28 days. The mixture composition of the examined mortar cubes is presented in Table 1. Five different amounts of two compounds (CaL and CaA) were tested; 0%, 0.56%, 1.12%, 1.68% and 2.24% per cement weight. The examined percentages were representing the amount of healing agent that could possibly leak in the mortar matrix; 0%, 10%, 20%, 30% and 40% respectively. An example of the calculation of those percentages is presented below.

- The amount of the (unloaded) LWA added in the mortar mixture is 257 g.
- The amount of cement added in the mortar mixture is 463 g.
- The LWA increase their dry weight by 10% after the impregnation. Therefore, the healing agent embedded is 25.7 g (total weight of loaded LWA is 257 g + 25.7 g ≈ 283 g).
- The 10% of the incorporated healing agent that might leak in the mortar matrix will be then 2.57 g and consequently 2.57 g / 463 g = 0.56% per cement weight.

The organic compound was dissolved in the mixing water. The mixing and casting of the mortars which contained CaL took place on a different period from the mortars with CaA. Therefore, the environmental conditions differed, as well as, the materials that were used for the casting (cement and aggregates) originated from different batches. Consequently, it was decided that the reference mixture (with 0% organic compound) was needed to be cast twice in order to have an objective comparison. Five cubic specimens per mixture were tested.

The mix design of the examined mixtures is presented in Table 3.1.

Table 3.1 Mix design of the mortars.

Compound	Amount (kg/m^3)
CEM I	463
Water	231.5
Sand 0.125/1 mm	855
Liapor	257

3.2.2 WATER ABSORPTION AND MERCURY INTRUSION POROSIMETRY TESTS

As stated above, the LWA were used as capsules for the biogenic healing agent. The LWA that were used for the research were the expanded clay particles. According to the manufacturer, the particles have a spherical shape and are created by burning the raw clay at a temperature of about 1,200 °C in a rotary kiln. During the burning process the organic substances found in the clay combust as well. The spheres expand and ceramic Liapor expanded clay particles with very fine pores come into existence [10]. A typical image from the outer and the inner surface of a Liapor particle is shown in Figure 3.3a. It can be seen from the ESEM picture shown in Figure 3.3b that the pores have either a spherical or an irregular shape, that they have varying sizes and that some are isolated, while others are interconnected.

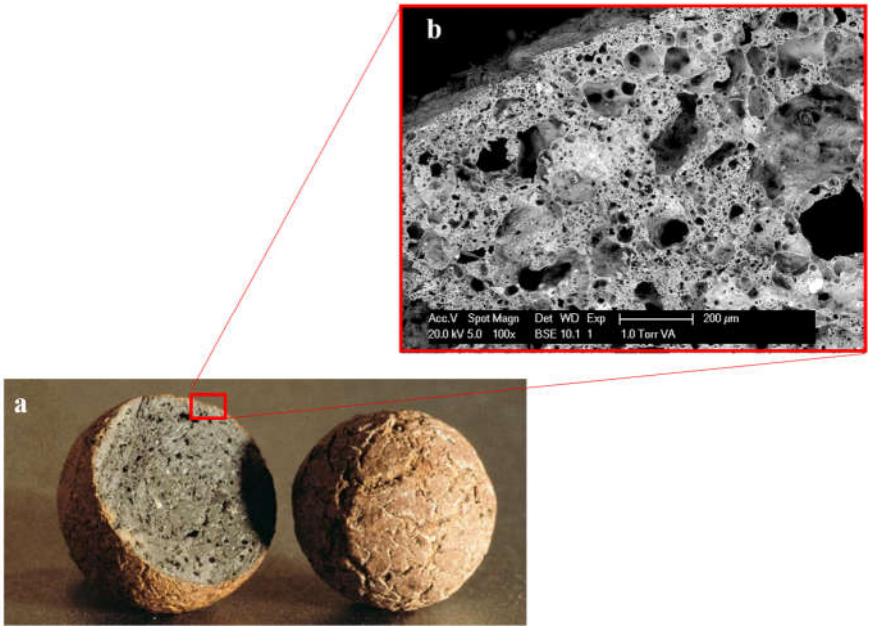

Figure 3.3 a. Outer and inner surface of a Liapor particle [11], b. ESEM picture from the inner surface of a Liapor particle.

Water absorption measurements were conducted on LWA. Before performing the test, the LWA were oven dried at 105 °C for 24 h to exclude any moisture that could be found in their mass. After drying, the LWA were divided in parts of 100 g and they were put in aluminium containers. 500 g of tap water was added in each container. After a certain time interval (5 min, 30 min, 1 hour, 2 hours, etc.), the water was removed from the container and the mass of the soaked aggregates was measured. In addition, the water intake of the LWA when subjected to vacuum treatment was also measured to compare the efficiency of the two methods. For this method, 100 g of oven dried LWA were put in a chamber and were vacuumed for 1 hour to remove the air contained in their pores. Then, water was slowly inserted in the chamber. After the release of the vacuum, the excessive water was removed and the mass of the impregnated LWA was measured.

Mercury intrusion porosimetry (MIP) measurements were conducted on three samples of LWA to investigate the total porosity and therefore the total volume that could accommodate the healing agent. The MIP tests were conducted with a Micrometrics PoreSizer 9320. Before the MIP test, the specimens were dried in a ventilated oven at 105 °C until a constant weight was obtained. During MIP test, the sample was placed into a chamber. First, the air was removed from the chamber and then mercury was introduced. As the pressure on the mercury increased (gradually), the mercury was forced from the surface of the sample into the pores.

By tracking pressures and intrusion volumes, it was possible to get a measure of the connecting pore necks of a continuous system or a breakthrough pressure in a discontinuous system [12]. MIP has been widely used in porous materials, whose pore sizes range over several orders of unit [13]. The technique is conceptually and experimentally simple, however, it might give moderately inaccurate results for mostly two reasons:

- The method assumes that all the pores have a cylindrical shape and
- The presence of ink-bottle pores designated by the trapped mercury in the pores during the extrusion phase (Figure 3.4).

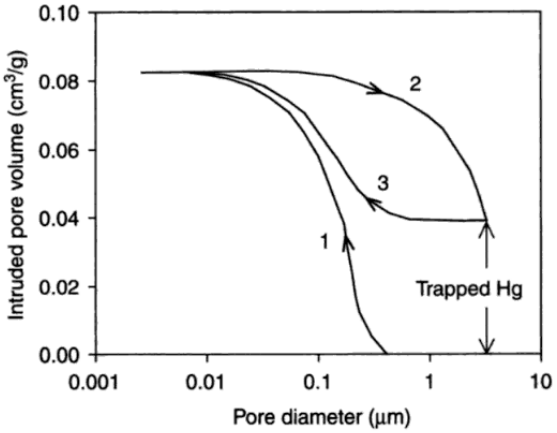

Figure 3.4 Intrusion-extrusion hysteresis and entrapment of mercury in a cement paste specimen. The arrows indicate the directions of intrusion (curve 1), extrusion (curve 2) , and re-intrusion (curve 3). [13].

3.2.3 INCORPORATION OF THE HEALING AGENT IN THE LWA AND FUNCTIONALITY OF THE SYSTEM

The LWA were impregnated with a solution containing the nutrients and the bacterial spores. For the optimization procedure two variables were considered; the impregnation technique and the drying temperature. The weight of the bulk amount of LWA was measured before and immediately after impregnation to determine the most efficient impregnation technique. The different drying temperatures that are presented in Table 3.2 concern only the samples that were treated with the most efficient impregnation technique. Unlike the procedure that was followed in 2.3.1 for measuring the increase in weight after impregnation and drying, which was conducted on the bulk amount of LWA, this investigation was performed on lightweight particles separately. In fact, the increase in weight was measured in a sample of 40 LWA (20 before and 20 after impregnation). The experiment was held as follows:

- The diameter and the weight of 20 empty LWA was measured before the impregnation procedure.
- After drying, 20 impregnated LWA having the same diameters as the empty LWA used before, were weighted.
- The difference in weight was calculated for each LWA and finally an average value was obtained.

Table 3.2 Healing agent incorporation approach.

Variable	Method
Impregnation technique	Without vacuum application (30 min soaking)
	Vacuum application
Drying temperature	Drying at 36 °C (for 72 h)
	Drying at 20 °C (for 72 h)
	Drying at 4 °C (for 24 h) and then at 20 °C (for 48 h)

After completing the procedures of impregnation and of drying, the LWA samples with the highest mass gain were further investigated. Continuous oxygen consumption measurements on loaded LWA submerged in carbonate-bicarbonate buffer (0.1 M, pH=10.5) were used to evaluate the effectiveness of the healing agent system. The tests were conducted in sealed glass flasks, as described in section 3.2.1. To confirm that the potential oxygen consumption is originating only from bacterial activity four different samples were tested:

- unloaded,
- loaded only with the selected organic compound
- loaded with organic compound and YE and
- loaded with the biogenic healing agent (bacterial spores plus organic compound plus YE).

After the completion of the oxygen consumption test, the precipitates found on the bottom of the flasks containing the biogenic healing agent were observed by Environmental Scanning Electron Microscope (ESEM, Philips XL30 Series) equipped with Energy Dispersive X-ray spectrometer (EDS).

3.3 RESULTS

3.3.1 EXPERIMENTAL RESULTS ON BACTERIAL NUTRIENT SELECTION

The continuous oxygen consumption test results from the respiration of vegetative cells pre-grown in the three media are presented in Figure 3.5. The graphs show the relative respiration rate (r) for each bacterial isolate respiring in the three different organic compound solutions after pre-growing in one of them. The calculation formula of r is shown in Equation 3.4. Where κ_a is the slope of the autogenous respiration curve (no organic compound in the flask) and κ_c is the slope of the curve from the respiration on a certain compound.

$$\boldsymbol{r = \frac{\kappa_c - \kappa_a}{\kappa_a} \times 100\%} \quad (3.4)$$

Isolates pre-grown on Lactate

The isolates pre-grown on lactate showed a definite preference in respiring on the same compound. Iso-06 exhibits a remarkable preference for CaL, almost 8 times more than the autogenous respiration. Iso-01 and Iso-10 also increased their autogenous respiration rate, however, considerably less than Iso-06. When CaA was used as nutrient for the vegetative cells, the respiration rates showed a rather limited increase. Iso-06 showed a bias for respiring in NaG, but the other two isolates did not. Respiration rates on NaG were noticeably lower for all three isolates. Slightly low negative relative respiration rates were observed for Iso-01 and Iso-06 respiring on CaA and NaG respectively. This phenomenon can be attributed to the "dilution" of the cell suspension. In fact, the density of the cell suspensions decreased when the solution with the organic compound was added, since the flasks contained of 13,5 ml instead 15 ml of cell suspension. This means that the oxygen consumption did not actually slow down, but it was the decreased number of cells in the flask that caused this effect.

Isolates pre-grown on Acetate

Iso-06 pre-grown on acetate, exhibited also a very significant increase in oxygen consumption rate for respiring on CaL. In addition, Iso-06 and Iso-10 pre-grown on acetate, increased their consumption rate (almost 4-5 times), when respiring on CaA. On the other hand, the respiration of Iso-01 pre-grown on acetate seemed unaffected regardless of the organic compound that was added. Furthermore, the presence of NaG in the flask did not influence the autogenous respiration of any of the isolates.

Isolates pre-grown on Gluconate

Iso-10 pre-grown on gluconate, was the only cell suspension that exhibited positive relative respiration values for respiring on CaL or on CaA. The other combinations of isolates and organic media showed negative relative respiration

rate values. In some cases, for example Iso-01 respiring on CaL or on CaA, the negative values exceeded the limit (approximately 20-30% lower than autogenous respiration) where it can be attributed to the dilution of the cell suspension.

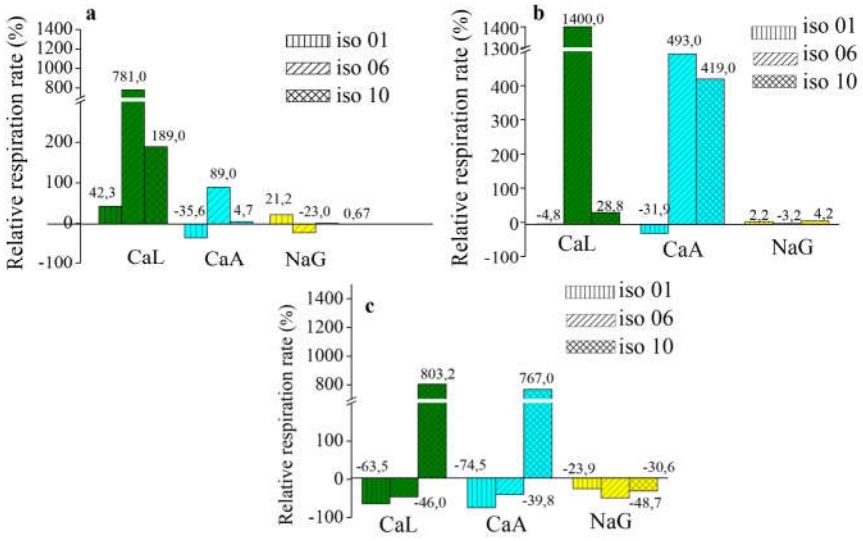

Figure 3.5. Relative respiration rate of vegetative cells pre-grown on: a. lactate, b. acetate and c. gluconate.

Biolog test results

The Biolog test follows essentially the same principle as the oxygen consumption test, since they both rely on oxygen reduction, due to respiration of vegetative cells. However, the duration of the tests and the way of monitoring the oxygen reduction are different. The results obtained by the Biolog test are shown in Figure 3.6. The y-axis of the graph indicates the air saturation in the control well at 48 hours. The results show that all three isolates show a preference for CaA, while they appear to be able to degrade CaL and NaG, but in a less efficient way. Iso-06 was the only isolate which was able to consume almost all oxygen within the incubation period when exposed to CaL and CaA.

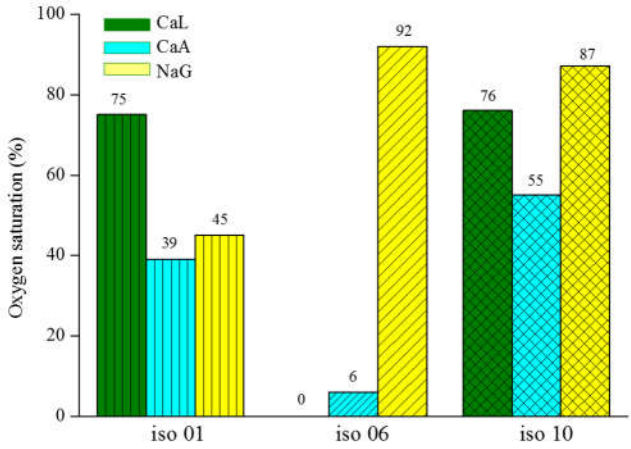

Figure 3.6. Oxygen saturation level of the three different bacteria isolates respiring on CaL, CaA or NaG.

Compressive strength results of mortar cubes

After considering the response of the three isolates respiring on the three different organic compounds in both continuous oxygen consumption- and the Biolog assay, it was decided that only two of them, namely CaL and CaA, would be tested for their effect on compressive strength development of mortar. The values presented in Figure 3.7 show the average (out of five cubic specimens) compressive strength of each mixture as well as the deviation from the reference mixture. The results revealed that in general the addition of the two organic compounds in the mixing water of mortar either increased or did not affect the compressive strength at the amounts that were tested. Mixtures with dissolved CaL and CaA in the mixing water showed the same trend in the development of strength in relation to the varying amounts of the organics. Specifically, for mixtures with dissolved CaL the compressive strength ranged from -1.46% to 7.98% compared to the reference mixture, while for CaA the increase varied from 0.12% to 13.43%. Although both organic compounds showed a relatively similar response when added in the mixing water of the mortar, it was decided that the research will be continued with CaL, as bacterial nutrient.

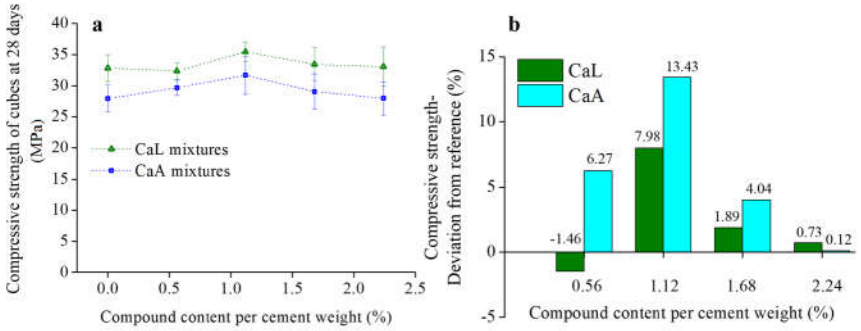

Figure 3.7. a. Compressive strength and b. Deviation of the compressive strength from the reference of mixtures containing different amounts of CaL and CaA.

3.3.2 EXPERIMENTAL RESULTS ON ABSORPTION CAPACITY AND POROSITY OF LWA

The water absorption of LWA was measured from 15 minutes until 5 days after immersion. The results (Figure 3.8) showed that the weight of wet LWA increased by 15% after 5 minutes, 18.7% after 30 minutes and continued in almost linearly until 48 hours where it reached an increase of 29.1%. From 48 hours and on, the weight increased with a rather slower rate and reached 31% after 5 days of immersion. Moreover, the water intake after vacuum treatment increased by 72.6% compared to the initial dry weight of Liapor particles.

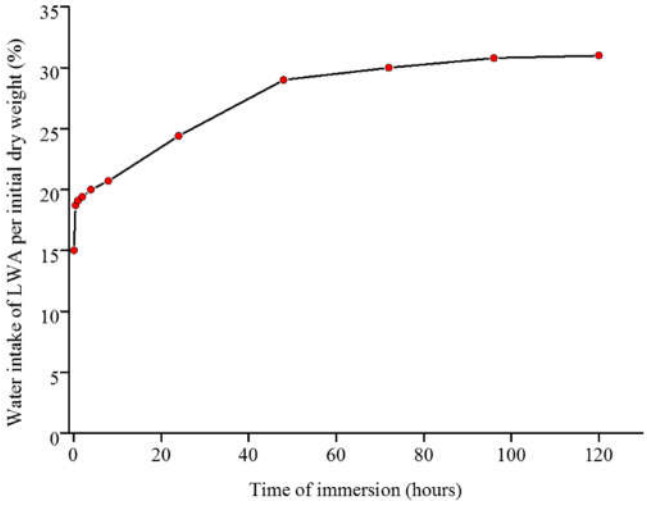

Figure 3.8 Percent water intake by initial dry weight of Liapor particles.

The MIP tests revealed that the average porosity of the Liapor particles occupied 59.7 ± 1.5% of their total volume (Figure 3.9a). However, as can be seen from

Figure 3.9a, during extrusion the mercury retention in the pores of the LWA was massive (almost 100%) what can be translated into a very pronounced ink-bottle-shaped pores effect. Figure 3.9b presents the differential intrusion plots of the tested LWA samples. Differential intrusion plots are frequently used in MIP to present, in a more straightforward way than the porosity curves, the pore size distribution of the specimens. Figure 3.9b shows that there are numerous diameter peaks for pore diameters ranging from approximately 0.15 μm until 6.5 μm. These peaks represent the pore diameters corresponding to the highest rate of mercury intrusion per change in pressure [14]. It could be therefore claimed that the most amount of the mercury volume was intruded when the pressure corresponded to pore diameters between 0.15 μm and 6.5 μm. Usually, if there is only one distinct peak, it can be concluded that the corresponding diameter is the most frequent one met among the pores of the material. Yet, the multiple peaks in the differential intrusion curve indicate random micro-cracking caused [14], due to the forced mercury in the mass of the particles.

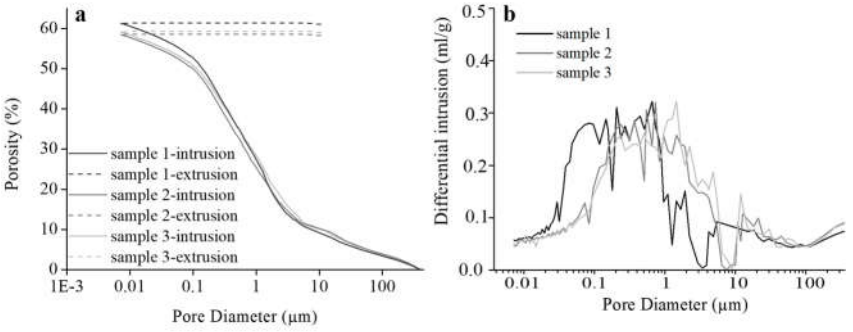

Figure 3.9 a. Cumulative intrusion (and extrusion) indicating the total porosity of the Liapor particles and the cumulative pore size distribution and b. Differential pore size distribution curves of Liapor particles.

3.3.3 EXPERIMENTAL RESULTS ON HEALING AGENT IMPREGNATION METHODS AND FUNCTIONALITY OF THE SYSTEM

Weight measurements on wet LWA after impregnation of the healing agent with and without vacuum application revealed that the use of vacuum increases substantially the incorporated amount of healing agent, as was already derived from the water absorption measurements. Therefore, different drying temperatures were applied to the samples that were vacuum treated. An overview of the average weight increase results can be found in Table 3.3. The healing agent solution, prepared at 80°C contained: CaL- (200 g/L, prepared), YE- (4 g/L) and bacteria spores (10^8 spores/L).

Table 3.3 Weight increase of LWA subjected to different impregnation and drying methods.

Variable	Method	Sample	Weight increase per initial dry weight (%)
Impregnation type	Without vacuum application	NV	4.6 [1]
	Vacuum application	V	17.6 [1]
Drying temperature	Drying at 36°C (for 72 h)	$V_{36\,°C}$	8.6
	Drying at 20°C (for 72 h)	$V_{20\,°C}$	11.3
	Drying at 4°C (for 24h) and then at 20°C (for 48 h)	$V_{4\,°C}$	12.2

The results obtained by the different drying temperatures were also supported by stereo-microscopic pictures. Figure 3.10 shows three typical broken-in-two Liapor particles that have been dried at different temperatures. From the observations, it was revealed that the most efficient drying method is the one with the intermediate cooling phase ($V_{4\,°C}$). A possible explanation could be that during cooling, the solubility of CaL and YE dropped, leading in separation of the water and the healing agent compounds resulting in the maximum amount of the nutrients left inside the pores of the particles after evaporation of the water. In contrary, during drying at 36 °C, the solubility of nutrients was still high. Consequently, the evaporating solution carried away on the outer surface of the LWA some of the nutrients. Thus, less healing agent remained in the pores of the LWA.

[1] Estimated values of dry healing agent contained in wet LWA (calculated from weight measurements on wet LWA).

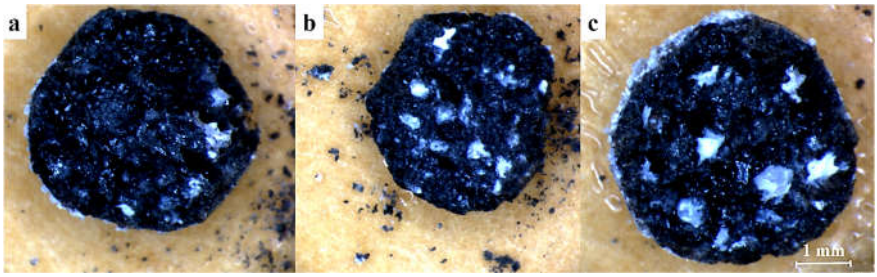

Figure 3.10 Broken-in-two Liapor particles subjected to different drying temperatures: a. Drying at 36 °C (for 72 h), b Drying at 20 °C (for 72 h) and c. Drying at 4 °C (for 24h) and then at 20 °C (for 48 h).

Nevertheless, the drying of the LWA at 20 °C was selected for the experiments that followed. The reason for this selection was in the simplicity of this procedure, which involves only one step, it requires less use of energy and finally its results did not differ substantially from the results of the most efficient drying method. Figure 3.11 shows two ESEM pictures of LWA impregnated with the biogenic healing agent and then dried at 20 °C. In the picture the pores which are filled with the healing agent are easily recognisable particularly due to the wool-shaped CaL formations.

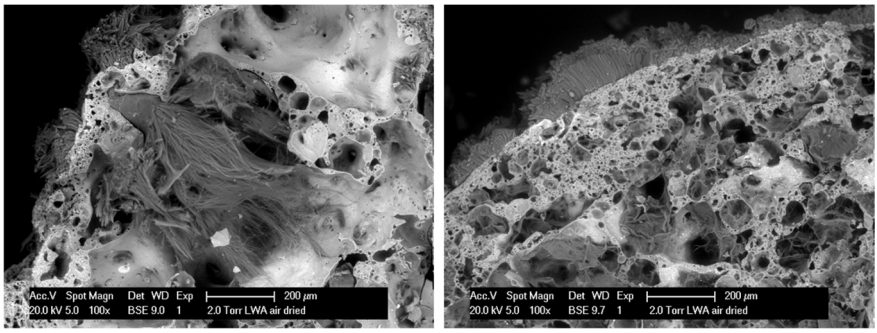

Figure 3.11 Inner surface and pores of LWA, which were impregnated with the biogenic healing agent and dried at 20 °C.

Oxygen concentration measurements (Figure 3.12) on unloaded and loaded Liapor particles indicated that only the samples containing the nutrients and the bacterial spores showed reduction in oxygen concentration, while the other samples exhibited a constant oxygen concentration profile. This reduction can be translated to bacterial activity. The results imply that the oxygen consumption originated only from the activated bacteria that were embedded in the LWA. Thus, the healing agent can be functional in relatively high pH conditions (pH =10.5), as it was designed for.

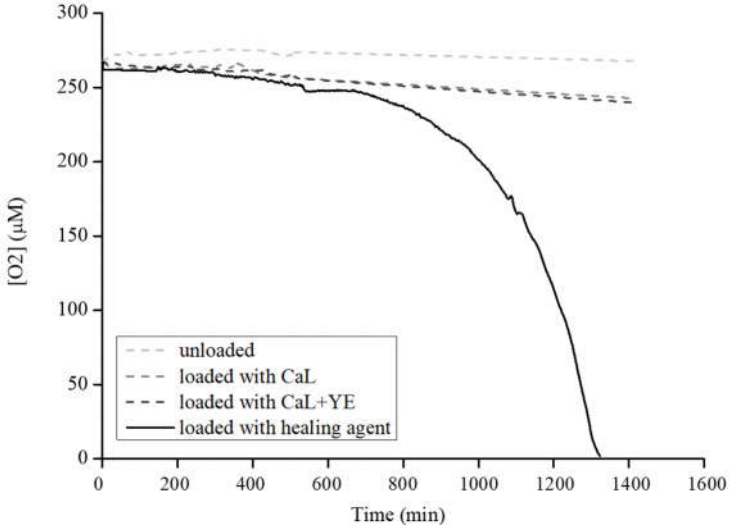

Figure 3.12 Oxygen consumption on: unloaded LWA, loaded with CaL, loaded with CaL+YE and loaded with healing agent.

The ESEM observations on the precipitates found on the bottom of the flasks containing the biogenic healing agent revealed that the crystals created during the experiment had the typical cubical shape of calcite, as it can be seen in Figure 3.13. The EDS (Figure 3.14) analysis on the abovementioned crystalline formations indicated high peaks of Ca, C and O, which suggested that precipitates were indeed $CaCO_3$ based.

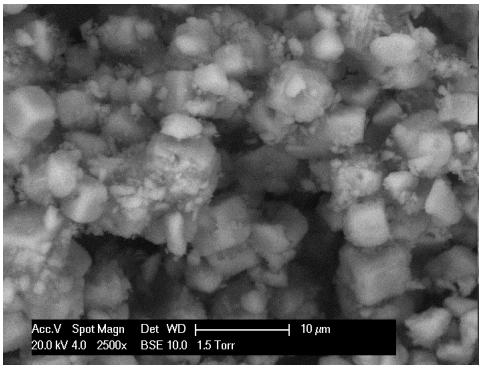

Figure 3.13 ESEM images from precipitates found on the bottom of the flasks which contained the LWA-based biogenic healing agent and carbonate-bicarbonate buffer solution.

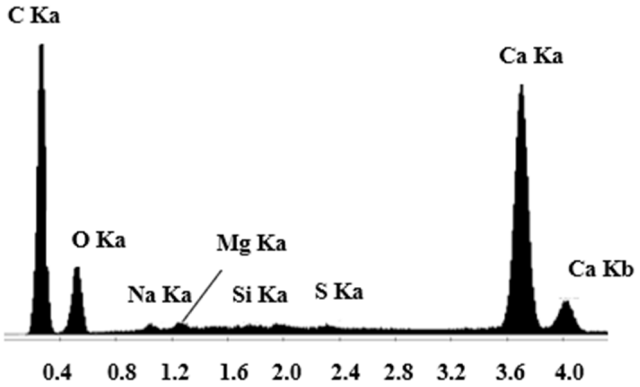

Figure 3.14 Indicative EDS results from precipitates found on the bottom of the flasks containing the LWA-based biogenic healing agent and carbonate-bicarbonate buffer solution.

3.4 DISCUSSION

The results of the continuous oxygen measurements on washed bacterial cultures showed that the vegetative cells have a preference to respire on lactate when pre-grown on it. The same holds for acetate, but only for two out of the three studied isolates (Iso-06 and Iso-10). Due to this fact, it can be assumed that the cells develop a sort of memory, probably by induction of specific metabolic enzymes, when pre-grown on a certain substrate, which allows them to degrade it rather fast when they encounter it in their environment. However, this was not the case for gluconate. The cells that were initially grown on gluconate did not "recognise" it afterwards in the flasks. This behaviour can possibly be explained by the fact that the cells were not pre-grown exclusively on the specific organic compound (lactate, acetate or gluconate), but also on a small amount of YE (1g/L). Thus, it seemed that the culture could initially grow only on YE and not on gluconate. It was therefore expected to exhibit slightly negative relative consumption rates when exposed to gluconate.

The Biolog test did not fully confirm the results that were obtained by the oxygen test. For example, it was derived (by the Biolog test) that NaG could be degraded by Iso-01, while the other two isolates exhibited much weaker response when exposed to it. On the other hand, the continuous oxygen consumption test revealed that none of the isolates could degrade NaG significantly, irrespectively of the pre-growth medium. In addition, the Biolog test revealed, in general, a higher preference for acetate than for lactate, which does not completely agree with the oxygen measurements. Although both tests work by measuring the oxygen

reduction, the results were slightly different. The variances in the results obtained by the two tests could be attributed to the two following facts:

- The duration of the tests. The continuous oxygen consumption measurements lasted between 30 and 120 minutes, while the Biolog test lasted 48 hours.
- The basis of comparison of each test. The continuous oxygen consumption test was based on comparison between consumption rates, while the Biolog test results were based only on a single value obtained 48 hours after the initiation of the test.

In this study, the compressive strength of mortar cubes was determined only at the age of 28 days and not earlier. It should be noted that in case the bacterial activity starts at an earlier age, the water produced during metabolic conversion of the organic compounds is insignificant and cannot alter the water-to-cement ratio. Consequently, the compressive strength cannot be affected by the metabolic reaction.

The compressive tests revealed a rather positive influence of the two organic components, when dissolved in the mixing water. In general, the compressive strength at 28 days was either slightly increased or remained unaffected compared to the reference mixture. Thus, both organic compounds (CaL and CaA) could be used as parts of the biogenic healing agent without expecting negative effects on the strength of the cementitious material.

The second part of the study concerned the investigation of the LWA and the incorporation method of the biogenic healing agent into them. The results from immersion of LWA in water gave an indication of the absorption capacity of the expanded clay material (31%). The MIP tests specified the total porosity, but also the pore size distribution and the most frequent pore diameters which ranged between 0.15 μm and 6.5 μm. However, the obtained curves gave evidence of micro-cracking occurring during testing, which can bring inaccuracy in the pore size distribution results. Nevertheless, in combination with ESEM observations the size of the pores seemed to be appropriate to accommodate the biogenic healing agent.

The vacuum impregnation method in combination with subsequent drying at low temperature (4 °C) proved to be the most efficient technique to include the highest possible amount of healing agent in the LWA. The loaded LWA could be directly added (after impregnation) in the cementitious mixture. Yet, sometimes dry mixing could be required. Thus, drying of the loaded LWA is essential. Drying at room temperature (20 ± 2)°C appeared to be a valid and applicable method,

especially for real scale applications, where the extra cooling step could not be always feasible.

Finally, the oxygen concentration measurements on unloaded and loaded LWA in sealed conditions revealed that the oxygen consumption originated only from the activated bacteria spores being part of the healing agent and were activated, due to certain conditions (nutrients and oxygen) present in the flask. In addition, the oxygen profiles obtained from the active cells and from the healing agent differed noticeably. In fact, during the respiration of active bacterial cells the oxygen concentration decreased in a rather linear way until it reached zero. On the other hand, as can be seen in Figure 3.12, the bacterial spores incorporated in LWA particles remained apparently dormant for more than 5 hours after which they germinated and subsequently multiplied, resulting in an exponential consumption of oxygen until depletion in the sealed flask. This was a desired behaviour which indicated that the bacterial spores were not woken up during their stay in the pores of the LWA, but only when they found favourable environmental conditions (humidity and alkaline pH) for them. This fact is quite promising, since it shows that the healing agent will not be falsely activated before finding a relatively alkaline pH environment and presence of water; conditions that could be met in a cracked cementitious material exposed to humid atmosphere.

3.5 CONCLUDING REMARKS

The nutrient preference of three different bacterial isolates that were used as part of biogenic healing agent for cementitious materials was studied. Two methods, based on oxygen consumption, were adapted. The continuous oxygen measurement method revealed a higher preference for CaL, while the non-continuous oxygen measurement for CaA. Both testing methods agreed that NaG is not an appropriate source of nutrient for the specific isolates. Additionally, the continuous oxygen measurements revealed that bacterial cells pre-grow on a certain organic compound can degrade it easily when they find it afterwards in their environment. Therefore, a sort of memory is developed. The compressive strength tests on 28-days-old mortar cubes indicated that the two organic components, namely CaL and CaA, either do not affect or positively affect compressive strength when dissolved in mixing water in amounts between 0.56 and 2.24% per cement weight. In addition, the highest absorption capacity of LWA soaked in water for 5 days resulted in mass increase of 31% compared to the initial dry weight, while through vacuum application the mass increase was 72.6%. MIP tests revealed that the total porosity of the Liapor particles was close to 60% of their total volume. Furthermore, the impregnation of the healing agent via vacuum treatment, followed by drying at room temperature resulted in mass increase of the LWA by 11.3% compared to the initial dry weight. Finally, the continuous oxygen consumption measurements showed that the encapsulated biogenic healing agent

was activated in the presence of water and in high pH conditions. Consequently, it can become functional when used in cementitious materials as it can provide them with self-healing properties.

REFERENCES

[1] Tziviloglou, E., Wiktor, V., Jonkers, H.M., and Schlangen, E., *Selection of Nutrient Used in Biogenic Healing Agent for Cementitious Materials.* Frontiers in Materials, 2017. 4(15).

[2] Tziviloglou, E., Wiktor, V.A.C., Jonkers, H.M., and Schlangen, E., *Preparation and optimization of bio-based and light weight aggregate-based healing agent for application in concrete*. 2015. In: 5th international conference on self-healing materials. Durham, North Carolina, USA.

[3] Anbu, P., Kang, C.-H., Shin, Y.-J., and So, J.-S., *Formations of calcium carbonate minerals by bacteria and its multiple applications.* SpringerPlus, 2016. 5: p. 250.

[4] Jonkers, H.M., Thijssen, A., Muyzer, G., Copuroglu, O., and Schlangen, E., *Application of bacteria as self-healing agent for the development of sustainable concrete.* Ecological Engineering, 2010. 36(2): p. 230-235.

[5] Jonkers, H.M., *Bacteria-based self-healing concrete.* HERON 2011. 56(1/2): p. 1-12.

[6] Wiktor, V. and Jonkers, H.M., *Quantification of crack-healing in novel bacteria-based self-healing concrete.* Cement and Concrete Composites, 2011. 33(7): p. 763-770.

[7] Kubantseva, N. and Hartel, R.W., *Solubility of calcium lactate in aqueous solution.* Food Reviews International, 2002. 18(2-3): p. 135-149.

[8] Apelblat, A. and Manzurola, E., *Solubilities of magnesium, calcium, barium, cobalt, nickel, copper, and zinc acetates in water fromT= (278.15 to 348.15) K.* The Journal of Chemical Thermodynamics, 1999. 31(10): p. 1347-1357.

[9] Pedrosa, A. and Serrano, M.L., *Solubilities of sodium gluconate in water and in aqueous solutions of ethanol and methanol.* Journal of Chemical and Engineering Data, 2000. 45(3): p. 461-463.

[10] *Liapor fabrication*, retrieved from: http://www.liapor.com/en/basic.php?n=0101 (24/02/2017).

[11] *Liapor-ökologischer Baustoff mit Speicherkapazität*, retrieved from: http://www.kastell-pro.com/liapor-werkstoff.html (01/03/2017).

[12] Cook, R.A. and Hover, K.C., *Mercury porosimetry of hardened cement pastes.* Cement and Concrete Research, 1999. 29(6): p. 933-943.

[13] Aligizaki, K.K., *Pore structure of cement-based materials: testing, interpretation and requirements*. 2006, London, UK: Taylor and Francis.

[14] Zhang, Q., Microstructure and deterioration mechanisms of Portland cement paste at elevated temperature. 2013. PhD Thesis, Delft University of Technology, Delft, The Netherlands.

4

Characterization and healing efficiency of biogenic self-healing mortar

The innovative technology of self-healing cementitious materials allows the repair of cracks, which can endanger their durability, due to ingress of aggressive substances. Various concepts target on the recovery of water-tightness or the recovery of mechanical properties after cracking. Among those, biogenic self-healing concrete has shown promising results regarding the improvement of crack sealing performance. In this chapter, the developed and optimised biogenic healing agent embedded in lightweight aggregates was mixed with fresh mortar. The study first focused on the investigation of the effect of the addition of the healing agent on the fresh- and the hardened-state properties of the mortar. Moreover, the evaluation of the recovery of water-tightness and the recovery of flexural strength after cracking and exposure to two different healing regimes (water immersion and wet-dry cycles) was also studied. Oxygen concentration measurements, ESEM observations and FTIR analyses were used for further investigation of the crystals found inside the healed cracks. The results of the study revealed that the compressive strength of the mortar containing lightweight aggregates was not affected by the presence of the healing agent. The study also showed that the recovery of water-tightness did not differ substantially either for specimens with or without healing agent when immersed continuously in water. Conversely, the recovery of water-tightness increases significantly for specimens containing the healing agent compared to specimens without it, when subjected to wet-dry cycles. Oxygen concentration measurements and bacterial traces on calcite formations confirmed the bacterial activity on specimens containing the healing agent.

Parts of this chapter have been published in the journal paper "Bacteria-based self-healing concrete to increase liquid tightness of cracks", in Construction and Building Materials, 2015 [1] and in the conference paper "Performance requirements to ensure the crack sealing performance of bacteria-based self-healing concrete", in FraMCos-9, held in Berkeley, CA, USA [2].

4.1 INTRODUCTION

Concrete is a structural material that has been widely used in the modern age [3]. Yet, unavoidable surface micro-cracking can increase its permeability, making it susceptible to aggressive agents and will consequently affect the durability of the material [4-6]. Cracking of concrete structures is triggered by temperature and humidity fluctuations, mainly at an early age, and by external loading, mainly at a later age, creating a pathway through which harmful substances enter the material and decay it gradually over time [6]. Self-healing cementitious materials target on preventing the ingress of those substances through self-triggering crack blockage. In the case of biogenic self-healing cementitious materials, where adequate humidity is present, the healing agent can be "activated" by ingress water upon crack formation. Ultimately, after cracking and activation of the healing agent, the open cracks are filled with inorganic crystals (often calcium based), which are products of bacterial metabolic activity.

Previous researches have demonstrated the enhanced performance of biogenic self-healing cementitious materials in comparison to the conventional ones. However, for the performance conditions to be satisfied, prove of the efficiency of the biogenic self-healing material is required. For example, Stuckrath et al. [7] quantified the amount of calcium carbonate ($CaCO_3$) precipitation in bacteria-based self-healing mortar through image analysis (photographic pictures), thermal analysis and Scanning Electron Microscopy (SEM). However, they did not include in their research the proof of either bacterial activity or recovery of lost functionality after cracking and healing. On the other hand, Wiktor and Jonkers [8] noted the improved crack closure of the biogenic mortar through stereo-microscopic observations and confirmed the bacterial activity in mortar through oxygen consumption measurements. Yet, from their experimental results no definite conclusion could be drawn regarding the loss and the regain of functionality (e.g. water-tightness or flexural strength/stiffness) before and after healing treatment. The same for Sierra-Beltran et al. [9], who characterized the bio-based self-healing agent in repair mortar through Environmental Scanning Electron Microscopy (ESEM) observations and oxygen consumption measurements. Moreover, Wang et al. [10] investigated the strength regain and the recovery of water-tightness on cracked and healed mortar specimens. In their study, they also included SEM observations on $CaCO_3$ precipitates and bacterial activity investigation via conductivity measurements. Yet, those tests were conducted in silica gel and polyurethane foam with bacteria, which were not incorporated in the cementitious matrix.

The conclusions of the previous studies are based on experimental results which at best only indicate the efficiency of the system rather than proving full evidence. For example, $CaCO_3$ formations on the crack surface combined with reduced crack

permeability or visual crack closure after the healing treatment can also occur due to autogenous healing. In fact, studies that compared samples with and without biogenic healing agents have shown that crystals in partially- or fully-sealed cracks can be found also in non-biological specimens. This behaviour might exclusively originate from autogenous healing (carbonation of cement matrix and/or continued cement hydration) and not from bacterial healing. Moreover, $CaCO_3$ formations on the crack surface have been found to co-occur with bacterial activity that was derived either from microscopic evidence of bacterial imprints in formed $CaCO_3$ crystals, or from oxygen consumption measurements. Although providing evidence for bacterial activity, the latter two observations did not provide quantitative information on reduction of actual crack permeability. As a matter of fact, it might be feasible that biological activity leading to the formation of precipitates does not significantly contribute to the reduction of the crack permeability. Vice versa, evidence of bacterial activity combined with reduced crack permeability in comparison to non-biological reference specimen is very likely to be always accompanied by bacterial controlled mineral formation inside the crack. Yet, one needs to confirm that crack sealing is not caused, for example, by abiotic swelling of cement matrix or by non-biological derived impurities blocking the crack.

Considering the previous, it can be stated that by focusing only on individual test results, the functionality of the biogenic self-healing system cannot be assured. Therefore, in this research, it was proposed to apply a more complete investigation method based on three performance requirements (Figure 4.1). These are: the presence of mineral formation inside the crack, the concomitant reduced crack permeability, and the evidence of bacterial activity in the mortar. Measuring and quantification of these three processes would not only be able to assess the healing behaviour of the cementitious material, but also prove that the enhanced behaviour is originating from the bacterial activity. In the current chapter the biogenic healing agent developed and optimized, as presented in chapter 3, is introduced into mortar. At first, the biogenic self-healing mortar is characterized and compared with mortars without the healing agent. The basis of comparison was the results obtained by mostly applying standardised tests on fresh and hardened mixtures. Along with the material characterization, the healing efficiency of the biogenic self-healing mortar was also investigated. The second part of this chapter proposes a standardized experimental procedure to be applied on mortar specimens which can quantify and confirm the efficiency of the biogenic self-healing system through combined crack permeability, strength regain tests, microscopic observations, and oxygen consumption measurements.

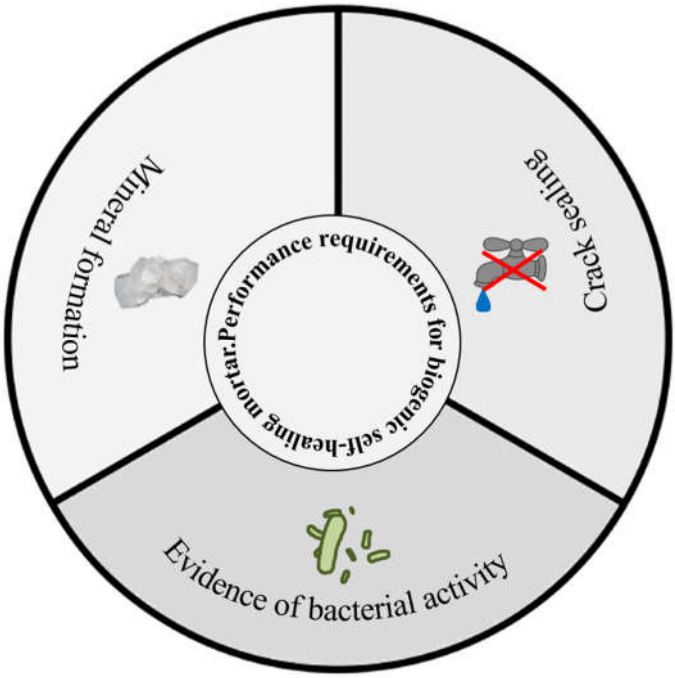

Figure 4.1 The three performance requirements to ensure quantification of the desired crack sealing performance of a biogenic self-healing agent incorporated in cementitious materials [2].

4.2 MATERIALS AND METHODS

4.2.1 PREPARATION OF THE HEALING AGENT

The biogenic healing agent, as described in the previous chapter, consisted of spores derived from alkaliphilic bacteria of the genus *Bacillus* and organic mineral compounds. The healing agent was incorporated in expanded clay particles (Liapor 1/4 mm, Liapor GmbH Germany) via an impregnation under vacuum with calcium lactate (CaL, Corbion Group Netherlands B.V.)- (200g/L), Yeast Extract (YE, Leiber GmbH Germany) - (4 g/L) and bacterial spores (10^8 spores/L) solution. Following the impregnation, the LWA were dried for approximately 5-6 days at standard temperature (20 ± 2 ˚C) with (60 ± 10)% RH, until a constant weight was obtained.

4.2.2 PREPARATION OF THE MORTAR SPECIMENS

Three types of mixtures were investigated. One reference mixture (REF) with normal weight aggregates, one control mixture (CTRL) with non-impregnated LWA and one mixture with impregnated LWA (BAC). The REF mixture contained ordinary Portland cement (CEM I 42.5 N, ENCI, The Netherlands) and

0/4 mm sand, while the CTRL and BAC mixtures contained 0.125/1 mm sand and 1/4 mm LWA. The detailed mixture proportions are presented in Table 4.1. The LWA used for the CTRL mixture were pre-wetted to avoid consuming part of the mixing water. This is a well-known procedure that is often used in the common practise. Water (10% of the weight of the LWA) was poured in a bucket containing the LWA, 30 min prior to mixing. The bucket remained covered until mixing to avoid water evaporation. This procedure was not followed before the casting of the BAC specimens, since it was known from previous experience that the impregnated LWA can significantly increase the workability of the mixture. Therefore, there was no need to previously add extra water in the mixture. Moreover, the addition of water might have caused dilution of the healing agent components in the pre-wetting water and it could have led to loss of some part of the healing agent.

For the examination of the influence of the healing agent on hardened-state properties of the mortar, 9 prisms (40 mm x 40 mm x 160 mm) were cast per mixture. In addition, for the investigation of the recovery of water-tightness (R_{WT}) and the recovery of flexural strength (R_S), 15 reinforced mortar prisms (40 mm x 40 mm x 160 mm) modified with a hole in their centre, as illustrated in Figure 4.2, were cast per mixture. The hole was created by introducing a smooth (greased) metal bar (ø 5mm) while casting, which was pulled-out during demoulding. REF and CTRL prisms were demoulded 24 h after casting, while BAC specimens after 72 h. All specimens after demoulding were kept in a room with standard temperature (20 ± 2)°C and > 95% RH for 28 days.

Table 4.1 Mortar mix designs.

Mixture	CEM I	Water	0.125/1 mm Sand	1/4 mm Sand	1/4 mm LWA
	(kg/m^3)	(kg/m^3)	(kg/m^3)	(kg/m^3)	(kg/m^3)
REF	463	231.5	855	825	0
CTRL	463	231.5	855	0	257
BAC	463	231.5	855	0	283[2]

[2] This weight includes the weight of impregnated healing-agent into the pores of the LWA.

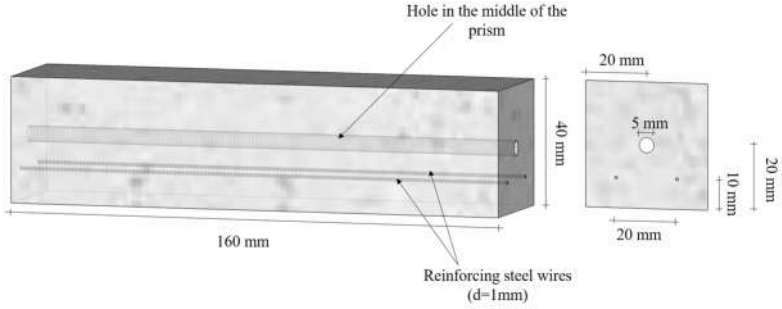

Figure 4.2 Specimens for evaluation of R_{WT} and R_S.

4.2.3 MATERIAL CHARACTERIZATION, CRACK INTRODUCTION AND HEALING REGIMES

Immediately after mixing, four fresh-state mortar properties were tested, i.e. consistency, bulk density air content and setting time. The tests were performed according to EN 1015-3, EN 1015-10, EN 1015-7 and EN 480-2 respectively. Flexural and compressive strength was determined (in triplicates) on 3-days-, 7-days- and 28-days-old unreinforced prismatic specimens according to the procedure described at EN 1015-11.

MIP tests were performed on 3-months-old specimens from all the three mixtures. The tests were conducted with a Micrometrics PoreSizer 9320. The PoreSizer 9320 machine can determine pore sizes in the range 0.007-500 μm. The measurements comprised of two pressure modes, namely the low-pressure mode (0.004-0.17 MPa) and the high-pressure mode (0.17-210 MPa). A surface tension of 480 N/m and a contact angle of 139° were used as suggested by Cook and Hover [11]. Before the MIP test, the specimens were crushed into small pieces (≈ 5 g) and then dried in a ventilated oven at 40 °C until a constant weight was succeeded. The MIP tests were also conducted in triplicates.

Damage introduction was performed on 28-days-old reinforced prismatic specimens via three-point-bending test (Figure 4.3a). The specimens were loaded until the formation of a single stable and rather large crack (350 μm), without being fractured completely into two parts. Each specimen was placed on the testing machine (INSTRON 8872 Testing System), where a vertical load was applied at the middle span of the specimen, so that the crack opening increased constantly by 0.5 μm/s. When a crack opening of approximately 400 μm was reached, the specimens were slowly unloaded. After unloading, the crack width reduced to approximately 350 μm (Figure 4.3b).

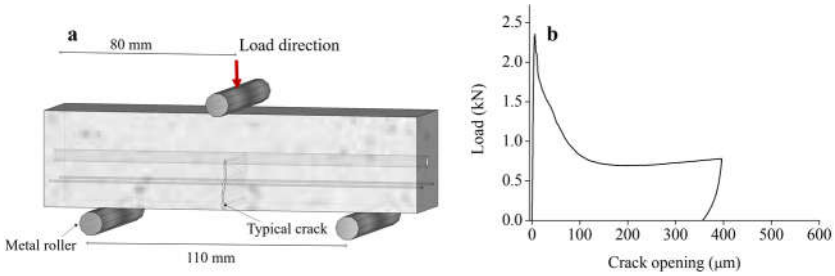

Figure 4.3 a. Three-point-bending set-up and b. Typical load-deflection graph obtained during the crack introduction on mortar prisms.

Following the crack creation, 6 specimens of each mixture were placed horizontally in a plastic container filled with tap water for crack healing. The specimens were placed on the top of spacers (10 mm high), so that there was space between them and the bottom of the container. The container was kept open to the atmosphere at standard room temperature (20 ± 2)°C with (60 ± 10)% RH for 28 or 56 days. Extra water was added (on a weekly basis), to keep a constant liquid-to-solid ratio. Another 6 specimens of each mixture were subjected to wet and dry cycles for 28 or 56 days. The specimens were placed on spacers in plastic containers. Each cycle lasted 12 hours. An external pump was either supplying the container with water or was removing it. The container was kept open to the atmosphere at standard room temperature (20 ± 2)°C with (60 ± 10)% RH.

4.2.4 CRACK PERMEABILITY TEST

The recovery of water-tightness (R_{WT}) after cracking and healing was initially investigated through stereomicroscopic images. Although stereomicroscopic observations can give an indication for the crack closure, the results should be combined with a crack permeability test to link the functional property (crack permeability) with the visual observations. The test was performed on three specimens (with the 5-mm hole) before, and on another three specimens after the healing treatment. Before performing the test, one of the two end-sides (40 mm x 40 mm) of the specimens was covered with an insulating layer, to prevent water passage from this side. On the other end-side a connector was fixed, and a plastic tube was adjusted to it. Via a water-column (500 mm above the specimen), water passed through the plastic tube in the 5 mm-hole and leaked out through the crack. The dripping water fell in a container placed on an electronic scale. The scale was connected to a computer that recorded the experimental data, i.e. water weight and time [12]. The set-up of the crack permeability test is presented in Figure 4.4a Although each test lasted approximately 10 minutes, the flow was rather stable from the beginning (Figure 4.4b). After the completion of the crack permeability tests, the R_{WT} for each set of the three healed specimens was calculated as follows:

$$\boldsymbol{R_{WT} = (1 - \frac{\bar{m}_h}{\bar{m}_{n-h}})x\ 100\%} \quad (4.9)$$

Where $\bar{m}_{n-h}$ is the average (out of three specimens) mass of water that has passed through the unhealed cracks of the three specimens in 5 minutes and $\bar{m}_h$ is the average (out of three specimens) mass of water that has passed through the healed cracks of another three specimens in 5 minutes.

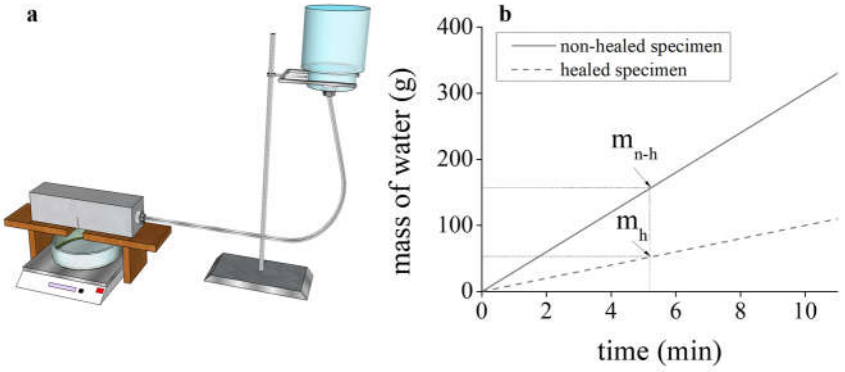

Figure 4.4 a. Crack permeability test set-up of prismatic specimens and b. typical water flow graphs obtained by performing the crack permeability test on specimens before and after healing treatment.

4.2.5 INVESTIGATION OF THE HEALING PRODUCT INSIDE THE CRACK

For the investigation of the healing product formed inside the crack during healing treatment, the prisms were separated in two parts, so that both crack surfaces were exposed. The morphology of the precipitates was investigated by examination of the crack surface via ESEM (Philips XL30 Series) equipped with Energy Dispersive X-ray spectrometer (EDS). In addition, Fourier-Transform Infrared (FT-IR) spectrometry (Perkin-Elmer Spectrum 100 Series equipped with Attenuated Total Reflexion) was used for identification of the precipitates (2-3 mg) scraped from the crack surface. The spectra obtained consisted of 16 scans with a resolution of 2 cm^{-1} in the range of 4000-600 cm^{-1}.

4.2.6 RECOVERY OF FLEXURAL STRENGTH

The recovery of flexural (R_S) strength was examined through three-point-bending tests. The initially cracked specimens at the age of 28 days were again subjected to three-point-bending after the end of the healing period. The load was applied in the middle of the specimens with the same load rate as during the first cycle. The second loading cycle lasted until the crack was further opened above approximately 200 μm. Afterwards, the specimen was slowly unloaded. Figure 4.5 shows a typical graph of two loading-unloading cycles on the same specimen

before and after the healing treatment. The R_S for a single specimen can be calculated, as seen in Equation 4.2, based on the values obtained by the loading-unloading cycles shown in Figure 4.5.

$$\boldsymbol{R_s = (1 - \frac{F_3}{F_2})x\ 100\%} \quad (4.10)$$

Where F_2 is the load value that corresponds to a crack opening of 400 μm during the first loading cycle (before healing treatment) and F_3 is the peak load value of the second loading cycle (after healing treatment).

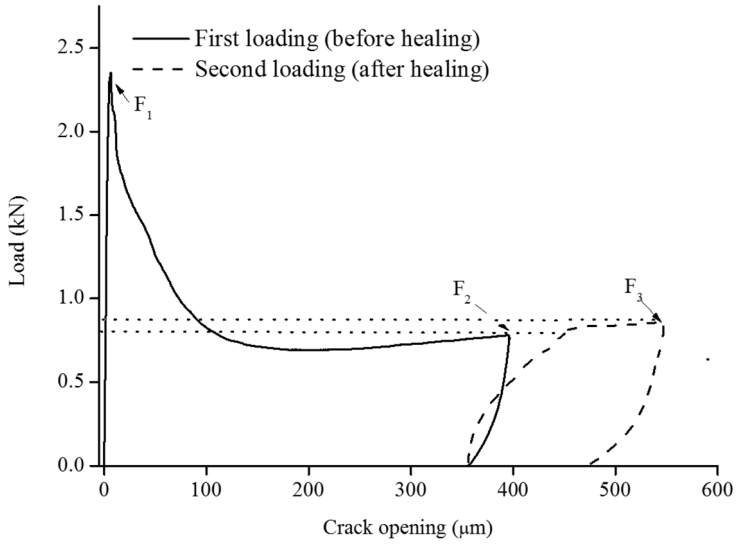

Figure 4.5 Typical graph obtained by the two loading-unloading cycles before and after healing treatment.

4.2.7 OXYGEN CONSUMPTION MEASUREMENTS

The oxygen consumption measurements were conducted to prove the existence of bacterial activity when the bacteria and the nutrients were packed in the cementitious matrix. The measurements were performed on mortar pieces, as seen in Figure 4.6. The pieces were either submerged in water or in an alkaline aqueous solution (carbonate-bicarbonate buffer). For this test, micro-sensor type Oxy50M (Presens, Germany) was used. The micro-sensor, fixed to a motorized micromanipulator on the vertical axis, was measuring the oxygen concentration in vertical steps of 50 μm from 5 mm above and down to the surface of the specimen. The specimen was placed in a 4-litres tank filled either with tap water or with carbonate-bicarbonate buffer (0.1 M, pH= 10.5 at 20 ± 2 °C). Each set of measurements ran for 10 minutes and after 10 minutes of pause the next set was starting (3 tests/hour). After the completion of the test, which lasted for 5 hours

for the specimens in water and 9 days for the specimens in buffer, oxygen micro-profile measurements were obtained.

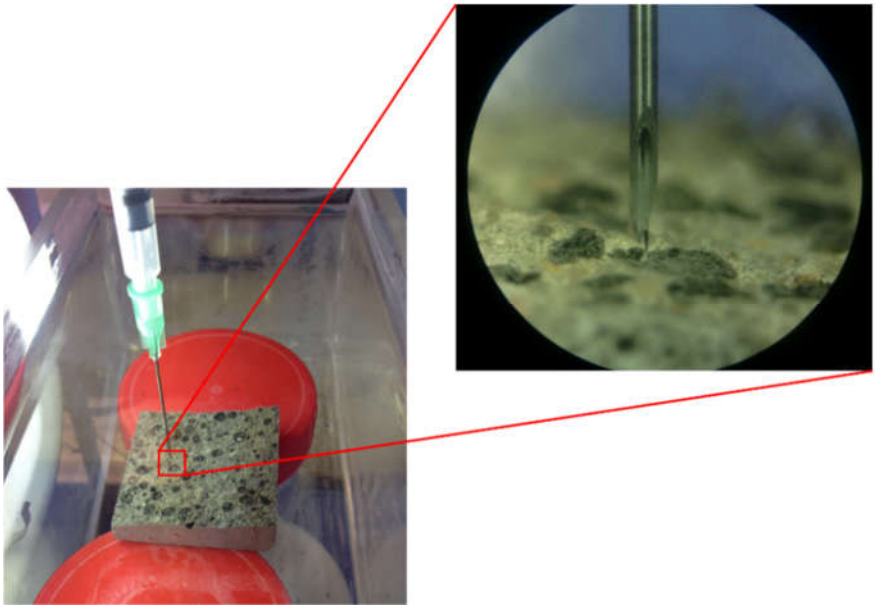

Figure 4.6 Mortar piece submerged in water or in alkaline solution. Over the mortar piece and on the top of an expanded clay particle the oxygen sensor needle is positioned. The sensor measures the oxygen concentration at its current position.

The schematic representation of the complete experimental procedure that was followed during this research is depicted in Figure 4.7.

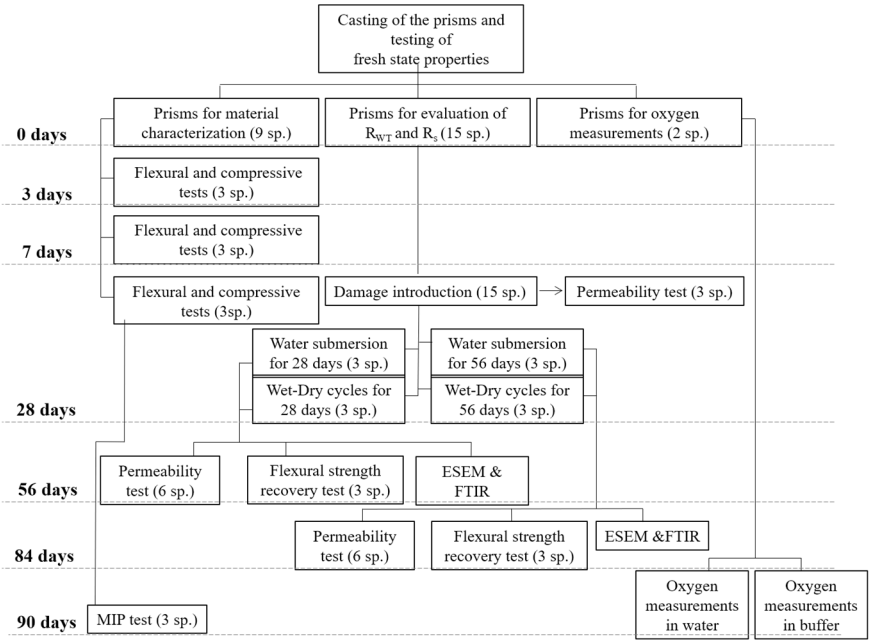

Figure 4.7 Schematic representation of the experimental procedure (sp. stands for specimens).

4.3 RESULTS

4.3.1 INVESTIGATION OF FRESH-STATE PROPERTIES

The effect that the healing agent has on the fresh as well as on the hardened mortar was examined through the comparison of several properties of the mixtures with and without healing agent. The comparison was conducted in two steps; first on fresh mixtures and then on hardened prisms. Table 4.2 presents the results obtained by the tests performed on the fresh mixtures. The tests revealed that the replacement of sand with LWA in CTRL mixture led to a substantial decrease of the bulk density and tended to increase the air content, while it hardly affected the consistency of the fresh mixture (Figure 4.8). These changes in the fresh mortar are quite expectable, since the normal weight sand with a higher specific mass is replaced with the almost 3 times lighter and porous LWA. Thus, the density is decreasing while at the same time air voids are introduced into the mixture. Furthermore, the presence of the healing agent seems to affect all the above-mentioned characteristics leading to a lighter and more flowable mixture with increased air content. The bulk density of the BAC mixture is comparable to that of the CTRL one (6% difference). Conversely, the flow and the air content show an increase of 16% and 43% respectively. Those two properties were most probably affected due to the presence of CaL and YE.

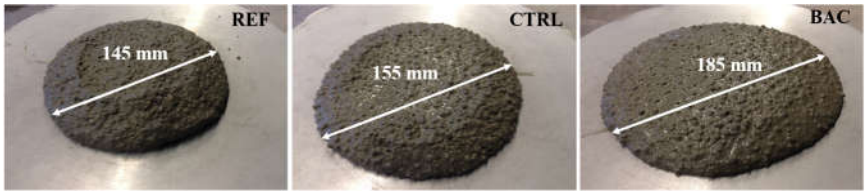

Figure 4.8 Flow table diameters (indication of consistency) of the different mixtures.

Table 4.2 Flow, density and air content values for the three different mixtures.

Property	REF	CTRL	BAC
Flow (mm)	145	155	185
Density (kg/m^3)	2192	1652	1546
Air content (%)	5	8	14

Figure 4.9 shows the results of the setting time test on the three mixtures. The REF mixture showed a tendency to reduce the penetration depth of the VICAT needle from the start of the test. The initial and final setting were reached in approximately 1.5 hours and 5.25 hours respectively. The CTRL mixture showed a delay only in the initial setting compared to REF mixture, probably due to the extra pre-wetting water. In fact, the initial setting time was 2.7 hours, while the final setting was reached in 5.8 hours. Finally, the BAC mixture exhibited an initial setting at 3.1 hours, while final setting was succeeded at around 10 hours. The exact setting time values can be found in Table 4.3.

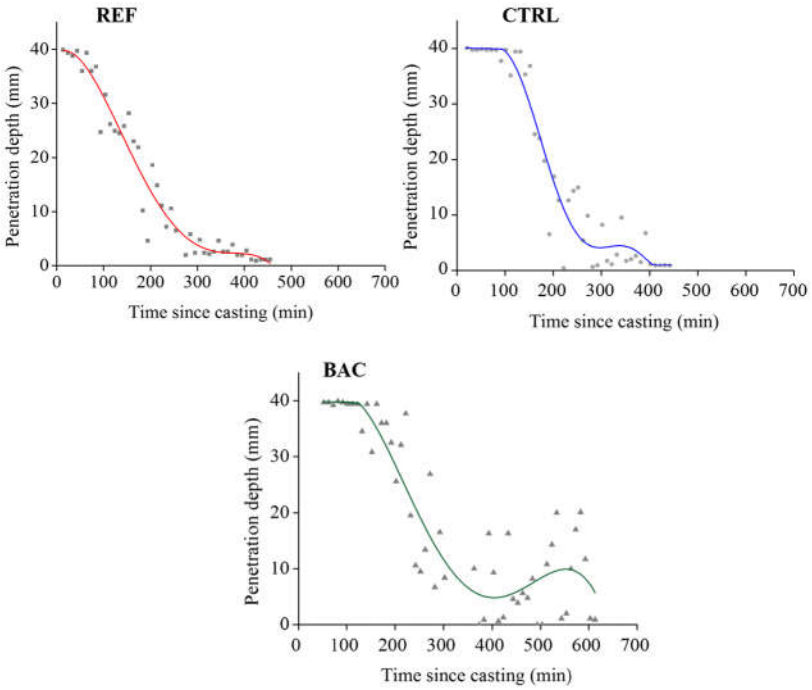

Figure 4.9 Setting time results for the three different mixtures.

Table 4.3 Initial and final setting values of the examined mixtures.

Mixture	Initial Setting (min)	Final Setting (min)
REF	94	315
CTRL	160	350
BAC	192	603

4.3.2 INVESTIGATION OF HARDENED-STATE PROPERTIES

Figure 4.10 shows the results obtained by flexural and compressive strength tests on hardened prisms. The tests revealed that the replacement of normal weight sand with LWA moderately affected the flexural strength (3%-12% reduction) at all testing ages, however, it resulted in significant decrease in compressive strength (26%-37% reduction) compared to the mortar with normal weight sand. On the other hand, the addition of the healing agent affects significantly both flexural and compressive strength (53% and 63% reduction respectively) at the age of 3 days leading to a weaker material in comparison with the CTRL mixture. However,

after the age of 7 days the flexural and compressive strength of CTRL and BAC fell in the same range.

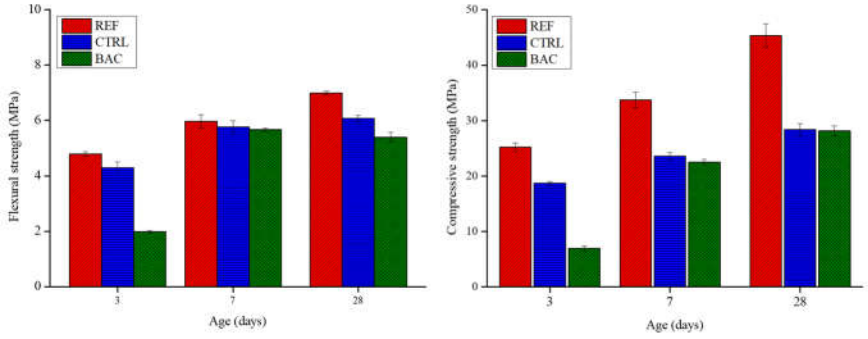

Figure 4.10 Average flexural and compressive strength of prismatic specimens at 3, 7 and 28 days.

Moreover, Figure 4.11 shows the crack surface of three BAC specimens which were broken into two pieces via three-point-bending at different ages. As can be seen from the pictures, at 3 days the LWA were not fractured by the crack. This means that the crack did not intersect the LWA, since they were not the weakest and therefore the crack-attraction points. As a result, the crack passed around the aggregates and the healing agent was not exposed. However, at 7 and 28 days, while hardening process has proceeded, the crack seemed to intersect the LWA and did not pass around them. The white spots inside the LWA can be easily distinguished in the two pictures representing the healing agent found in the pores of the Liapor particles. This means that from the age of 7 days and further on the healing agent system could become available for the cementitious material.

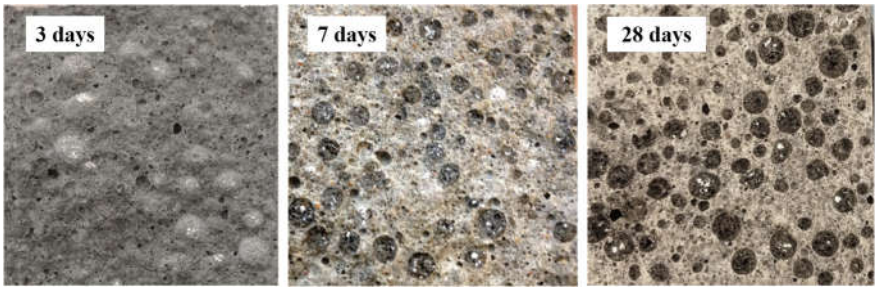

Figure 4.11 Broken-into-two BAC prisms after flexural strength test at different ages.

The MIP tests revealed that the total porosity of the two mixtures with the LWA (CTRL and BAC) was significantly higher (almost 20% higher) than the REF mixture. This increase can be certainly attributed to the replacement of the normal weight sand with the porous expanded clay particles. Three typical curves

displaying the different porosities of the examined mixtures are presented in Figure 4.12. Moreover, there were only small differences in the total porosity of CTRL and BAC mixtures. In fact, CTRL tend to exhibit slightly higher (around 2%) porosity values than BAC. Figure 4.12 presents also typical differential intrusion plots of the three mixtures. As can be seen from the graphs below, all mixtures contain several peaks, while the more pronounced peaks are found at around a diameter of 0.1 μm. The pore size distribution of the CTRL and BAC mixtures was quite similar. Both mixtures had a very distinct critical diameter peak at around 0.15 μm and several other peaks up to 5 μm. On the other hand, the REF mixture showed diameter peaks at around 0.1 μm, while the frequency of appearance of larger pore sizes than 1 μm was quite lower than CTRL and BAC mixtures.

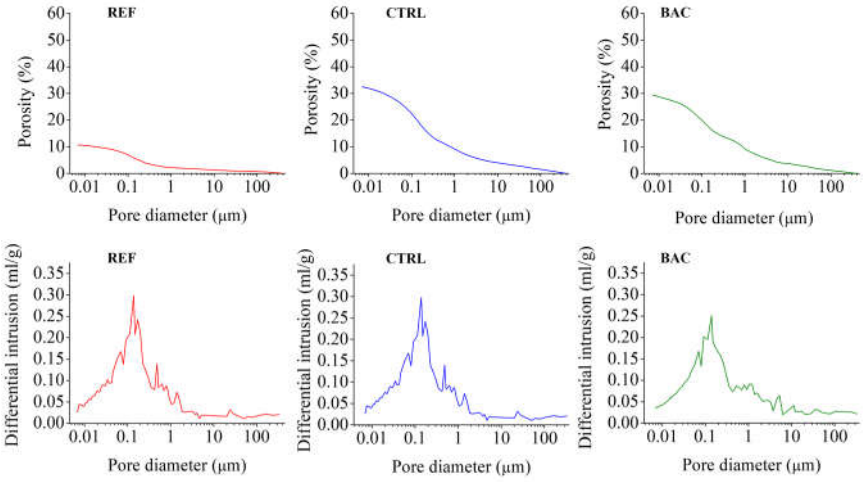

Figure 4.12 Typical total porosity and differential intrusion graphs from MIP tests on REF, CTRL and BAC specimens.

4.3.3 RECOVERY OF WATER-TIGHTNESS AND HEALING PRODUCT INVESTIGATION

The efficiency of the healing agent was investigated initially through stereomicroscopic images and later through crack permeability tests. Figure 4.13 shows examples of cracks before and after each healing treatment. The stereomicroscopic images revealed that REF and CTRL specimens that were immersed in water for 28 or 56 days showed partial or full crack closure, but when subjected to wet-dry cycles the healing was substantially less or even non-existent. On the other hand, the cracks of BAC specimens that were immersed in water for 28 or 56 days exhibited obviously improved crack closure, compared to REF and CTRL specimens subjected to the same healing treatments. Furthermore, the

cracks of BAC specimens which were exposed to wet-dry cycles demonstrated almost complete crack closure.

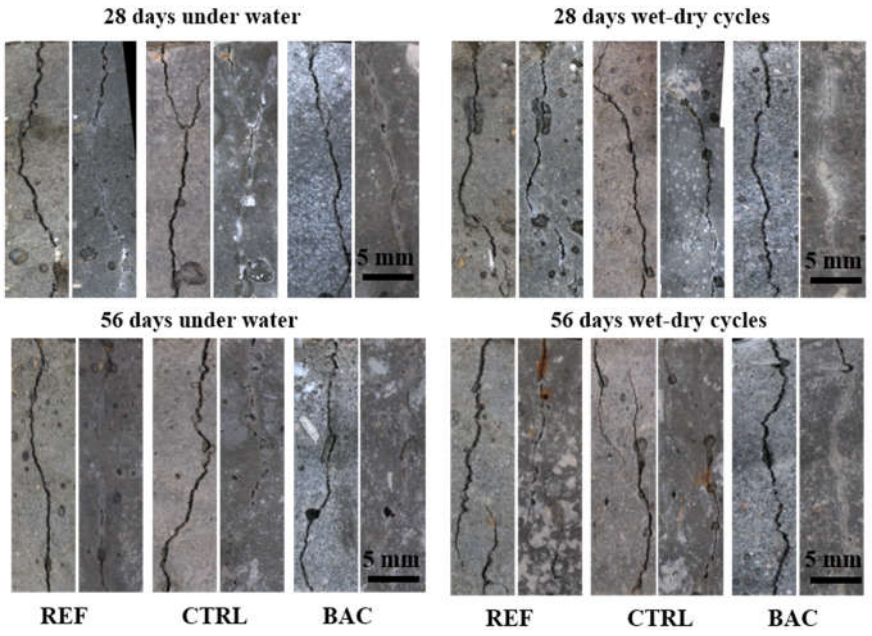

Figure 4.13 Stereomicroscopic observations of cracks subjected to different healing treatments and for different duration (images on the left are before water treatment).

Figure 4.14 shows the R_{WT} of the three types of prismatic specimens. These quantitative results are in good agreement with the qualitative stereomicroscopic observations. In fact, the specimens without healing agent show a relatively high R_{WT} when immersed under water, i.e. 71% and 80% for the REF specimens and 31% and 82% for the CTRL specimens, for healing treatment of 28 and 56 days respectively. Very similar was also the behaviour of BAC specimens under water. The R_{WT} was 69% for 28 days and 91% for 56 days of water submersion. The results differed for the specimens that were subjected to wet-dry cycles. The specimens without healing agent exhibited considerably lower R_{WT} when compared to REF and CTRL specimens under water. Especially, for CTRL specimens subjected to wet-dry cycles the flow of water out of the crack was even higher than the flow before the healing treatment (negative values). In contrast, the R_{WT} on BAC specimens subjected to wet-dry cycles reached 76% for 28 days and 98% for 56 days healing treatment.

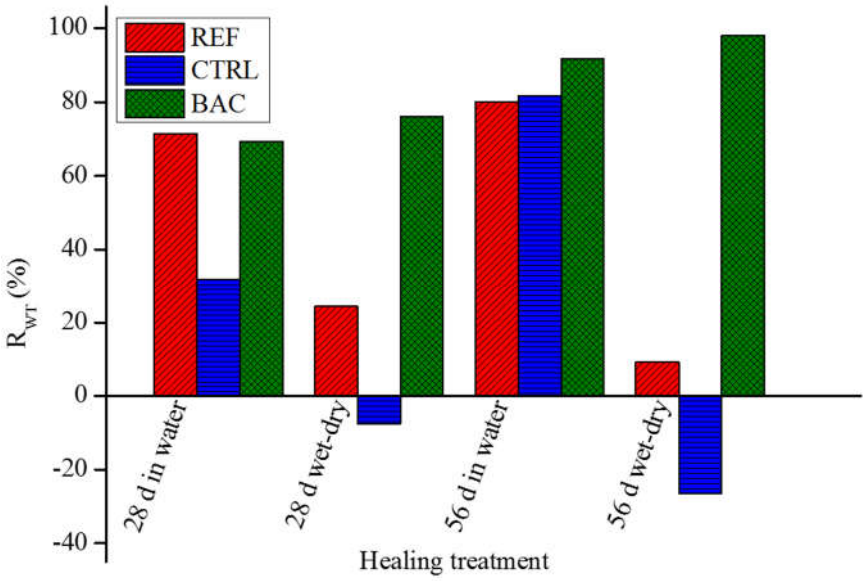

Figure 4.14 R_{WT} in specimens subjected to 28 and 56 days healing treatment.

ESEM observations revealed that the main crystal shapes that were found in the cracks of the three different types of mortar samples were in almost all cases either cubic or clustered asymmetric rhombohedral, possibly formations of $CaCO_3$. Figure 4.15 shows formations lying on the surfaces of the cracks that were found by ESEM observations. During the 28 days of healing treatment on REF and CTRL sample crack surfaces the crystals that were created were considerably smaller than those formed in the cracks of BAC specimens. Despite the larger size, small holes and cavities (1-2 μm wide,~5 μm long) similar to bacterial imprints were observed on the surface of the crystals found in BAC specimens. After 56 days of healing treatment the crystals created inside the cracks of REF and CTRL specimens were fairly larger compared to those of 28 days treatment, yet smaller than the crystals in BAC specimens. However, this time the surface of the precipitates found in BAC specimens was rather smooth. The EDS analysis on the abovementioned crystalline formations indicated high peaks of Ca, C and O, which suggested that crystals were indeed $CaCO_3$ based.

The FT-IR spectra revealed very similar peaks for the three different types of specimens. As shown in Figure 4.16, all spectra exhibited strong calcite bands that appear at around wave numbers 1400 cm^{-1}, 870 cm^{-1} and 712 cm^{-1}, typical of carbonate vibrations in calcite, and some weaker bands at 2511cm^{-1} and at 1796 cm^{-1} [13-15].

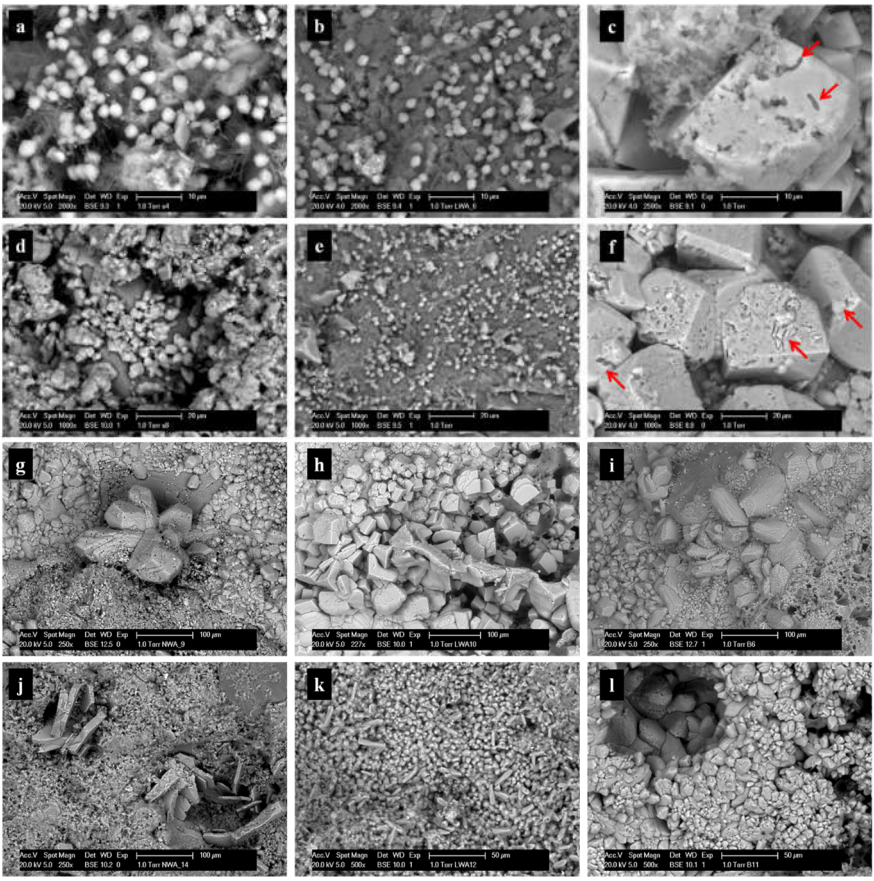

Figure 4.15 ESEM images of precipitates that were found on the surface of the crack after healing treatments a. REF specimen, b. CTRL specimen, c. BAC specimen submerged in water for 28 days; d. REF specimen, e. CTRL specimen, f. BAC specimen subjected to wet-dry cycles for 28 days; g. REF specimen, h. CTRL specimen, i. BAC specimen submerged in water for 56 days; j. REF specimen, k. CTRL specimen, l. BAC specimen subjected to wet-dry cycles for 56 days.

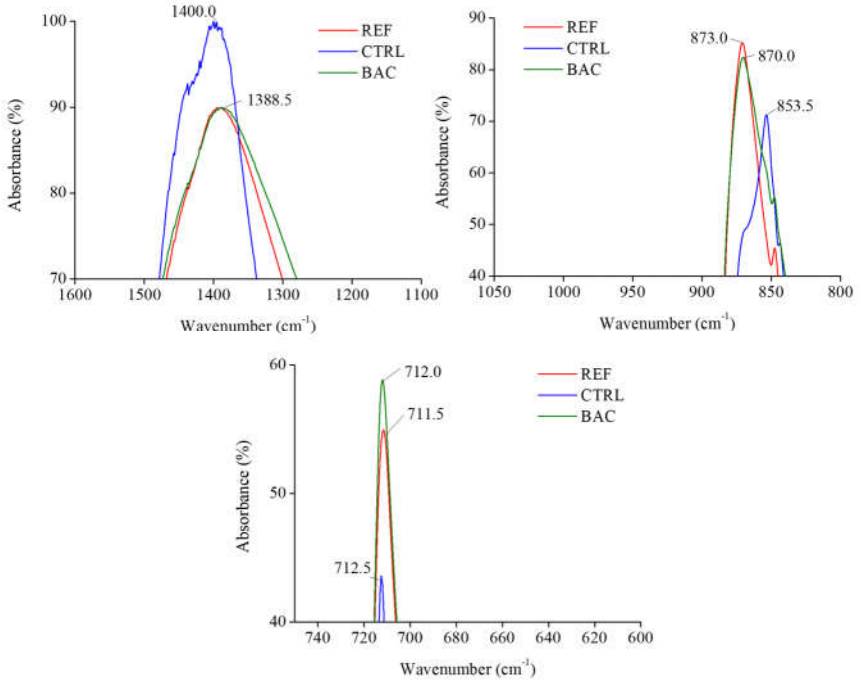

Figure 4.16 Details of FT-IR spectra obtained by analyses of healing products found inside the cracks of REF, CTRL and BAC samples.

4.3.4 RECOVERY OF FLEXURAL STRENGTH

The results on the recovery of flexural strength are shown in Figure 4.17. The values obtained were ranging from approximately - 3.0% until 7.3%, which were very low considering the values obtained by testing the recovery of water-tightness. Furthermore, the scatter in almost all strength recovery calculations proved to be quite high, which means that there was no consistency among the specimens of the same batch regarding the flexural strength results after the healing treatment. Figure 4.17 shows that the REF and BAC specimens tend to increase their flexural strength as the duration of the healing treatment increases. Additionally, it seems that the wet-dry cycles are working in favour of the R_S, for both REF and BAC specimens. On the other hand, no clear trend can be distinguished for the CTRL specimens. However, due to the large scatter, care should be taken with the interpretation of the findings of the specific tests. It could be claimed that no determinative conclusion can be derived from this set of experiments.

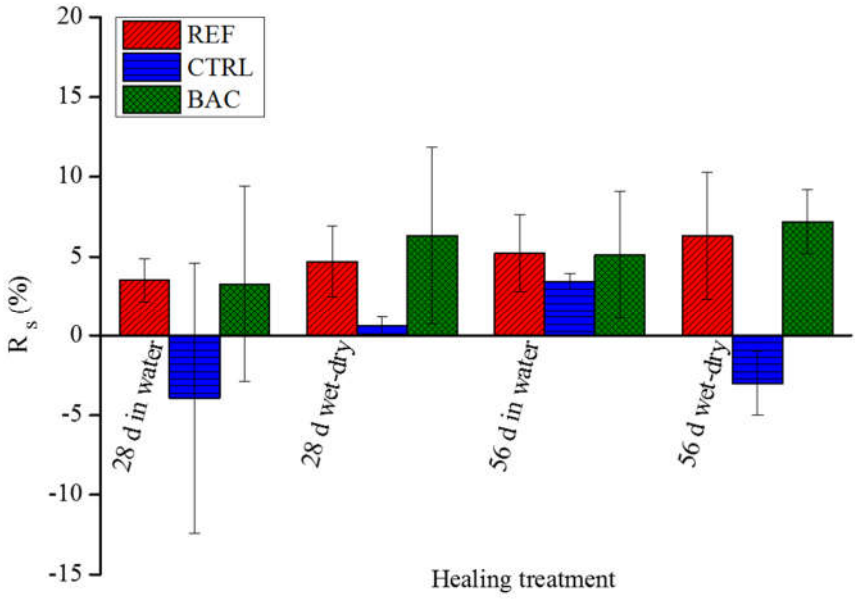

Figure 4.17 Average R_S (flexural strength recovery) in specimens subjected to 28 and 56 days healing treatment.

4.3.5 OXYGEN CONSUMPTION MEASUREMENTS

Oxygen profile measurements showed that oxygen consumption occurred only for the specimens that contained the biogenic self-healing agent. For REF and CTRL specimens the profiles obtained were fairly straight (constant oxygen concentration) along the measuring distance, while the profiles derived from BAC specimens were stable down to 500 μm above their surface but clearly decreased from 500 μm down to the specimen surface. Figure 4.18a and Figure 4.18c show typical oxygen profiles obtained from specimens immersed in tap water and in carbonate-bicarbonate buffer respectively. Moreover, Figure 4.18b and Figure 4.18d show the oxygen consumption rate in time for BAC specimen submerged in tap water and in carbonate-bicarbonate buffer respectively. The values of oxygen consumption rate were obtained by calculating the change in oxygen concentration in the linear part of the gradient in the diffusive boundary layer using Fick's first law of diffusion as seen in Equation 4.3 [16],

$$\boldsymbol{J = -D_{O_2} \frac{d(C_z)}{dz}} \quad (4.11)$$

where D_{O2} is the diffusion coefficient of O_2 in water, and C(z) is the concentration of O_2 at depth z [8]. Although, there was oxygen consumption in both liquids (tap water and buffer), the starting time, the duration and the magnitude of

consumption were different. In fact, for the BAC specimen in tap water the consumption started almost immediately after immersion, it lasted approximately 2.5 hours, and the highest rate reported was - 0.25 μM·mm^2/s at 1 hour after the immersion. For the BAC specimen in carbonate-bicarbonate the consumption started after 20 hours of immersion, it lasted approximately 8 days and the highest value reported was -0.5 μM·mm^2/s at 170 hours after the immersion.

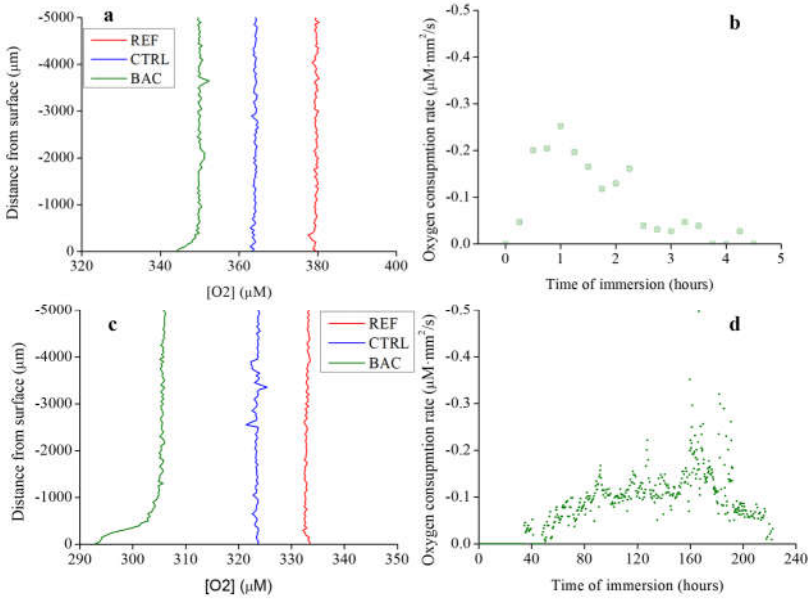

Figure 4.18 a. Typical profiles obtained from specimens in tap water, b. Oxygen consumption rate in time from bacterial specimen immersed in tap water c. Typical profiles obtained by specimens in buffer, d. Oxygen consumption rate in time from bacterial specimen immersed in buffer.

4.4 DISCUSSION

The results of this chapter revealed that replacement of sand with the porous LWA in the mortar specimens (CTRL) led to:

- a considerable reduction of the bulk density of the cementitious material,
- an increase in the air content and
- a reduction in the compressive strength.

Contrary, the replacement of sand with the porous LWA moderately affected the consistency of the mixture, since extra water was added before mixing to avoid loss of workability. The flexural strength was also not significantly affected.

On the other hand, the replacement of sand with impregnated LWA created a rather liquid fresh mixture with increased air content, but it also delayed the setting of the cement. As a consequence, the early age (3 days) flexural and compressive strength of the BAC prisms were respectively 54% and 63% lower than the CTRL specimens.

The increased setting time and workability can be attributed to the introduction of CaL in the fresh mixture triggered either by the leakage of the component from the pores of the LWA or from the remainings of the healing agent on the external walls of the LWA. An organic compound such as CaL can act as retarder causing a delay in the setting of the cement paste and thus inhibit the development of early strength. The action mechanism of organic retarders in general has not been established with certainty. However, it is likely that the organic compound is rapidly adsorbed on the formed membrane of the hydrated cement and it is slowing down the growth of calcium hydroxide nuclei [17].
Moreover, CaL acted also as water reducing admixture, which means that it enhanced the workability of the mixture without increasing the water-to-cement ratio. The function of a water reducer is to disperse the cement grains that tend to flocculate after the addition of water. The water reducing admixtures, which are also associated with retardation of setting, can be hydroxylated carboxylic acids and their salts [17], such as CaL. It can be assumed that CaL is adsorbed by cement particles charging them negatively and resulting in the development of repulsive forces between them. Thus, the water is trapped among the cement particles and the early hydration is delayed.

The introduction of the healing agent in the fresh cementitious mixture caused also an increase in the air content. The same effect has been reported by Megalla [18], where the air content of the fresh paste with a biogenic healing agent of the same nature was almost 38% higher compared to the reference mixture. The air content increase could be attributed the presence of YE (yeast extract). The YE that was used for this study contained proteins in a proportion of 65.1 g/100 g. Proteins are large molecules consisting of smaller chains of amino acids linked with a peptide bond. In alkaline environment, the peptide bond of the protein breaks and smaller hydrophobic molecules are formed. This procedure has been known to facilitate the formation of air bubbles in concrete by reducing the surface tension of the fresh cement paste and increasing the stability of air bubbles [19]. Therefore, the air that has been introduced during high-speed mixing is trapped by the protein molecules and kept inside the mixture.

At a later age (> 7 days) the healing agent presence did not seem to affect either the flexural or the compressive strength of the material. This means that the healing agent slowed down the hardening of the mortar (< 3 days), but did not alter the composition or the identity of the hydration products [17]. It can be therefore

safely argued that the biogenic self-healing mortar can have similar mechanical performance in comparison to a conventional lightweight mortar mixture.

Further, the pictures of the fractured BAC specimens during three-point-bending test revealed that the biogenic mortar cannot provide self-healing properties to the cementitious material before the age of 7 days. In fact, the crack leaves the LWA intact, since it passes around them. Therefore, the impregnated LWA cannot break and expose the embedded healing agent to the crack. Consequently, it could be stated that the healing agent system is rather inert at a very early age of the mortar (<7 days). However, even after 7 days there are more conditions that need to be satisfied to activate the healing agent. These are the presence of water and oxygen and the relatively low pH of the cementitious matrix pore water (between 8.5 and 11.0).

Another focus of this study was to investigate whether the autogenous healing can be enhanced due to the addition of the biogenic healing agent in mortar. This investigation was carried out through water permeability experiments on cracked mortar prisms exposed to two different healing regimes and through three-point-bending tests. The crack permeability results showed that there was indeed reduction of the initial water flow from the cracks of REF and CTRL specimens that were submerged under water for 28 as well as for 56 days. This reduction can be attributed to the autogenous healing mechanisms/reactions that can take place during water immersion. On the other hand, the same type of specimens exhibited substantially lower R_{WT} when exposed to wet-dry cycles. The same behaviour has been reported by Roig-Flores et. al. [20], who proved through water permeability tests that concrete samples immersed in water achieved higher healing rates than samples exposed to wet-dry cycles. BAC specimens showed similar R_{WT} results with REF and CTRL specimens, when immersed in water. However, the differentiation in R_{WT} for BAC specimens was well emphasized by the significantly higher values obtained by specimens that were subjected to wet-dry cycles. The higher concentration of oxygen in the air during the dry cycles seems to promote the bacterial activity leading in increased amount of $CaCO_3$ precipitates. In published studies on biogenic cementitious materials, the healing treatment is traditionally under water. However, this study proved the enhanced crack sealing behaviour of the biogenic mortars subjected to wet-dry cycles, which also represents a more realistic curing scheme than continuous water immersion.

The results on the recovery of strength (R_S) showed very limited increase in flexural strength after the healing treatment, regardless the type of the mixture. Moreover, the scatter of the results was rather high and therefore no solid conclusions could be drawn for the mechanical regain of each mixture. Nevertheless, the increase in strength for REF and BAC specimens could be also linked to the later age of testing where hydration process has progressed causing

an increase in strength. Further, the limited or the non-existent recovery of strength was expected since the presence of $CaCO_3$ has not been related before to enhanced strength at least in the crack range that was studied. Regularly in the literature, the recovery of stiffness is studied along with the R_S. However, in this study the investigation of the former was deliberately skipped after the results obtained by the investigation of the R_S.

Traces of bacteria were found on the surfaces of the crystals formed inside the cracks of BAC specimens that were exposed for 28 days to complete water immersion or to wet-dry cycles. The shape and the size of holes and cavities that were observed are very similar to those described in the literature [21-25], as bacteria imprints on microbially induced calcium carbonate precipitates. However, those imprints could not be found on crystals after 56 days of healing treatment, possibly because the crystals gradually grew in time [26] and covered the bacterial traces.

The oxygen concentration profiles were used as a supplementary tool to investigate the existence of bacterial activity on the mortar specimens with the biogenic healing agent. The results of experiments on BAC specimens submerged in tap water showed that the consumption of oxygen near the surface of the crack was lower and lasted less than in BAC specimens submerged in carbonate-bicarbonate buffer. The explanation may be in two facts:

- The bacteria that exist in the tap water are already active vegetative cells that find the CaL incorporated in the healing agent and start to metabolize it immediately after the immersion of the specimen. In contrast, when the sample is immersed in the buffer the bacteria possibly contained in the water that was used for the preparation of the buffer solution are not active due to the high alkalinity. Therefore, the recorded oxygen consumption is caused only by the bacteria incorporated into the healing agent. Since those bacteria need some time to turn from dormant to active state, the consumption is delayed.
- The solubility of CaL is such that it can dissolve very fast in the bulk water. During this study, it was observed that CaL was dissolving quite slow in the alkaline buffer solution. Thus, the healing agent could stay for longer period undissolved at the same place until bacterial spores are activated and start their metabolic activity.

4.5 CONCLUDING REMARKS

This chapter characterized the biogenic self-healing mortar regarding its fresh- and hardened-state properties and investigated its healing efficiency through crack permeability and mechanical tests. It was proven that the fresh state properties

were significantly affected by the addition of the healing agent, while the properties of the hardened mortar were hardly altered compared to the same lightweight mortar without the healing agent. It was also shown that the lightweight mortar with biogenic healing agent exhibited improved crack sealing, particularly when subjected wet-dry cycles, compared to when subjected to continuous water immersion. On the other hand, the flexural strength showed very limited improvement for the mortar specimens with and without the biogenic healing agent. The proof that the enhanced sealing behaviour of the biogenic mortar originated from the bacterial activity was supported by oxygen consumption measurements and ESEM observations.

In conclusion, the experimental test results not only indicated but also proved the sealing efficiency of the biogenic healing system through a series of laboratory tests, which examine the overall healing behaviour and its origin. It was confirmed that the studied biogenic mortar cannot restore the lost mechanical properties caused by cracking. Yet, a structure could benefit from the use this material, since the enhanced crack sealing behaviour can prevent durability problems that are related to micro-cracking.

REFERENCES

[1] Tziviloglou, E., Wiktor, V., Jonkers, H.M., and Schlangen, E., *Bacteria-based self-healing concrete to increase liquid tightness of cracks.* Construction and Building Materials, 2016. 122: p. 118-125.

[2] Tziviloglou, E., Wiktor, V., Jonkers, H.M., and Schlangen, E., *Performance requirements to ensure the crack sealing performance of bacteria-based self-healing concrete*. 2016. In: 9th International Conference on Fracture Mechanics of Concrete and Concrete Structures. Berkeley, California, USA.

[3] van Oss, H.G., *Background facts and issues concerning cement and cement data*, in *Open-File Report*. 2005. p. 88.

[4] Karr, A.F., Aldea, C.M., and Shah, S.P., *Effect of Microcracking on Durability of High-Strength Concrete.* Transportation Research Record, 1999(1668): p. 86-90.

[5] Yang, Z., Weiss, W.J., and Olek, J., Interaction Between Micro-Cracking, Cracking, and Reduced Durability of Concrete: Developing Methods for Considering Cumulative Damage in Life-Cycle Modeling. 2004, Publication FHWA/IN/JTRP-2004/10, Joint Transportation Research Program, University, I.D.o.T.a.P., West Lafayette, Indiana, USA.

[6] Schlangen, E. and Joseph, C., *Self-Healing Processes in Concrete*. in *Self-Healing Materials: Fundamentals, Design Strategies, and Applications*, Eds. Gosh, S.K. 2009, Wiley-VCH Verlag GmbH & Co. KGaA : Weinheim, Germany. p. 141-182.

[7] Stuckrath, C., Serpell, R., Valenzuela, L.M., and Lopez, M., *Quantification of chemical and biological calcium carbonate precipitation: Performance of self-healing in reinforced mortar containing chemical admixtures.* Cement and Concrete Composites, 2014. 50: p. 10-15.

[8] Wiktor, V. and Jonkers, H.M., *Quantification of crack-healing in novel bacteria-based self-healing concrete.* Cement and Concrete Composites, 2011. 33(7): p. 763-770.

[9] Sierra-Beltran, M.G., Jonkers, H.M., and Schlangen, E., *Characterization of sustainable bio-based mortar for concrete repair.* Construction and Building Materials, 2014. 67: p. 344-352.

[10] Wang, J., Van Tittelboom, K., De Belie, N., and Verstraete, W., *Use of silica gel or polyurethane immobilized bacteria for self-healing concrete.* Construction and Building Materials, 2012. 26(1): p. 532-540.

[11] Cook, R.A. and Hover, K.C., *Experiments on the contact angle between mercury and hardened cement paste.* Cement and Concrete Research, 1991. 21(6): p. 1165-1175.

[12] Tziviloglou, E., Jonkers, H.M., and Schlangen, E., *Bacteria-based self-healing concrete to increase durability of structures*. 2014. In: 1st

conference on ageing of materials and structures. Van Breugel, K. and Koenders, E.A.B. Delft, The Netherlands.

[13] Miller, F.A. and Wilkins, C.H., *Infrared Spectra and Characteristic Frequencies of Inorganic Ions. Analytical chemistry.* Analytical chemistry, 1952: p. 1253-1294.

[14] Peloci, C., Agresti, G., Andaloro, M., Baraldi, P., Pogliani, P., and Santamaria, U., *The rock hewn wall paintings in Cappadocia (Turkey). Characterization of the constituent materials and a chronological overview.* . 2012. In: 10th International Conference of the Infrared and Raman Users Group (IRUG). Barcelona, Spain.

[15] Ramachandran, V.S. and Beaudoin, J.J., *Handbook of Analytical Techniques in Concrete Science and Technology-Principles, Techniques and Applications*. First edition, ed(s). Ramachandran, V.S. and Beaudoin, J.J. 2000.

[16] Gundersen, J.K. and Jorgensen, B.B., *Microstructure of diffusive boundary layers and the oxygen uptake of the sea floor.* Nature, 1990. 345: p. 604.

[17] Neville, A., *Properties of concrete*. Fourth Edition. 1997, London: Longman Group Limited.

[18] Megalla, M., Bacteria based self - healing concrete. 2017. Master Thesis, Delft University of Technology, Delft, The Netherlands.

[19] Panesar, D.K., *Cellular concrete properties and the effect of synthetic and protein foaming agents.* Construction and Building Materials, 2013. 44: p. 575-584.

[20] Roig-Flores, M., Moscato, S., Serna, P., and Ferrara, L., *Self-healing capability of concrete with crystalline admixtures in different environments.* Construction and Building Materials, 2015. 86: p. 1-11.

[21] Stocks-Fischer, S., Galinat, J.K., and Bang, S.S., *Microbiological precipitation of CaCO3.* Soil Biology and Biochemistry, 1999. 31(11): p. 1563-1571.

[22] Cacchio, P., Ercole, C., Cappuccio, G., and Lepidi, A., *Calcium Carbonate Precipitation by Bacterial Strains Isolated from a Limestone Cave and from a Loamy Soil.* Geomicrobiology Journal, 2003. 20(2): p. 85-98.

[23] Abo-El-Enein, S.A., Ali, A.H., Talkhan, F.N., and Abdel-Gawwad, H.A., *Utilization of microbial induced calcite precipitation for sand consolidation and mortar crack remediation.* HBRC Journal, 2012. 8(3): p. 185-192.

[24] Polka, J.K. and Silver, P.A., *Induced sensitivity of Bacillus subtilis colony morphology to mechanical media compression.* PeerJ, 2014. 2: p. e597.

[25] Dhami, N.K. and Mukherjee, A., *Can We Benefit from the Microbes Present in Rammed Earth? CRC Press 2015; 2015 p.* 2015. In: 1st International Conference on Rammed Earth Construction. University of Western Australia.

[26] Baskar, S., Baskar, R., Mauclaire, L., and McKenzie, J.A., *Microbially induced calcite precipitation in culture experiments: Possible origin for stalactites in Sahastradhara caves, Dehradun, India.* Current Science. 90(1): p. 58-64.

5

Assessment of experimental methodology to evaluate self-healing

The research groups that work on self-healing cementitious materials often apply several experimental methodologies on the newly developed materials. Indeed, to prove the efficiency of self-healing cementitious materials, experimental technologies are needed. Within HEALCON project, the need to establish an experimental methodology, which could be applied on self-healing mortars with different implemented self-healing strategies, was considered. Consequently, an experimental methodology, which comprises of crack permeability, water absorption and flexural tests for evaluating the ability of a cementitious material (mortar) to regain water-tightness and mechanical properties, has been developed based on commonly used tests procedures. The first part of the chapter presents the test methodology and the calculations for estimating the healing efficiency of the self-healing mortar. Towards standardization, the reproducibility and therefore the quality of the obtained results was investigated through a round robin test. The second part of the chapter presents and compares the results obtained by the round robin test among four laboratories within the framework of RILEM/TC 253 MCI (Micro-organisms-Cementitious Materials Interactions) and it concerns only the part that examines the sealing efficiency of the biogenic self-healing mortar, which has been studied in the previous chapters. The comparison revealed high scatter in the results of the proposed experimental methodologies, due to the large variations of crack widths obtained within the different laboratories. The chapter closes with recommendations, regarding the methodology of crack introduction and the execution of permeability test, which can ultimately improve the quality of the results.

Parts of this chapter have been published in the conference paper "Evaluation of experimental methodology to assess the sealing efficiency of bacteria-based self-healing mortar: Round robin test", in RILEM TC 253-MCI symposium, held in Delft, The Netherlands [1].

5.1 INTRODUCTION

Self-healing in cementitious materials is a concept that has recently received a lot of attention. Several research groups focus on the development of different self-healing agents for cementitious materials. The techniques that have been commonly used to assess the efficiency of the developed self-healing materials are based on the investigation of the recovery of a certain property or on a function after cracking and healing treatment. Often, the recovery of a mechanical property or the ability to regain water-tightness after an imposed damage are studied using varying specimen sizes and shapes according to the experimental technique that is applied. The development of a mutual or 'standard' methodology to quantify self-healing, which could be applied to various self-healing cementitious materials, has not been a priority so far.

Within the HEALCON project and towards the standardization of an experimental methodology that can test the healing efficiency, several activities have been carried out. Tests procedures were designed to quantify the extent of the recovery of water-tightness and of flexural strength and stiffness on mortar prisms. The testing methods were adapted from techniques that are regularly used in mortar characterization studies and modified by two participants of the HEALCON consortium (Delft University of Technology and Ghent University). The ultimate target was to create a normative document, which includes an experimental methodology that would be scientifically sound and relatively easy to be implemented by other scientists. As a part of the effort to fulfil this target, a round robin test (RRT) was carried out, concerning only the part that examines the sealing efficiency (and not the recovery of flexural strength) through crack permeability via water flow and water absorption. The testing sequence included:

- Flexural and compressive strength tests for material characterization,
- Crack introduction on mortar prisms using three-point-bending,
- Crack permeability tests via water flow and
- Water absorption tests.

The same three mixture categories of mortar specimens that were studied in chapter 4 were considered also for this study; i.e. a reference mixture (REF) with normal weight sand without biogenic healing agent, a mixture with LWA without biogenic healing agent (CTRL) and a mixture with lightweight aggregates (LWA) loaded with the biogenic healing agent (BAC). The focus of the current study was to investigate the robustness of the suggested test methodology rather than drawing conclusions for the healing ability of the biogenic mortar, which has been investigated in the previous chapters.

The RRT was held within the framework of RILEM/TC 253 MCI (Micro-organisms-Cementitious Materials Interactions), WG4 (Engineered bacteria-based protective systems for cementitious materials) among four different testing laboratories with Delft University of Technology being the task coordinator. The laboratories in alphabetical order were:

- Delft University of Technology (TU Delft)
- Ghent University (U Ghent)
- Northumbria University (NU)
- University of Bath (UBath)

Before starting the RRT, all the participants received, from the coordinator, pre-cast mortar prisms and detailed instructions regarding the testing procedures. After the completion of the tests the participants sent the test data to TU Delft for further processing.

A schematic representation of the experimental procedure that was followed during the RRT in every laboratory for each set of mortar prisms received is shown in Figure 5.1.

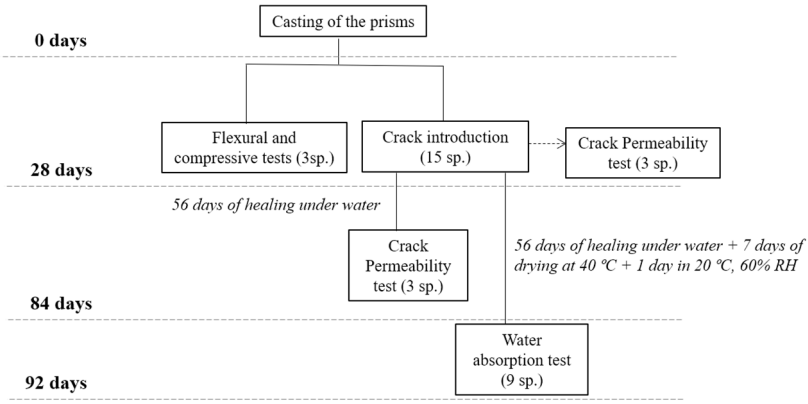

Figure 5.1 Schematic representation of experimental procedure that was followed in every laboratory for each set of prisms received from TU Delft starting at t=28 days.

5.2 MATERIALS AND METHODS

5.2.1 PREPARATION OF THE MORTAR PRISMS

The mortar prisms were prepared at TU Delft and were shipped to the other four laboratories at the age of 7 days. The mixture compounds and their proportions are

presented in Table 4.1. The preparation of the healing agent was according to 4.2.1. All specimens were cast in polystyrene moulds and were kept in sealed plastic bags until they were tested.

For the material characterization three mortar prisms (40 mm x 40 mm x 160 mm) were cast. For the water absorption test, nine mortar prisms (40 mm x 40 mm x 160 mm) reinforced with two steel wires (ø1 mm) were cast (Figure 5.2). Finally, for the water flow test, six mortar prisms (40 mm x 40 mm x 160 mm) with a 5-mm diameter cylindrical hole in the centre, reinforced with two steel wires (ø1 mm), as described in 4.2.2 (Figure 4.1) were used. A notch of approximately 2-3 mm deep was manually made in the middle of every reinforced prism at the age of 28 days to ensure that the crack will initiate from the designated point.

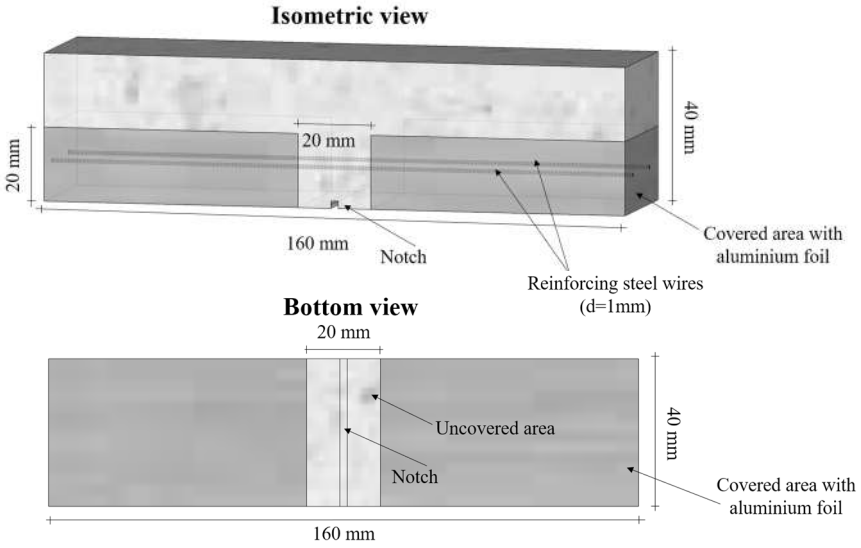

Figure 5.2 Isometric and bottom view of waterproofed specimens designed for the water absorption test.

5.2.2 MATERIAL CHARACTERIZATION, CRACK INTRODUCTION AND HEALING REGIME

The material characterization tests included flexural and compressive tests on prisms as described in EN 1015-11 [2]. The loading speed was 30 N/s and 250 N/s for flexural and compressive strength test respectively. Even though the flexural and compressive strengths do not interfere with the healing efficiency of the studied material, these characterization tests were initially held to evaluate the uniformity of the distributed material.

Cracks were introduced on the reinforced mortar specimens, destined for both crack permeability and water absorption tests, at the age of 28 days by means of three-point-bending, as described in 4.2.3. During bending, the prisms were placed on the testing machine, where a vertical load was applied at their middle span, so that the crack opening increased constantly by 0.5 μm/s up to 350 μm. After achieving a crack width of 350 μm, the samples were slowly unloaded. The laboratories of TU Delft, UGhent and UBath were monitoring and controlling the increase of crack width via Linear Variable Differential Transducers (LVDT). The three-point-bending set-up for NU laboratory was not equipped with LVDT, therefore, the vertical displacement reading was converted to horizontal deformation value. The details of the three-point-bending setup as indicated by the RRT coordinator, including the number and position of the LVDT is shown in Figure 5.3. Following the crack creation, the samples were submerged horizontally (on spacers of 5 to 10 mm) for 56 days in a plastic bucket filled with 5 litres of tap water per three specimens to heal the cracks.

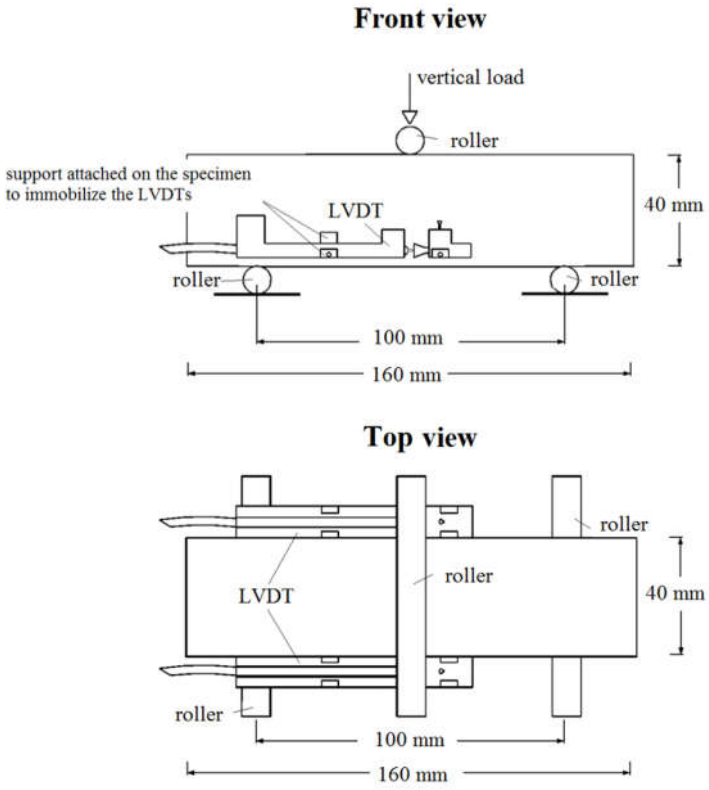

Figure 5.3 Three-point-bending test setup as indicated by the RRT coordinator.

5.2.3 ASSESSMENT OF WATER-TIGHTNESS THROUGH CRACK PERMEABILITY TESTS

The crack permeability test that was described in 4.2.4 was used to evaluate the ability of a crack to resist a flow after the healing treatment. The test was performed before water submersion on three specimens and after water submersion on another three. As it has been mentioned before, the test was performed on different set of prisms before and after healing to avoid loss of healing agent during the first testing, which could negatively affect the healing process. Each crack permeability test lasted for 5 minutes. The available obtained graphs showed a linear relation between the mass of water leaked from the crack and the time. The test data (mass of water and time) should have been continuously recorded. However, in U Bath the mass of water was recorded once; at the end of the test. Considering that the resulting curve from this test is linear, it was assumed that this would not affect the RRT test results. After the completion of the crack permeability tests, the R_{WT} (recovery of water-tightness) for each set of the three healed specimens was calculated as follows:

$$\boldsymbol{R_{WT} = 1 - \frac{\bar{m}_h}{\bar{m}_{n-h}} x\ 100\%} \quad (5.12)$$

Where $\bar{m}_{n-h}$ is the average (out of three specimens) mass of water that has passed through the unhealed cracks of the three specimens in 5 minutes and $\bar{m}_h$ is the average (out of three specimens) mass of water that has passed through the healed cracks of another three specimens in 5 minutes.

Another test was developed to investigate the ability of a cracked and healed specimen to absorb water. The procedure was based on the test described in EN 13057 [3]. During the test, the bottom of the specimens (the side containing the notch) came into contact with water and the water uptake was monitored/measured at certain time intervals. The data was then used to plot a graph, where x-axis and y- axis represented the square root of time and the water uptake, respectively. According to EN 13057, the resulting lines should be linear unless there is a variation in the properties of the mortar with the depth or a change in the system with the time (Figure 5.4).

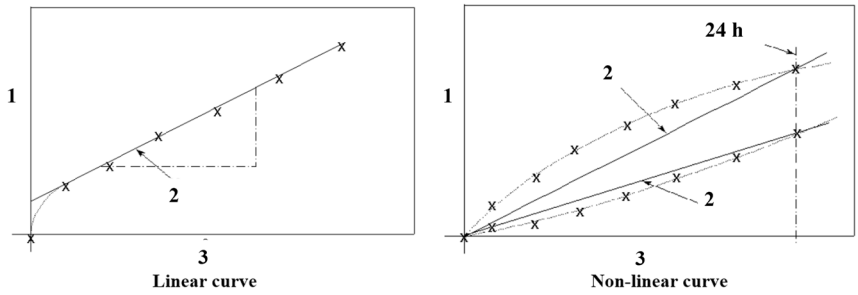

Key
1 Water uptake (kg/m^2)
2 Gradient
3 Time under test (h^{0,5})

Figure 5.4 Resulting lines from capillary absorption test on repair mortar according to EN 13057[3].

The water absorption test that was performed to prove self-healing efficiency on mortar specimens used reinforced prismatic mortar specimens; non-cracked, cracked non-healed and cracked healed. The test concept implied that the non-cracked specimens would absorb the least, while the cracked non-healed specimens would absorb the most amount of water. In addition, the water absorbed by the cracked healed specimens should be between the amount absorbed by the non-cracked and the non-healed specimens, as depicted in Figure 5.5.

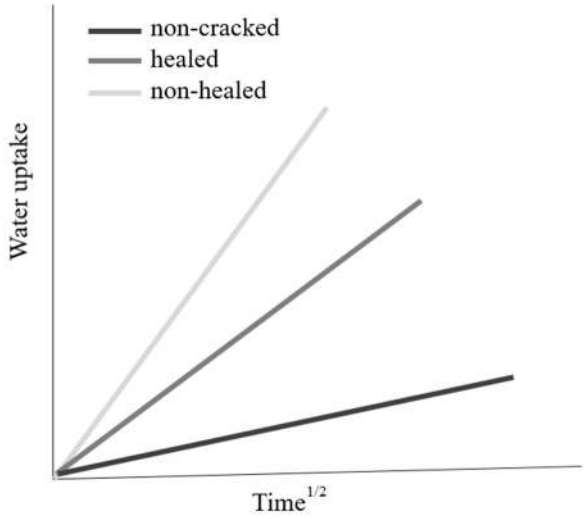

Figure 5.5 Theoretical curves of non-cracked, non-healed and healed specimens subjected to the water absorption test.

For this test, the non-cracked specimens were also immersed in water for 56 days (the same as cracked-healed specimens), while the cracked non-healed specimens were kept in sealed plastic bags for the same time. For a minimum of 7 days before performing the test, the specimens were kept at 40 °C, until a stable weight change was obtained. Then, the specimens were stored for 24 h at 20 °C with 60% RH. Right before the test, the specimens were partially waterproofed (with aluminium adhesive foil), as seen in Figure 5.2 and weighed. During testing, the specimens were put in a plastic container standing on spacers, so that there was a gap between them and the bottom of the container. The water level in the container exceeded the bottom of the specimens by approximately 2-3 mm.

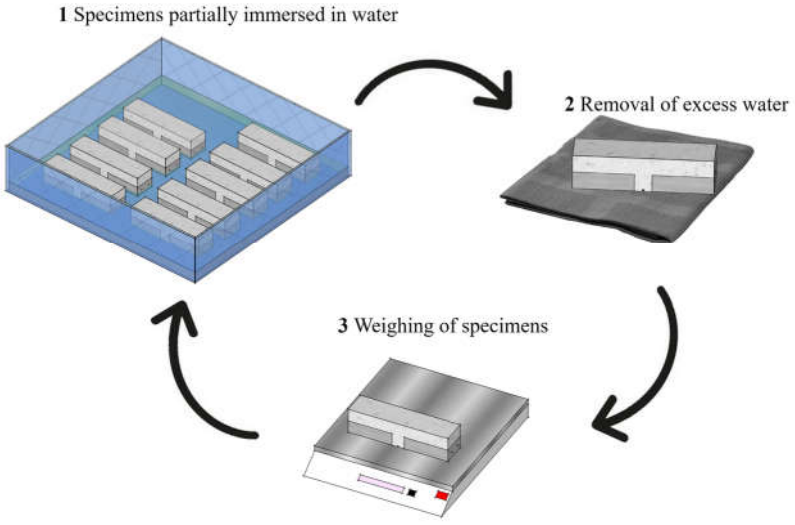

Figure 5.6 The procedure of water absorption test.

The water uptake was monitored frequently for a period of 8 h (after 0.25 h, 0.5 h, 1 h, 2 h, 4 h, 6 h, 8 h), after removing the excess of water on their surfaces with a cloth (Figure 5.6). This data were used to plot the graph of the water uptake with the square root of time. By plotting this graph, it is possible to calculate the sorption coefficient (SC) of each specimen. According to EN 13057, the SC of a specimen should be calculated as the gradient of the obtained curve in case that the resulting line is linear. After the completion of the test, the average SC (average out of three specimens) for non-cracked ($\overline{SC}_{uncracked}$), cracked non-healed ($\overline{SC}_{unhealed}$) and cracked healed specimens ($\overline{SC}_{healed}$) were calculated. The average SC values were used for the calculation of the recovery of water absorption resistance (R_{WA}, Equation 5.2).

$$\boldsymbol{R_{WA}} = \frac{\overline{\mathbf{SC}}_{\mathbf{non-healed}} - \overline{\mathbf{SC}}_{\mathbf{healed}}}{\overline{\mathbf{SC}}_{\mathbf{non-healed}} - \overline{\mathbf{SC}}_{\mathbf{non-cracked}}} \mathbf{x\ 100\%} \quad (5.2)$$

5.3 RESULTS

5.3.1 FLEXURAL AND COMPRESSIVE STRENGTH

The results obtained from flexural and compressive strength tests from each mixture category are presented in Figure 5.7 and Figure 5.8 respectively.

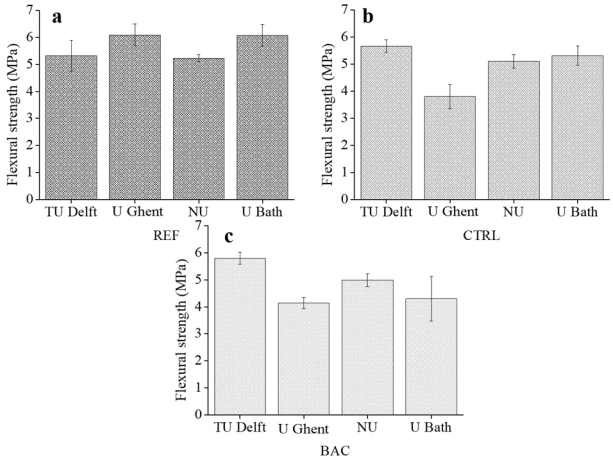

Figure 5.7 Flexural strength test results: a) REF specimens, b) CTRL specimens and c) BAC specimens.

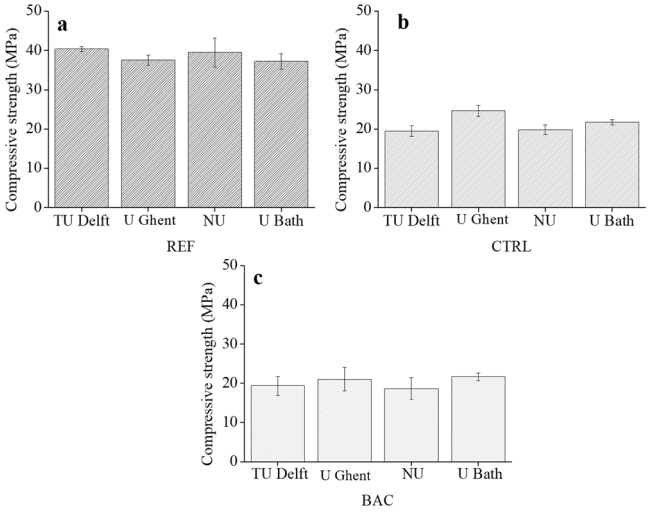

Figure 5.8 Compressive strength test results: a) REF specimens, b) CTRL specimens and c) BAC specimens.

The flexural strength results revealed that the REF specimens tended to show slightly higher values than CTRL and BAC specimens. The average flexural strength values as obtained by each laboratory ranged from 5.2 up to 6.1 MPa, from 3.8 up to 5.7 MPa and from 4.3 up to 5.8 MPa for REF, CTRL and BAC specimens respectively. The intra-lab variations (within one laboratory) were relatively low (approximately 6.6% for REF, 6.9% for CTRL and 8.1% for BAC), while the inter-lab variations (among the different laboratories) were higher (14.1% for REF, 33.3% for CTRL and 28.0% for BAC) in view of the observed standard deviations.

The compressive strength results revealed the effect of the replacement of normal weight sand with LWA. In fact, the compressive strength of REF mixture on average was approximately 39 MPa, while CTRL and BAC specimens showed a reduction of almost 50%. However, the intra- as well as the inter-lab scatter were lower than those obtained by the flexural strength tests. The laboratory averages ranged from 37.2 up to 40.4 MPa, from 19.5 up to 24.7 MPa and from 18.7 up to 21.7 MPa for REF, CTRL and BAC specimens respectively. Moreover, the inter-lab variations were 7.7% for REF, 21.0% for CTRL and 13.8% for BAC specimens.

Overall, it could be stated that the 'under-investigation' mixtures exhibited a comparable behaviour regarding their compressive strength. However, the flexural strength results showed slightly more variations among the different laboratories.

5.3.2 CRACK INTRODUCTION

As it was mentioned above, the crack introduction on the mortar prisms was performed via three-point-bending. The final crack width after unloading of the specimens was measured either via microscopy on the bottom of the specimen or from the readings of the LVDT. There was no designated method for the crack width measurements. The values displayed in the graphs of Figure 5.9 were obtained via microscopy for TU Delft, U Ghent and NU. The crack values for TU Delft and U Ghent were the average from a range of values measured on the bottom of the specimens via stereomicroscopy. NU laboratory obtained the crack values via microscopy software (ALICONA), while for U Bath the crack width values were taken straight from the readings of the LVDT.

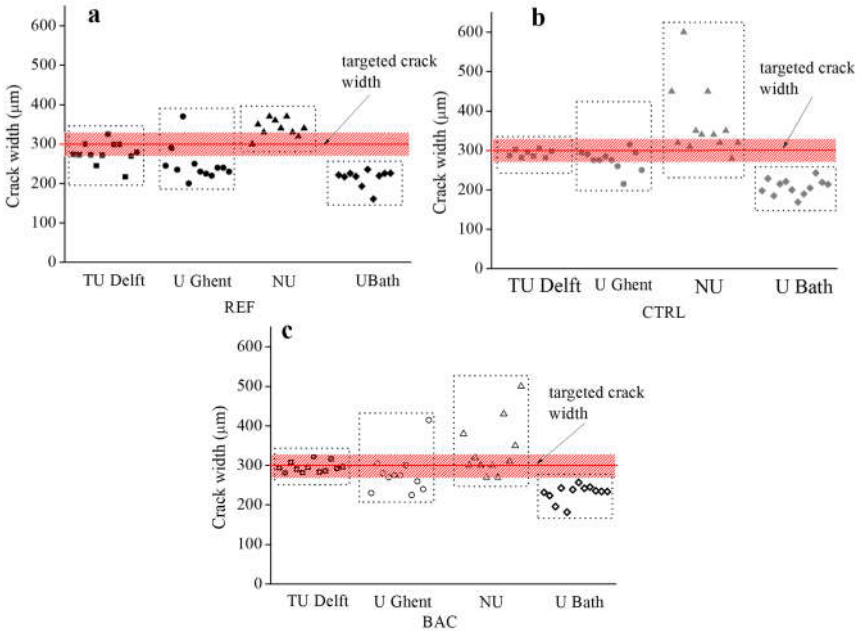

Figure 5.9 Crack width values after the loading-unloading cycle for: a) REF specimens, b) CTRL specimens and c) BAC specimens.

The intra-lab variations regarding the crack width values were relatively moderate regardless of the proximity to the targeted crack width value (300 ± 20 µm). Yet, NU produced quite larger crack widths than the targeted value. The differences in the crack width values among the laboratories were obvious and can be attributed either to the different microscopic technique that was implemented by each laboratory or to the different way of monitoring and controlling the crack opening during three-point-bending (Figure 5.10). For example:

- TU Delft used two LVDT on the front and on the back of the specimens,
- U Ghent used a single LVDT on the bottom of the specimens,
- U Bath used a single LVDT on the front of the specimens and
- NU monitored indirectly the crack width; by conversion of the vertical displacement of the machine to the horizontal crack opening.

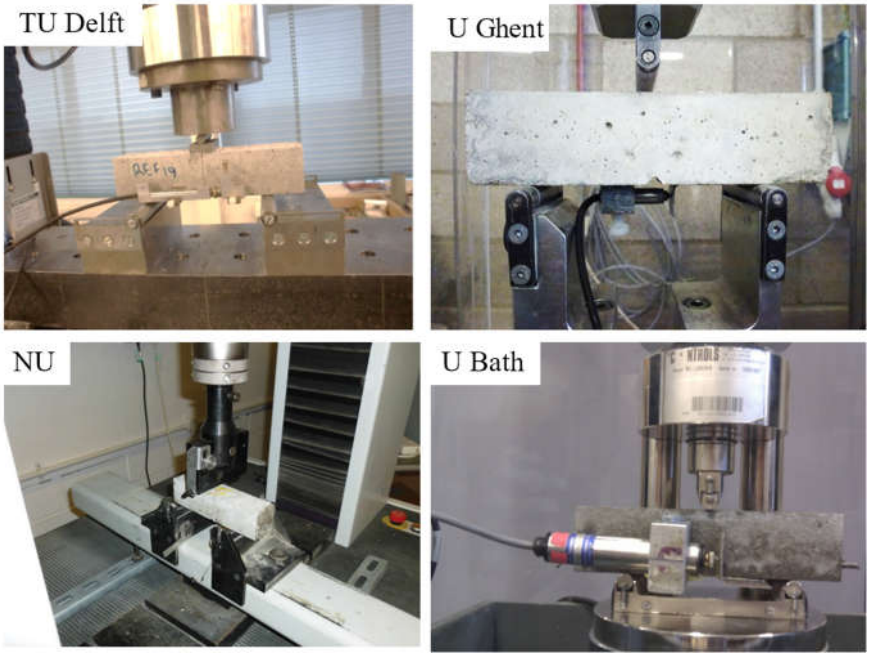

Figure 5.10 Crack introduction set-ups of the four different laboratories.

5.3.3 CRACK PERMEABILITY TEST VIA WATER FLOW

Figure 5.11 shows the results obtained by the crack permeability tests via water flow before and after the healing treatment. The R_{WT} values for REF, CTRL and BAC specimens are shown in Table 5.1. In cases where some test data was missing the calculations were made on basis of the values available.

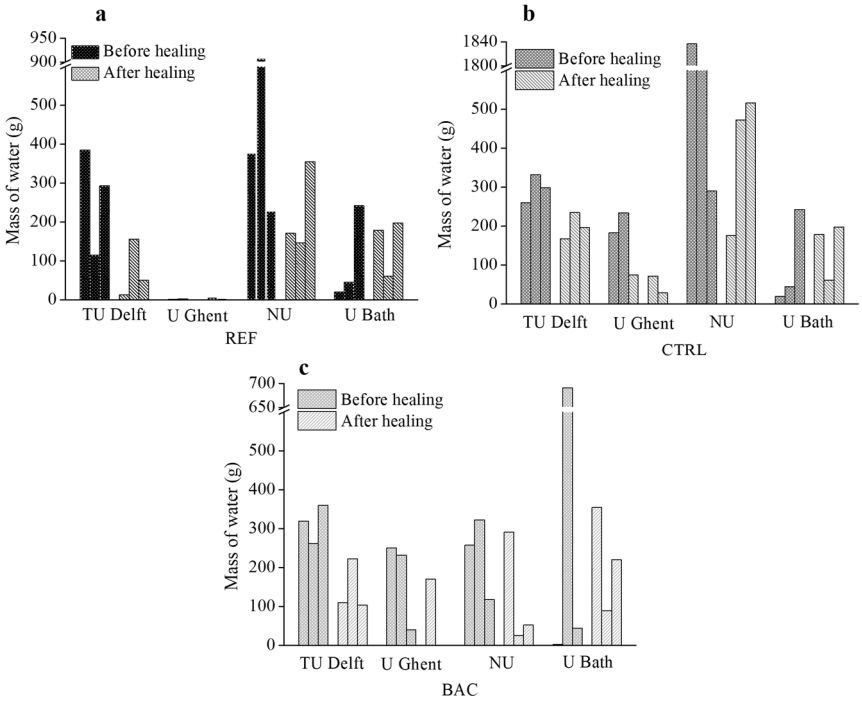

Figure 5.11 Mass of water from the crack permeability test.

Table 5.1 Sealing efficiency values obtained by the laboratories for the various mixtures

Laboratory	$R_{WT\text{-}REF}$ (%)	$R_{WT\text{-}CTRL}$ (%)	$R_{WT\text{-}BAC}$ (%)
TU Delft	72.4	32.9	53.8
U Ghent	76.4	71.9	56.7
NU	55.4	32.9	47.2
U Bath	-42.7	62.4	10.0

The intra- as well as the inter-lab variations were significant. Particularly, the inter-lab variations for REF and CTRL specimens regarding the initial as well as the final flow were very pronounced. Subsequently, the R_{WT} values showed a rather high scatter. For the REF specimens, negative values of R_{WT} were observed, as well. For the BAC specimens, the differences in average values among the laboratories were slightly decreased. However, no obvious trend was revealed within the same mixture or from one mixture to another, apart from a slight

decrease in water flow for the specimens that were tested after the healing treatment.

The high scatter of the intra-lab results within a mixture and for the same set of prisms (prisms test before or after healing) can be explained by the numerous crack geometries/widths that were obtained in the different specimens. It was, therefore, assumed that the most governing factor for this test was obviously the crack width, but at the point of the intersection between the crack and the cylindrical hole in the middle of the specimen.

In some cases, higher flow values were oddly observed after than before healing. This can be explained by the fact that the test was performed on different triplicates before and after healing. Occasionally, the (average) crack width of the specimens tested before healing was smaller than those tested after healing. Accordingly, the (average) water flow before healing was less than the flow of the specimens tested after healing, in the case where no significant healing had taken place. Thus, it was possible to acquire higher flow values for the triplicates tested after healing, which led to negative R_{WT} values.

5.3.4 WATER ABSORPTION TEST

The concept of the water absorption test was based on the hypothesis that there is always a certain behaviour regarding the absorption of each of the three types of specimens (non-cracked, non-healed and healed). The hypothesis states that the non-cracked specimens would soak up the least and the cracked non-healed specimens the maximum amount of water, since the presence of a crack could decrease the resistance to water uptake. In addition, the absorption capacity of the healed specimens would be somewhere between the values of the other two types of specimens. Another assumption is that the resulting curve of the water uptake in function with the square root of time would be linear and therefore the slope of each line will indicate the SC of each specimen. By combining the above, someone would expect that the SC classification would be as follows: $SC_{non\text{-}healed} > SC_{healed} > SC_{non\text{-}cracked}$.

However, none of the above-mentioned hypotheses were confirmed. Figure 5.12 shows the curves from three BAC specimens (a non-cracked, a non-healed and a healed one) that were tested at TU Delft. As can be seen from the graph, the curves were non-linear, and the SC classification hypothesis was not verified as well. It should be noted though that the SC classification derived from this graph was not representative of the results that were obtained among the four laboratories and for all mixture categories.

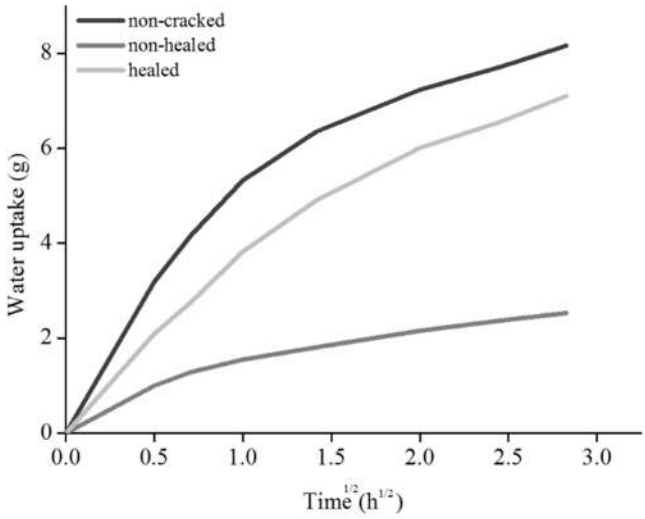

Figure 5.12 Water uptake as function of the square root of time for a non-cracked, a non-healed and a healed BAC specimen, tested at TU Delft.

According to Hall [4] capillary water absorption into porous building materials frequently increases with the square root of the elapsed time. The deviations from linear bahaviour arise from the lateral spreading of the wetting front that could be caused either by a 'leaky seal' and/or by a 'cut' on the face of the specimen that comes in contact with water as depicted in Figure 5.13.

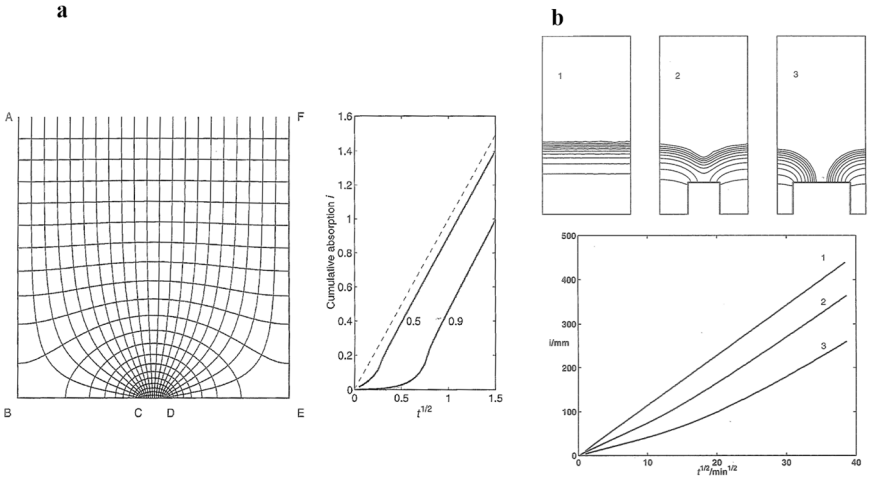

Figure 5.13 a. Left: The leaky seal problem. BC and DE are impermeable stripes and CD is a leak Right: The cumulative absorption plotted against $t^{1/2}$ for two different fractions of the covered surface (β); i.e. β=0,5 and β=0,9. The dashed

line shows the absorption for the unsealed surface. b. Advance of wetting front into complete and reduced (notched) areas in contact with water. The lower graph shows the cumulative absorption versus $t^{1/2}$ for the three cases.[5]

The curves in Figure 5.13 show some upward curvature (increase of water absorption with time), while the curves in Figure 5.12 show a downward curvature. Therefore, the deviation from the linear behaviour cannot be explained by the presence of either the sealed area or of the notch. Hall [4] mentions that the materials with coarse pore structures may show downward curvature in the absorption plot. In such cases, the data can fit to the following equation:

$$\boldsymbol{i = A_1 + St^{1/2} - A_2 t} \quad (5.3)$$

Where i is the cumulative water amount absorbed, S is the sorptivity of the material, t is the elapsed time and A_1 and A_2 are constants.

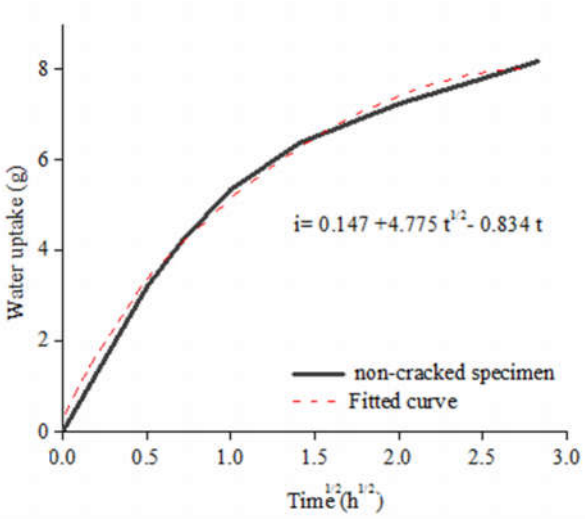

Figure 5.14 Curve fitting on the absorption curve of a non-cracked specimen.

Indeed, the data of the curves obtained by the water absorption tests could fit to such an equation as is shown in Figure 5.14. Consequently the SC values were calculated as indicated by Hall by applying equation 5.3, with the SC value being the factor (S) of the $t^{1/2}$.

Figure 5.15 presents the average SC of each specimen category (out of three replicates). The results of the water absorption test revealed a very random behaviour for all categories of specimens when results of the different testing laboratories are being compared. The SC values exhibited a high standard deviation even within the measurements of each individual laboratory, without

showing any particular trend. The initial hypothesis ($SC_{non\text{-}healed} > SC_{healed} > SC_{non\text{-}cracked}$) was certainly not confirmed.

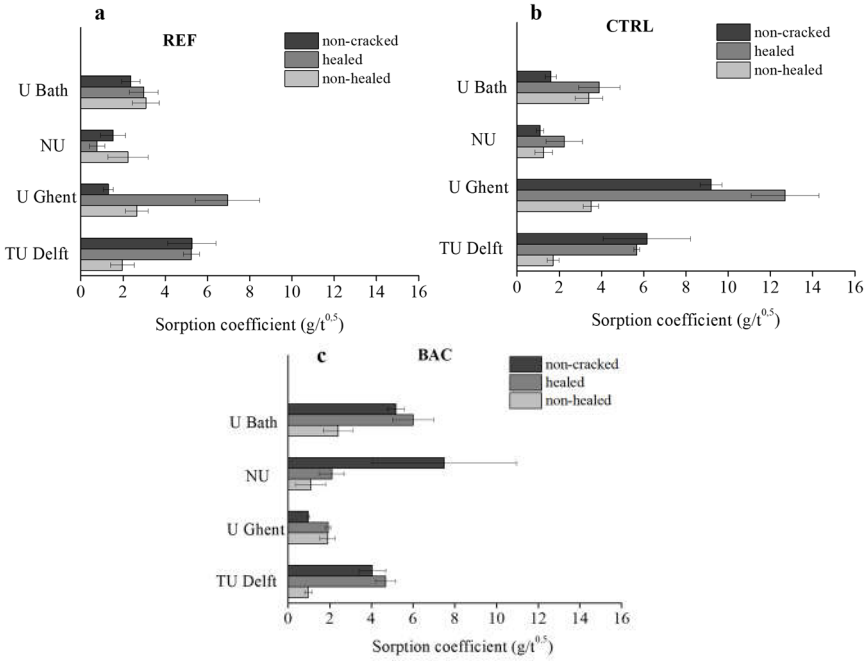

Figure 5.15 Average SC calculated from water absorption test for: a. REF specimens, b. CTRL specimens and c. BAC specimens.

5.4 DISCUSSION AND RECOMMENDATIONS

The permeability and the water absorption test results led to the conclusion that the crack width was the most governing factor for the outcome of the RRT. Even though each laboratory targeted the same crack width, the obtained results exhibited a large scatter. The reasons for such differences could be attributed partly to the non-consistent way of the applied cracking procedure as well as the procedure used for measuring the crack width or to the positioning of the LVDT, as mentioned earlier. Moreover, it was observed that the crack geometries obtained by the different laboratories were quite different even in the intra-lab level. The specimens were notched for purposes of controlling the position and the number of cracks. In other words, the notches were made to attract the crack at the specific point and to avoid multiple cracking. Yet, in some cases crack branching was detected at a height of a few millimetres over the notches as depicted in Figure 5.16.

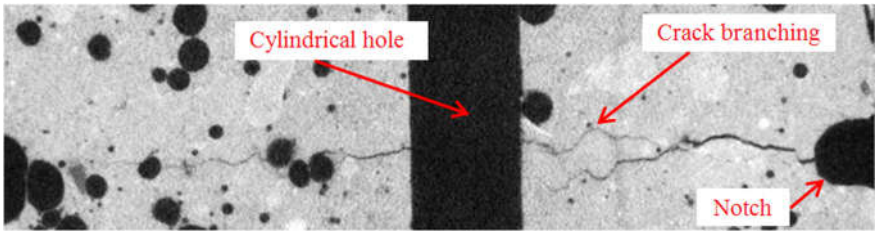

Figure 5.16 X-ray computed tomographic image on a cracked mortar specimen with cylindrical hole, cracked at U Ghent, showing crack branching.

The variations in crack shape and width can be additionally explained by:

- The different dimensions of the notches in every specimen. The notches were manually introduced and were targeted to have a 2-3 mm depth. However, there were only few cases where the correct notch was achieved. Furthermore, the method of the notch introduction varied among the laboratories.
- The type of the reinforcement. The steel reinforcing wires that were used were quite bendable. Thus, the reinforcement, after placed in the casting moulds, resembled more to a curved/corrugated wire rather than a straight steel bar. Consequently, the reinforcement prevented the total fracture of the prisms, however, it influenced the crack development by creating different crack geometries in each specimen.

The large scatter in shapes and crack width values was translated in equally large, if not larger, scatter in the results of the crack permeability test via water flow. The most influential factor that could have affected the uniformity of the results is the crack (width and geometry) dissimilarity. It is therefore recommended to reduce, as much as possible, this variability by:

- creating the notches during casting (in specially shaped moulds) rather than making them manually after casting and
- using steel bars with larger diameter to avoid arbitrary bending of the reinforcement.

In addition, to avoid the uncertainty in the results of the crack permeability test via water flow, it is of great importance to perform the initial (before healing) and final test (after healing) on the same set of specimens. This contributes to an objective comparison between the unhealed and the healed state of a sample, since every sample has its own features. Dissolution and loss of healing agent can be avoided either by using a liquid that is not in favour of dissolving the healing agent, for example a solution of water and ethanol, or a solution with higher pH

(carbonate-bicarbonate buffer), or by using gas, which means that the set-up should be redesigned. Yet, by employing those changes the test could give less heterogeneous results due to more homogenous specimen preparation regarding the actual healing performance of a specific specimen rather than an average trend of a set of specimens.

The results of the absorption test did not exhibit an unambiguous relation between water absorption and healing performance. The classification of the SC of a certain type category of specimens (REF, CTRL, BAC) varied significantly, depending on the laboratory that was performing the test. In reality, there are more factors than the crack opening and the potential (or not) presence of healing product, which can affect the absorption capacity of each specimen. As is suggested by the literature, the porosity, the presence and dimensions of a notch, and the sealing characteristics of each specimen can also influence the results. Therefore, the specimen preparation procedure, particular with respect to consistent crack formation, used in this round robin test experiment was not proved to be appropriate for accurate evaluation of the recovery of water-tightness in mortar specimens.

5.5 CONCLUDING REMARKS

The current chapter presented the results of a preliminary study from a round robin test that studied a set of proposed methodologies to evaluate the efficiency of self-healing in cementitious materials. This study revealed a large scatter in the obtained test results examining the water-tightness after the healing of the cracks. The bottleneck of the research regarding self-healing in cementitious materials is to find a way to produce identical cracks. Considering the inhomogeneity of mortar and of concrete this achievement was quite challenging. However, recommendations were given towards limiting the heterogeneity in shape and size of the cracks. The suitability of the proposed test methodologies was also questioned after the collection and comparison of the results. It seemed that the crack permeability test via water flow, which was performed on water saturated specimens, was mostly influenced by the crack width at intersection point between the cylindrical hole and the crack, while the water absorption test was affected by more factors than the crack opening and the occurrence of healing. Finally, the given recommendations should be further tested to evaluate the quality and reproducibility of the results obtained by the modified experimental methodology and to examine the possibility to come up with a standard procedure to investigate and quantify the healing potential of a cementitious material.

REFERENCES

[1] Tziviloglou, E., Wiktor, V., Wang, J., Paine, K., Alazhari, M., Richardson, A., Gueguen, M., Jonkers, H., Bertron, A., De Belie, N., and Schlangen, E., *Evaluation of experimental methodology to assess the sealing efficiency of bacteria-based self-healing mortar : Round Robin test*. 2016. In: RILEM Symposium in Microorganisms-Cementitious Materials Interactions. Delft, The Netherlands.

[2] EN 1015-11: Specifies a method for determining the flexural and compressive strenght of moulded mortar specimens.

[3] EN 13057: Products and systems for the protection and repair of concrete structures - Test methods - Determination of resistance of capillary absorption.

[4] Hall, C., *Water sorptivity of mortars and concretes: a review.* Magazine of Concrete Research, 1989. 41(147): p. 51-61.

[5] Hall, C. and Hoff, W.D., *Unsaturated flow in building physics*. in *Water Transport in Brick, Stone and Concrete*, Eds. 2011, CRC Press. p. 152-169.

6

Crack sealing efficiency of biogenic self-healing mortar studied by experimental and numerical methods

This chapter discusses the crack healing efficiency of biogenic healing mortar that was developed in the previous chapters. The investigation of sealing performance is conducted through experimental and computational approaches. Image processing and crack permeability test results are compared with results obtained by computer simulations. It is concluded that the experimental approaches might overestimate the crack closure percentage, while the computer simulation mostly underestimates the crack sealing. Finally, the study reveals that some modifications on both the experimental and the computational methodologies are needed to improve obtained results. The modifications are related to the shape of the crack that has been used, the set of specimens on which the permeability test has been performed, the replacement of 2-dimensional to 3-dimensional microscopic observations and the consideration of an additional factor in the crack filling equation used in the numerical model.

Parts of this chapter have been published in the journal paper entitled "Bio-based self-healing mortar: An experimental and numerical study", in the Journal of Advanced Concrete Technology, 2017 [1].

6.1 INTRODUCTION

The research on self-healing of cementitious materials often focuses on laboratory and experimental work [2]. Experimental studies are very useful to test and evaluate each self-healing concept and its functionality. There are various ways to examine and quantify the degree of self-healing. The most commonly used experimental techniques are presented below:

- Visual observations before and after the healing treatment mostly via optical microscopy [3-12], as an indication of the extent of (surficial) crack closure that took place.
- Mechanical testing to evaluate the strength and stiffness recovery [12-24].
- Crack water absorption tests [9, 12, 24-28] on non-cracked, cracked non-healed and cracked healed specimens, as described in 5.3.4.
- Crack permeability tests via water flow [4, 5, 19, 26, 29-35] on cracked non-healed and cracked healed specimens,
- Non-destructive testing techniques, based on ultrasonic measurements [36-38], acoustic emission [37-41], vibration analysis [37, 38] and resonance frequency [16, 42, 43].

There are only few publications that include modelling studies regarding self-healing in cementitious materials. It is a challenge for the researchers to simulate, apart from the crack development, the physico-chemical reactions that take place inside a crack due to self-healing processes. Several studies have simulated the healing of cracks based on the autogenous healing reaction and particularly on the further hydration of the unhydrated cement particles [44-48]. Other publications focus on specific self-healing systems [49-52]. However, there is only one study that is related to the modelling of biogenic self-healing concrete [2].

The aim of this chapter is to quantify and compare the crack closure of mortar specimens after healing treatment by two different experimental techniques (crack inspection via stereomicroscopic pictures and crack permeability tests via water flow) and a computer simulation. Although the crack permeability test and its reproducibility have been discussed in chapters 4 and 5, here results are combined with crack width measurements from microscopic observations and compared with two other methodologies that have been developed to quantify the crack closure of mortar specimens. The model that is described in this chapter was developed by Pan and Schlangen [53] and was initially used to obtain a mathematical basis for the choice of optimum amount of loaded lightweight aggregates (LWA) to be applied in the biogenic self-healing mortar. The three different methodologies give results regarding the healing efficiency of the

biogenic system. The chapter discusses and evaluates the obtained results. Finally, recommendations are given for improving crack healing evaluation methods.

6.2 MATERIALS AND METHODS

6.2.1 PREPARATION AND CRACKCING OF THE MORTAR PRISMS

The mortar mixture compounds and their proportions are presented in Table 4.1. The healing agent was prepared according to 4.2.1. Additionally, results of some prisms investigated in chapter 4 were also used in the results analysis in the current chapter.

Nine reinforced mortar prisms (40 mm x 40 mm x 160 mm) were considered in the present study. As described in chapter 4.2.3, three-point-bending (with a span of 100 mm) was used for crack introduction in 28-days-old mortar prisms. A single crack was created in each specimen. After unloading, the crack width reduced to approximately 0,27 - 0,36 mm. The depth of the crack was not monitored during bending, but it was observed through microscopic analysis. The microscopic images revealed that the crack was developed along the whole height of the specimens (larger on the bottom and zero on the top), therefore, the crack depth was almost equal to the height of the specimen, namely, 40 mm.

Following the crack creation, 6 out of 9 specimens were placed horizontally in a plastic container filled with tap water for crack healing, while 3 of them were immediately tested for water permeability. The 6 specimens were completely immersed in water while placed on the top of 10-mm-high spacers. The container was kept open to the atmosphere at standard room temperature (20 ± 2)°C at (60 ± 10)% RH. Three out of 6 specimens were left to heal for 28 days, while the other 3 for 56 days. Extra water was added, to keep a constant liquid-to-solid ratio.

6.2.2 CRACK INSPECTION

In chapter 4, the visual crack inspection was used only as an indication for the healing that took place. In this chapter, the crack inspection was used to primarily evaluate, but also quantify, the healing efficiency of the biogenic healing agent. The inspection was conducted in two steps; i.e. right after crack creation and after healing treatment. Images of the cracks were taken by a Leica MZ6 stereomicroscope with a Leica DFC420 camera. Image processing software (ImageJ) was used to estimate the width, the area on the bottom of each specimen and ultimately the volume of the crack. The crack width was considered as the average ($\overline{w}$) out of four measurements (w_1, w_2, w_3 and w_4) taken from the bottom of the specimen as seen in Figure 6.1. In many cases, shape imperfections (rough surface, air voids, etc.), due to casting procedure or poor compaction could cause unexpected local damages after cracking. Therefore, it was decided that the

estimation of the crack width should be undertaken by the above described methodology, where the measuring points were predetermined, but they could also be adjusted by the user in case that the point was coinciding with a matrix flaw. In addition, the specific measuring method has also been used in published studies [6, 11, 54].

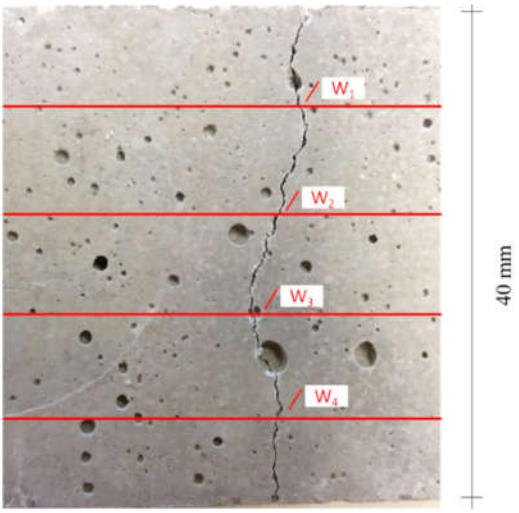

Figure 6.1 Measurements of crack width on the bottom of the specimen.

The assessment of crack volume was performed as follows: The stereomicroscopic image was thresholded to a grey value of 120 (Figure 6.2). Afterwards, the crack area (in pixels) was measured and converted to mm^2. In the microscopic images that were taken, the grey values of the mortar matrix and of the healing products were quite similar. Therefore, the thresholded grey value that was used was sufficient to separate and detect the solids (mortar and healing product) from the crack voids.

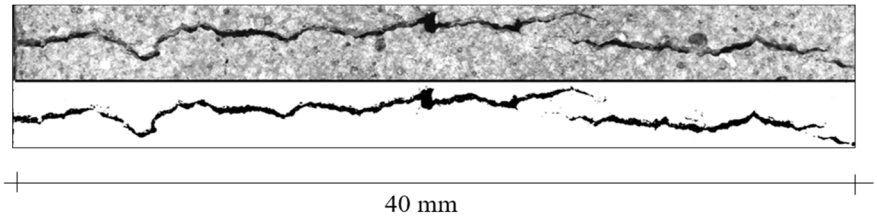

Figure 6.2 Crack geometry on the bottom of a specimen as determined by stereomicroscopy.

Figure 6.3 shows a strip of a cracked specimen before subjection to healing treatment. The picture was taken by a Phoenix Nanotom X-ray system (Phoenix X-ray Wunstorf, Germany). As can be seen, the crack is developed almost along

the whole height of the prismatic specimen. Moreover, the crack width decreases from the bottom to the top until it reaches zero. For simplicity in the estimation of the crack volume, it was therefore assumed that:

- the crack had a triangular shape,
- it was formed along the full height of the specimen and
- it exhibited identical geometry on the bottom as well as on the other crack sections.

Consequently, the crack volume was calculated by using the following formula:

$$\boldsymbol{V = \frac{1}{2} A \cdot h} \quad (6.1)$$

Where V is the volume of the crack, A is the area of the crack on the bottom section of the specimen as calculated by using image processing and h is the height of the specimen (40 mm). Furthermore, the sealing percentage α_m (for every specimen), i.e. the percentage of the crack volume that it is filled with healing product, was calculated as seen in Equation 6.2.

$$\boldsymbol{a_m = \frac{V_i - V_t}{V_i} \cdot 100\%} \quad (6.2)$$

Where V_i is the initial crack volume and V_t is the crack volume after healing time t (28 or 56 days).

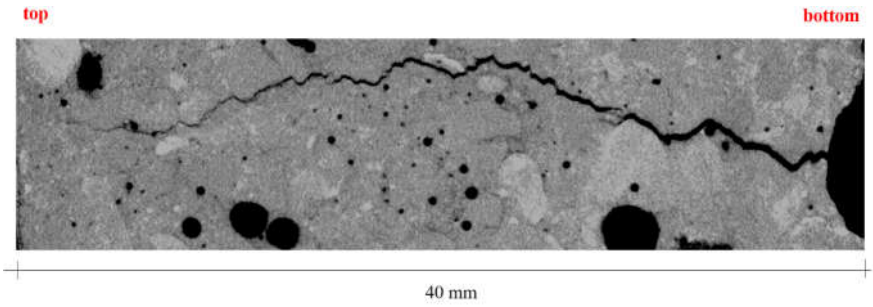

Figure 6.3 X-ray image of the crack of a specimen.

6.2.3 CRACK PERMEABILITY TEST

Following the crack inspection, the healing efficiency was also studied through a crack water permeability test in order to link the functional property (crack permeability) to the visual observations. The test was performed before and after the healing treatment. The set-up and the experimental process are described in 4.2.4. After the completion of the crack permeability tests, the R_{WT} for each set of the three replicate healed specimens was calculated as follows:

$$R_{WT} = 1 - \frac{\bar{m}_h}{\bar{m}_{n-h}} x\ 100\% \quad (6.3)$$

Where $\bar{m}_{n\text{-}h}$ is the average (out of three specimens) mass of water that has passed through the unhealed cracks of the three specimens in 5 minutes and $\bar{m}_h$is the average (out of three specimens) mass of water that has passed through the healed cracks of another three specimens in 5 minutes. Unlike the sealing percentage α_m, which was calculated for every specimen, the R_{WT} was calculated for the set of the tested specimens (in this case three). As has been explained in the previous chapters, the reason for this lies in the fact that the test was performed on different specimens sets before and after the healing treatment. The test was performed before healing treatment on a set of three and after healing on another set. The reason for testing different sets before and after healing was to avoid any loss of healing agent during the first permeability test that could possibly affect the healing process. This fact can influence the obtained results, in a sense that the tested cracks are not identical and might heal differently. Yet, the results can give a good indication for the extend of healing that has taken place during the healing treatment and can be used for comparison.

6.3 MODEL DESCRIPTION

A numerical simulation was conducted at meso-scale to estimate the sealing efficiency of the biogenic healing system and to determine the optimized usage of the healing agent. The model used in the simulation was the same as used for the experiments (a prism of 40 mm x 40 mm x 160 mm). In the meso-scale model, the mortar (hardened cement paste and sand) and the lightweight aggregates are taken as a homogeneous matrix and spherical inclusions respectively. Figure 6.4 shows a typical example of the simulated meso-scale model. The meso-scale model can also be extended to concrete in which the coarse aggregates are explicitly modelled.

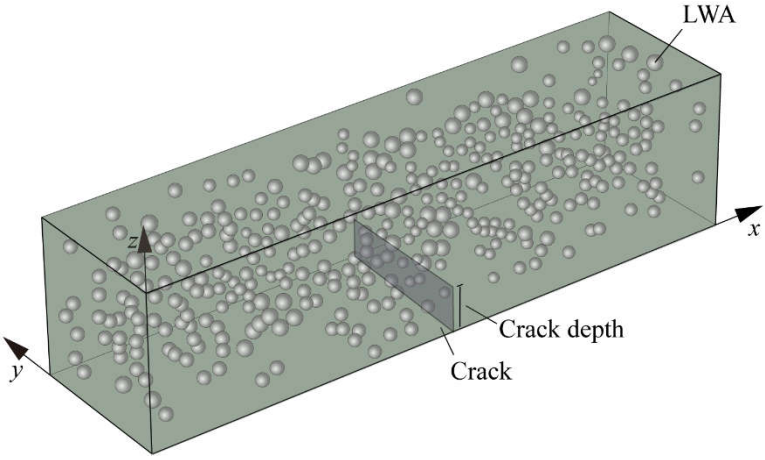

Figure 6.4 A schematic representation of the meso-scale mortar model containing LWA (based on the model described [53]).

To get the meso-scale model of the mortar, the size of each lightweight particle was randomly generated based on the gradation curve which was obtained by a sieve test (Figure 6.5). The process stopped when the volume fraction of all generated LWA reached the requirement. Then a packing algorithm based on the "take-and-place" method [55] was adopted to place the LWA into the meso-scale model. During this procedure, a separation check for each particle was conducted to ensure that it was not overlapping with any other particle that already existed in the model.

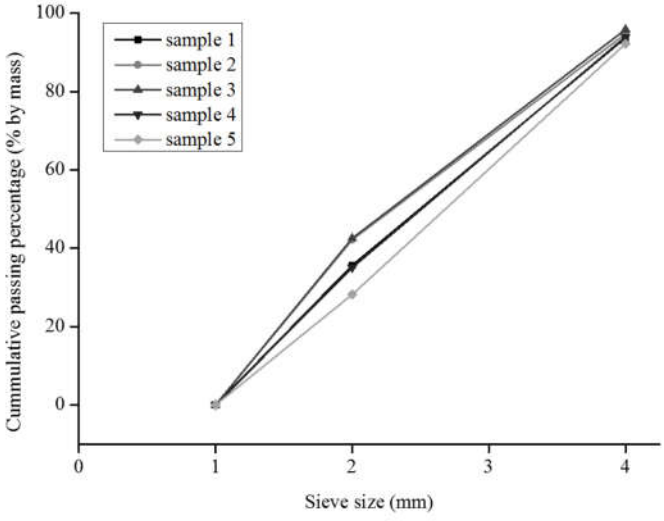

Figure 6.5 Liapor particle (LWA) size distribution

Following the creation of the meso-scale model, an artificial V-shaped crack was assumed in the middle of the prism, according to the experimental observations. Based on the size and the position of the LWA, all the lightweight particles which were intersected by the crack could be identified. These LWA were considered as damaged by the crack. Consequently, the healing agent lying inside the pores of the LWA would be released to form the chemical products which can seal the crack. The sealing percentage (α_s) according to the simulation can be expressed as in Equation 6.4:

$$\boldsymbol{a_s = \frac{V_{sp}}{V_{cr}} = \frac{V_{cp} \cdot \beta}{0.5 \cdot d_{cr} \cdot w \cdot l_y}} \ \% \quad (6.4)$$

Where V_{sp}, V_{cr} and V_{cp} represent the volume of the healing product, the volume of the crack and the volume of the cracked particles respectively; d_{cr} is the crack depth which in this case (to compare with the experimental results) coincides with the height of the specimen; w is the crack width; l_y is the length of the model in the y direction and β is a dimensionless parameter which represents the amount of sealing product that can be formed for each unit of volume of LWA. In the simulation of a three-point bending test, the crack is assumed to be initiated in the middle of the specimen, i.e., $x = 0.5l_x$, where l_x is the model size along the x-direction. It is also assumed that the crack can propagate through a lightweight particle, due to its lower strength compared to a normal aggregate. Thus, the cracked LWA can be identified by checking whether they have been intersected by the crack surface. Then, the total volume of cracked LWA, i.e., V_{cp}, can be calculated according to the diameter of each cracked particle.

The concept of the biogenic self-healing concrete indicates that in the presence of oxygen and water inside the crack, the dormant bacterial spores are activated. Subsequently, the active bacterial cells convert the calcium lactate present in the healing agent to calcium carbonate ($CaCO_3$) by using oxygen. Thus, when the healing agent of the cracked LWA is released into the cement paste, the following chemical reaction will occur [6]:

$$\boldsymbol{CaC_6H_{10}O_6 + 6\,O_2 \rightarrow CaCO_3 + 5CO_2 + 5H_2O} \quad (6.5)$$

Carbon dioxide (CO_2) formed during the above reaction can further react with portlandite ($Ca(OH)_2$) present in the mortar matrix as a product of cement hydration:

$$\boldsymbol{Ca(OH)_2 + CO_2 \rightarrow CaCO_3 + H_2O} \quad (6.6)$$

Based on the above chemical reactions, $CaCO_3$ is considered as the product which seals the crack. Thus, β in Equation 6.4 can be calculated as:

$$\boldsymbol{\beta} = \frac{\boldsymbol{\gamma \cdot 650 \cdot 6 \cdot 0.10009}}{\boldsymbol{0.218\ 22 27\ 11}} = \boldsymbol{0.66 \cdot \gamma} \quad (6.7)$$

In Equation 6.7, 650 (kg/m^3) is the packing density of the LWA used in the experiment; 0.21822 (kg/mol) is the molar mass of calcium lactate; 0.10009 (kg/mol) and 2711 (kg/m^3) are the molar mass and density of $CaCO_3$, respectively; the coefficient 6 represents the (total) mol of $CaCO_3$ that can be produced by 1 mol of calcium lactate (from Equations 6.5 and 6.6); γ is the mass of the healing agent inside the unit mass of the LWA which is measured in the experiment. Based on a test on several LWA, it was found that γ varies between 1.4 and 38.7. Thus, γ was taken as a random variable following a uniform distribution in [1.41, 38.69]. With the value of β in Equation 6.7, the sealing percentage (α_s) can be calculated according to Equation 6.4. However, since the meso-scale model is randomly generated, α_s should be considered as a random variable. Hence, in the following part of this chapter, not only the average, but also the standard deviation of the sealing percentage was considered. The reason to consider the standard deviation is that this parameter (γ) has a large degree of variation (γ=1.4~38.7). Thus, the simulation is performed in a probabilistic approach. In addition, the standard deviation was also considered to know whether the variation of input parameters can significantly affect the output result.

An overview of the numerical simulation steps that were undertaken to establish the sealing percentage (α_s) is depicted in Figure 6.6.

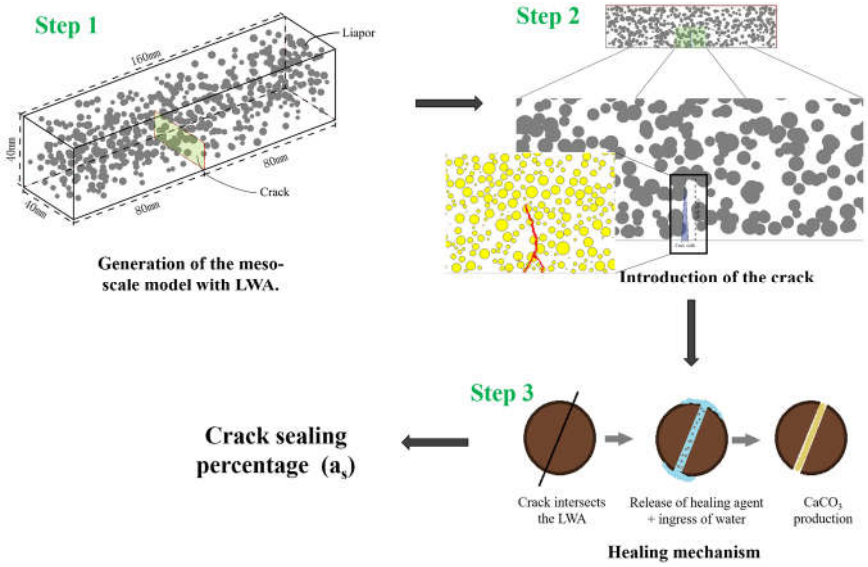

Figure 6.6 Overview of the numerical simulation steps, as described in [1].

6.4 RESULTS

6.4.1 CRACK HEALING ESTIMATION

The specimens were loaded until the crack opening reached 0.4 mm. However, after unloading the crack width was varying from 0.266 to 0.356 mm, based on the average values obtained by the stereomicroscopic observations. The crack width exhibited an almost linear relation with the crack volume as seen in Figure 6.7. The relation between crack width and volume is not perfectly linear since the crack width values come from the average values at different points of the crack, while the crack volume from Equation 6.1, uses the total area on the bottom of the crack. However, the fact that they exhibit this linearity shows that both crack magnitude estimation methods are in good agreement.

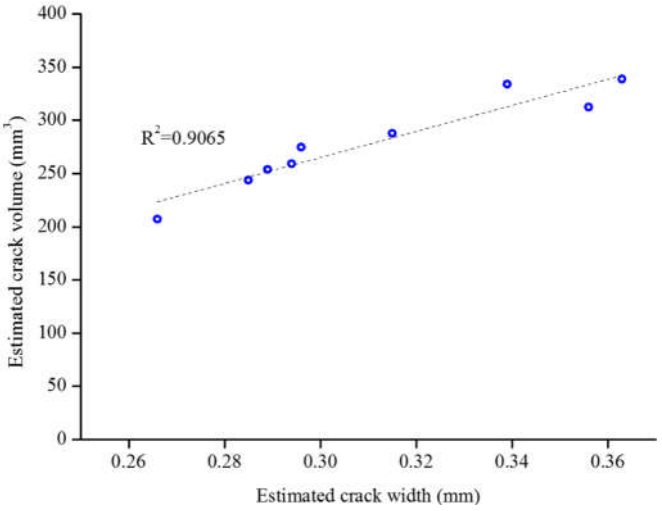

Figure 6.7. Estimated crack width versus estimated crack volume of mortar specimens.

Table 6.1 shows the average measured crack width, the crack volume before and after the healing treatment, and the calculated sealing percentage (α_m) based on microscopic observations (from Equation 6.2). Specimens 1, 2, and 3 were used as reference for the crack permeability test, and thus were not subjected to healing treatment. Specimens 4, 5, and 6 and 7, 8, and 9 were submerged in water for 28 and 56 days respectively. From the results it can be stated that crack closure percentage increased for the specimens immersed in water for 56 days in comparison to those immersed for 28 days. In addition, it could have been expected that the smaller crack volumes would result in more efficient crack closure. However, this was not concluded from the microscopic observations.

Table 6.1 Estimated crack width, volume and closure percentage.

Specimen	$\overline{w}$	V		α_m
		before healing	after healing	
	(mm)	(mm^3)		(%)
1	0.289	253.98	-	-
2	0.315	287.90	-	-
3	0.266	207.26	-	-
4	0.339	334.22	114.04	65.88
5	0.294	259.32	172.24	33.60
6	0.356	312.5	52.66	83.15
7	0.363	338.92	27.66	91.83
8	0.285	243.78	77.02	68.41
9	0.296	274.74	3.56	98.70

Table 6.2 shows the average measured crack width and the sealing percentage (α_s), as derived from the simulations. Contrary to the relation between $\overline{w}$ and α_m, the relation between $\overline{w}$ and α_s is linear (Figure 6.8). In other words, the model indicates that the narrower the crack the more efficient the sealing, while the microscopic observations did not support this result.

Table 6.2 Average measured crack width and corresponding sealing percentage as obtained by the simulations.

Specimen	$\overline{w}$	α_s
	(mm)	(%)
4	0.339	60.14 ±3.87
5	0.294	69.38 ±4.27
6	0.356	57.20 ± 3.50
7	0.363	56.23 ±3.63
8	0.285	71.43 ± 4.54
9	0.296	68.70 ±4.24

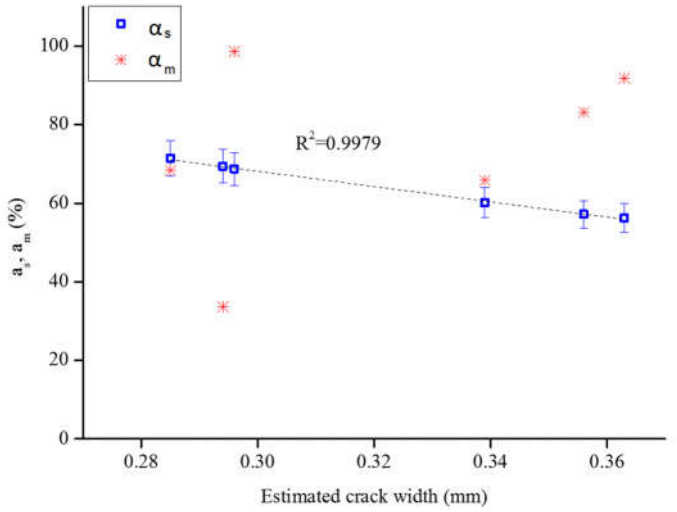

Figure 6.8 Estimated crack width versus crack closure percentage (microscopic observations) and sealing percentage (simulations).

6.4.2 CRACK PERMEABILITY RESULTS

The results from the crack permeability test as well as the R_{WT} for the two sets of specimens are presented in Table 6.3. The results from the water flow test on cracked non-healed specimens indicate that a larger crack area results in an increased flow. In addition, from the calculation of the recovery of water-tightness it was derived that a longer immersion period led to a decreased water flow, therefore, in a more efficient sealing. The results from the water flow test on cracked non-healed specimens indicate that a larger crack area results in an increased flow. In addition, from the calculation of the recovery of water-tightness it was derived that a longer immersion period resulted in a decreased water flow, therefore, in a more efficient sealing.

Table 6.3. Results from crack permeability test on prismatic mortar specimens.

Sample	$\bar{w}$	Mass of water collected		R_{WT}
		before healing	after healing	
	(mm)	(g)		(%)
1	0.289	405.1	-	
2	0.315	670.1	-	-
3	0.266	323.5	-	
4	0.339	-	137.3	
5	0.294	-	108.3	69.41
6	0.356	-	190.2	
7	0.363	-	54.5	
8	0.285	-	33.6	91.75
9	0.296	-	29.4	

6.5 DISCUSSION

This chapter used three different parameters to evaluate the healing efficiency of the biogenic self-healing system. All three (α_m, R_{WT} and α_s) are based on different ways of investigation, namely microscopy observations, crack permeability test and numerical simulations. However, they are designed to quantify the healing efficiency of cracks with a specified width. The comparison of α_m and α_s values (Figure 6.8) revealed that the sealing values obtained by the two different methods do not agree. In fact, microscopic observations proved that the healing that might take place in a crack is not inextricably linked with the crack width, while the numerical simulation showed exactly the opposite. This can be attributed to the assumptions made for both the crack volume calculations and the model. For example, for the calculation of the α_m it was presumed that the ratio filled-to-empty crack area, along the crack depth, is the same as on the bottom section of the specimen. This is probably overestimating the real volume of the $CaCO_3$ in the crack. Furthermore, the model took into account that all the healing agent included in the LWA, which were intersected by the crack, is released and then converted into $CaCO_3$. In reality, only a part of the healing agent is released and it depends on the plane that the crack has intersected the LWA and on the load of healing agent that each particle contains. In addition, the model did not consider that a potential blockage of the crack (from sealing products or from impurities) can cause depletion of oxygen and therefore limited conversion of the feed into sealing product, which might be the reason why narrower cracks are likely to show a

reduced healing. Moreover, in the model, the duration of the immersion period was not taken in consideration, consequently α_s was independent of the healing period. Thus, α_s exhibits roughly similar values for 28 or 56 days of immersion (62,24% and 65,45% respectively, see Table 6.4). The difference in α_s for 28 and 56 days is exclusively attributed to the different crack widths of the specimens.

Additionally, the comparison among α_s, α_m and R_{WT} was conducted for sets of specimens and not separately for each specimen. Thus, Table 6.4 presents the average values of α_m and α_s, as well as R_{WT} values for the sets of three specimens immersed in water for 28 and 56 days. In this case, the results of α_m and R_{WT} are in good agreement for both immersion periods. The α_s average value for 28 days of immersion is similar to the average values of the other two parameters, however, for 56 days the value is significantly lower for the reason that was previously discussed. In general, R_{WT} is higher than the average α_m and α_s, since the crack flow test is highly dependent on the crack opening at the position of the hole. Usually at this position (20 mm from the bottom of the specimen) the crack width is narrower than on the bottom and it is more likely to be fully sealed. In this case, the real R_{WT} value is probably overestimated.

Table 6.4. Values for sealing parameters (α_m, α_s and R_{WT}) for set of specimens immersed for 28 and 56 days in water.

Sealing parameter	Days of immersion	
	28	56
α_m	60.88	86.31
α_s	62.24	65.45
R_{WT}	69.41	91.75

6.6 CONCLUDING REMARKS

In conclusion, this chapter summarizes three different methodologies to evaluate the healing efficiency of the biogenic self-healing mortar; two of them are based on experiments (image processing and crack permeability test), while the last one is based on computer simulations. It was concluded that the experimental approaches might overestimate the crack closure due to:

- the hypothesis that the crack filling is constant along the crack length, or
- the fact that the crack permeability test is conducted on different sets of specimens before and after healing treatment, or

- the smaller crack width at the position of the (water passage) hole compared to the crack width on the bottom of the specimens.

In addition, the numerical model results can slightly overestimate the volume of the filling product, due to the assumption that all the healing agent included in the LWA intersected by the crack was released and converted to calcium carbonate. Yet, in general, the model underestimates the total volume of $CaCO_3$ produced in the crack because:

- the duration of the immersion period was not considered as a model variable; therefore, the sealing efficiency was independent of the healing period and
- the autogenous healing processes that occur during the healing treatment in water were also not considered.

Hence, some modifications on the experimental as well as on the computational part are needed to obtain more realistic results. The permeability test results can be improved if the test will be performed on the same set of specimens before and after healing, as has been discussed in chapter 5. The danger of losing the healing agent during the first cycle of testing can be avoided by using a liquid in which calcium lactate is less soluble than in water. In addition, a straight rather than a V-shaped crack could cause less heterogeneity in results. Moreover, the image processing could be more accurate if the microscopic observations will not only be limited to the outer surfaces of the crack, but also include other cross sections. Therefore, area (2-dimensional) will be replaced by volume (3-dimensional) observations. Further experimental research should also investigate whether the numerical model needs to include a "reduction factor", which will determine how much of initially existed healing agent participates in the crack filling process.

Finally, it could be stated that the reactions that take place inside the crack are quite complex and depend on several factors, such as the (local) crack width, the presence of humidity and oxygen, the duration of healing treatment, blockage of the crack etc. Although both experimental and computational methodologies need some improvements to mimic a more realistic situation, the current approaches can already provide an indication of the enhanced sealing behaviour originating from the biogenic self-healing system.

REFERENCES

[1] Tziviloglou, E., Pan, Z., H.M., J., and Schlangen, E., *Bio-based self-healing mortar: An experimental and numerical study.* Journal of Advanced Concrete Technology, 2017.

[2] Zemskov, S.V., Jonkers, H.M., and Vermolen, F.J., *Two analytical models for the probability characteristics of a crack hitting encapsulated particles: Application to self-healing materials.* Computational Materials Science, 2011. 50(12): p. 3323-3333.

[3] Lee, H.X.D., Wong, H.S., and NR, B., *Potential of superabsorbent polymer for self-sealing cracks in concrete.* Composites Part B: Engineering, 2010. 29(6): p. 819-827.

[4] Van Tittelboom, K., Adesanya, K., Dubruel, P., Van Puyvelde, P., and De Belie, N., *Methyl methacrylate as a healing agent for self-healing cementitious materials.* Smart Materials and Structures, 2011. 20(12): p. 125016.

[5] Ma, H., Qian, S., and Zhang, Z., *Effect of self-healing on water permeability and mechanical property of Medium-Early-Strength Engineered Cementitious Composites.* Construction and Building Materials, 2014. 68: p. 92-101.

[6] Wiktor, V. and Jonkers, H.M., *Quantification of crack-healing in novel bacteria-based self-healing concrete.* Cement and Concrete Composites, 2011. 33(7): p. 763-770.

[7] Li, V.C. and Herbert, N., *Robust Self-Healing Concrete for Sustainable Infrastructure.* Journal of advanced concrete technology, 2012. 10: p. 207-218.

[8] Wang, J.Y., Snoeck, D., Van Vlierberghe, S., Verstraete, W., and De Belie, N., *Application of hydrogel encapsulated carbonate precipitating bacteria for approaching a realistic self-healing in concrete.* Construction and Building Materials, 2014. 68: p. 110-119.

[9] Zhang, Z., Qian, S., and Ma, H., *Investigating mechanical properties and self-healing behavior of micro-cracked ECC with different volume of fly ash.* Construction and Building Materials, 2014. 52: p. 17-23.

[10] Krelani, V., Self-healing capacity of cementitious composites. 2015. PhD Thesis, Politecnico di Milano,

[11] Palin, D., Wiktor, V., and Jonkers, H.M., *Autogenous healing of marine exposed concrete: Characterization and quantification through visual crack closure.* Cement and Concrete Research, 2015. 73: p. 17-24.

[12] Alghamri, R., Kanellopoulos, A., and Al-Tabbaa, A., *Impregnation and encapsulation of lightweight aggregates for self-healing concrete.* Construction and Building Materials, 2016. 124: p. 910-921.

[13] Dry, C., *Matrix cracking repair and filling using active and passive modes for smart timed release of chemicals from fibers into cement matrices.* Smart Materials and Structures, 1994. 3(2): p. 118.

[14] Li, V.C., Lim, Y.M., and Chan, Y.-W., *Feasibility study of a passive smart self-healing cementitious composite.* Composites Part B: Engineering, 1998. 29(6): p. 819-827.

[15] Tziviloglou, E., Self-healing in ECC materials with low content of different microfibers and micro-particles. 2009. MSc, Delft University of Technology, Delft.

[16] Yang, Y., Lepech, M.D., Yang, E.H., and Li, V.C., *Autogenous healing of engineered cementitious composites under wet-dry cycles.* Cement and Concrete Research, 2009. 39(5): p. 382-390.

[17] Joseph, C., Jefferson, A.D., Isaacs, B., Lark, R.J., and Gardner, D.R., *Experimental investigation of adhesive-based self-healing of cementitious materials.* Magazine of Concrete Research, 2010. 62(11): p. 831-843.

[18] Kim, J.S. and Schlangen, E., *Self-healing in ECC stimulated by SAP under flexural cyclic load* In: 3rd International Conference on Self-Healing Materials. 2011. Bath, UK.

[19] Van Tittelboom, K., De Belie, N., Van Loo, D., and Jacobs, P., *Self-healing efficiency of cementitious materials containing tubular capsules filled with healing agent.* Cement and Concrete Composites, 2011. 33(4): p. 497-505.

[20] Yang, Z., Hollar, J., He, X., and Shi, X., *A self-healing cementitious composite using oil core/silica gel shell microcapsules.* Cement and Concrete Composites, 2011. 33(4): p. 506-512.

[21] Şahmaran, M., Yildirim, G., Ozbay, E., Ahmed, K., and Lachemi, M., *Self-healing ability of cementitious composites: effect of addition of pre-soaked expanded perlite.* Magazine of Concrete Research, 2014. 66(8): p. 409-419.

[22] Sierra-Beltran, M.G., Jonkers, H.M., and Schlangen, E., *Characterization of sustainable bio-based mortar for concrete repair.* Construction and Building Materials, 2014. 67: p. 344-352.

[23] Chen, H., Qian, C., and Huang, H., *Self-healing cementitious materials based on bacteria and nutrients immobilized respectively.* Construction and Building Materials, 2016. 126: p. 297-303.

[24] Feiteira, J., Gruyaert, E., and De Belie, N., *Self-healing of moving cracks in concrete by means of encapsulated polymer precursors.* Construction and Building Materials, 2016. 102, Part 1: p. 671-678.

[25] Sisomphon, K., Copuroglu, O., and Fraaij, A., *Application of encapsulated lightweight aggregate impregnated with sodium monofluorophosphate as a self-healing agent in blast furnace slag mortar* HERON, 2011. 56(1): p. 13-32.

[26] Wang, J., Soens, H., Verstraete, W., and De Belie, N., *Self-healing concrete by use of microencapsulated bacterial spores.* Cement and concrete research 2014. 56: p. 139-152.

[27] Kanellopoulos, A., Qureshi, T.S., and Al-Tabbaa, A., *Glass encapsulated minerals for self-healing in cement based composites.* Construction and Building Materials, 2015. 98: p. 780-791.

[28] Qureshi, T.S., Kanellopoulos, A., and Al-Tabbaa, A., *Encapsulation of expansive powder minerals within a concentric glass capsule system for self-healing concrete.* Construction and Building Materials, 2016. 121: p. 629-643.

[29] Tziviloglou, E., Wiktor, V., Jonkers, H.M., and Schlangen, E., *Bacteria-based self-healing concrete to increase liquid tightness of cracks.* Construction and Building Materials, 2016. 122: p. 118-125.

[30] Edvardsen, C., *Water Permeability and Autogenous Healing of Cracks In Concrete.* ACI materials journal, 1999. 96(4): p. 448-454.

[31] Reinhardt, H.W. and Jooss, M., *Permeability and self-healing of cracked concrete as a function of temperature and crack width.* Cement and Concrete Research, 2003. 33(7): p. 981-985.

[32] Lepech, M.D. and Li, V.C., *Water permeability of engineered cementitious composites.* Cement and Concrete Composites, 2009. 31(10): p. 744-753.

[33] Palin, D., Wiktor, V., and Jonkers, H.M., *A bacteria-based bead for possible self-healing marine concrete applications.* Smart Materials and Structures, 2016. 25: p. 084008.

[34] Gruyaert, E., Debbaut, B., Snoeck, D., De Belie, N., Diaz, P., Arizo, A., Tziviloglou, E., and Schlangen, E., *Self-healing mortar with pH-sensitive superabsorbent polymers: Testing of the sealing efficiency by water flow tests.* Smart Materials and Structures, 2016. 25(8).

[35] Mors, R.M. and Jonkers, H.M., *Feasibility of lactate derivative based agent as additive for concrete for regain of crack water tightness by bacterial metabolism.* Industrial Crops and Products.

[36] In, C.-W., Holland, R.B., Kim, J.-Y., Kurtis, K.E., Kahn, L.F., and Jacobs, L.J., *Monitoring and evaluation of self-healing in concrete using diffuse ultrasound.* NDT & E International, 2013. 57: p. 36-44.

[37] Malm, F. and Grosse, C.U., *Efficiency of self-healing agents for cementitious materials characterized by NDT*. 2016. In: 19th World Conference on Non-Destructive Testing 2016. Munich, Germany.

[38] Gruyaert, E., Feiteira, J., Nele De, B., Malm, F., Nahm, M., Grosse, C.U., and Tziviloglou, E., *Non-destructive testing techniques to evaluate the healing efficiency of self-healing concrete at lab-scale*. 2016. In: Emerging Technologies in Non-Destructive Testing VI. Aggelis, D.G., et al. Leiden, The Netherlands.

[39] Granger, S., Loukili, A., Pijaudier-Cabot, G., and Chanvillard, G., *Experimental characterization of the self-healing of cracks in an ultra high performance cementitious material: Mechanical tests and acoustic emission analysis.* Cement and Concrete Research, 2007. 37(4): p. 519-527.

[40] Feiteira, J., Tsangouri, E., Gruyaert, E., Lors, C., Louis, G., and De Belie, N., *Monitoring crack movement in polymer-based self-healing concrete through digital image correlation, acoustic emission analysis and SEM in-situ loading.* Materials & Design, 2017. 115: p. 238-246.

[41] Van Tittelboom, K., De Belie, N., Lehmann, F., and Grosse, C.U., *Acoustic emission analysis for the quantification of autonomous crack healing in concrete.* Construction and Building Materials, 2012. 28(1): p. 333-341.

[42] Jacobsen, S. and Sellevold, E.J., *Self healing of high strength concrete after deterioration by freeze/thaw.* Cement and Concrete Research, 1996. 26(1): p. 55-62.

[43] Yildirim, G., Aras, G.H., Banyhussan, Q.S., Şahmaran, M., and Lachemi, M., *Estimating the self-healing capability of cementitious composites through non-destructive electrical-based monitoring.* NDT & E International, 2015. 76: p. 26-37.

[44] He, H., Guo, Z., Stroeven, P., Stroeven, M., and Sluys, L.J., *Self-healing capacity of concrete - computer simulation study of unhydrated cment structure.* Image Analysis nad Stereology, 2007. 26: p. 137-143.

[45] Ye, G. and Van Breugel, K., *Potential use of HYMOSTRUC cement hydration model for self-healing of microcracks in cementitious materials*. 2007. In: First International Conference on Self Healing Materials Noordwijk aan Zee.

[46] Lv, Z. and Chen, H., *Modeling of self-healing efficiency for cracks due to unhydrated cement nuclei in hardened cement paste.* Procedia Engineering, 2012. 27: p. 281-290.

[47] Huang, H. and Ye, G., *Simulation of self-healing by further hydration in cementitious materials.* Cement and Concrete Composites, 2012. 34(4): p. 460-467.

[48] Krelani, V. and Ferrara, L., *A numerical model for the self-healing capacity of cementitious composites*. in *Computational Modelling of Concrete Structures*, Eds. Bícanić, N., et al. 2014, CRC Press. p. 471-474.

[49] Joseph, C., Experimental and numerical study of the fracture and self-healing of cementitious materials. 2008. PhD Thesis, Cardiff University, UK,

[50] Hilloulin, B., Hilloulin, D., Grondin, F., Loukili, A., and De Belie, N., *Mechanical regains due to self-healing in cementitious materials: Experimental measurements and micro-mechanical model.* Cement and Concrete Research, 2016. 80: p. 21-32.

[51] Savija, B., Feiteira, J., Araújo, M., Chatrabhuti, S., Raquez, J.-M., K., V.T., Gruyaert, E., N., D.B., and Schlangen, E., *Simulation-Aided Design of Tubular Polymeric Capsules for Self-Healing Concrete.* Materials, 2017. 10(1).

[52] Gilabert, F.A., Van Tittelboom, K., Van Stappen, J., Cnudde, V., De Belie, N., and Van Paepegem, W., *Integral procedure to assess crack filling and mechanical contribution of polymer-based healing agent in encapsulation-based self-healing concrete.* Cement and Concrete Composites, 2017. 77: p. 68-80.

[53] Pan, Z. and Schlangen, E., *A three-dimensional numerical research on probability characteristics of a crack hitting capsules for self-healing concrete* 2015. In: 5th international conference on self-healing materials. Durham, North Carolina, USA.

[54] Wang, J., Dewanckele, J., Cnudde, V., van Vlierberghe, S., Verstraete, W., and de Belie, N., *X-ray computed tomography proof of bacterial*

based self-healing in concrete. Cement and Concrete Composites, 2014. 53(289-304).

[55] Wang, Z.M., Kwan, A.K.H., and Chan, H.C., *Mesoscopic study of concrete I: generation of random aggregate structure and finite element mesh.* Computers & Structures, 1999. 70(5): p. 533-544.

7

Retrospection, conclusions and prospects

This chapter presents the highlights, a summary of the general conclusions that may be drawn from the current thesis and finally recommendations on the outlook of the research.

7.1 RETROSPECTION

Self-healing concrete has been introduced for almost two decades as an alternative to the conventual concrete repair systems. Research has proven that the self-healing technology can efficiently repair micro-cracks and avoid the limitations related to the application of ordinary concrete repair materials.

Numerous researchers worldwide have developed self-healing systems for cementitious materials using different types of healing agents, which often aim to limit the crack width, to expand the cement matrix or to release a(n) (encapsulated) healing agent in the cracks. Restrictions and recommendations for further improvements are presented in the related studies as well. Among the different self-healing systems, the use of biogenic healing agents has gained ground in the last decade. Biogenic self-healing agents can outbalance the other existing self-healing systems, since their nature and the way they work can prolong the functionality and increase the sustainability of a cementitious material. The different biogenic self-healing systems that have been known are based on three different bacterial metabolic pathways; namely, the hydrolysis of urea, the oxidation of organic compounds using oxygen under aerobic conditions or the oxidation of organic compounds using nitrate under anaerobic conditions.

The objective of this research project was to primarily develop the biogenic healing agent and investigate the mechanical and the crack sealing behaviour of biogenic self-healing mortar. Moreover, the research focused on developing an experimental methodology for quantifying and evaluating the recovery of crack sealing at laboratory scale.

The current thesis investigated the incorporation and the efficiency of the biogenic system, which works with the oxidation of organic carbon using oxygen, in mortar. Previous research has proven the potential in applying the specific biogenic healing agent for self-healing in cementitious materials. However, towards developing the healing agent, several aspects related to the physical properties of the lightweight aggregates (LWA), the selection of the organic carbon source, its encapsulation and activation in the LWA needed to be carefully considered and therefore were discussed in the third chapter. In direction of investigating the properties of the biogenic self-healing mortar, the compatibility and functionality of the biogenic healing agent when incorporated in the cementitious matrix was studied through fresh- and hardened-state properties, recovery of water-tightness and bacterial activity tests.

The final focus of the thesis was to develop a standardised methodology to assess self-healing at laboratory scale. The development of an experimental protocol originated from the need to establish an experimental methodology, which could be applied on self-healing mortars with different implemented self-healing

strategies. The methodology consisted of crack permeability, water absorption and flexural tests for the evaluation of the ability of a mortar to regain liquid-tightness and mechanical properties after cracking and healing. Towards standardization, a round robin test was organized to test and finally assess the reproducibility and the quality of the obtained results.

Finally, the experimental results were compared with the results of a computer simulation. Crack inspection via stereomicroscopy, crack permeability tests via water flow and a computer model were used to quantify the crack volume occupied by healing material after the healing treatment. The results suggested that there are limitations regarding both the laboratory tests and the computer simulation, however, these currently available methods can provide an indication of the efficiency of the biogenic healing agent.

7.2 GENERAL CONCLUSIONS

In this thesis, the biogenic healing agent embedded in expanded clay particles was developed and optimized. The healing performance of the biogenic agent incorporated in the mortar, was evaluated mostly through experimental techniques. The following conclusions were drawn:

- The bacterial cells that have been pre-grown on a certain organic compound can degrade it easily when they find it afterwards in their environment. Therefore, the bacteria cells can develop a sort of memory.
- Calcium lactate and calcium acetate are appropriate nutrient sources for the alkaliphilic bacteria that were used for the specific healing agent. In addition, these organic compounds do not negatively affect the compressive strength of the mortar when found in the mixture in amounts between 0.56 and 2.24% per cement weight.
- The impregnation of the healing agent was conducted via vacuum treatment, followed by drying at room temperature. The end result was that healing agent incorporated in the pores of the LWA increased their dry weight by 11.3%.
- By comparing two mortars with identical mixture proportions but with unloaded and loaded LWA, it was found that the setting time, the density and the air content of the fresh mixtures can be significantly affected by the addition of the healing agent, while the flexural and compressive strength of the hardened mortar remained similar.
- The lightweight mortar with biogenic healing agent exhibited improved crack sealing, particularly when subjected to wet-dry cycles, compared to when subjected to continuous water immersion. Oxygen

consumption measurements and bacterial traces found on calcium carbonate ($CaCO_3$) crystals proved that the enhanced sealing behaviour of the biogenic mortar originated from the bacterial activity.

- The recovery of flexural strength was very limited for the mortar specimens with and without the biogenic healing agent.
- The large scatter in the results of the tests that examine the recovery of water-tightness after the healing treatment reveal that the bottleneck of the research regarding quantification of self-healing in cementitious materials is to find a way to produce identical cracks, so that there is a common base for the comparison of the healing performance of the different specimens.
- The porosity and the presence of a notch in test specimens affected the results of the water absorption test. The fact that those factors are not related with the crack opening or the presence of healing agent can question the suitability of the suggested assessment method.
- Image processing and crack permeability tests were used to evaluate the healing efficiency of the biogenic self-healing mortar. The methodologies might overestimate the efficiency of crack closure, due to assumptions related to the geometrical characteristics of the cracks and of the specimens.
- For the computer model, it was assumed that all the amount of the healing agent included in the LWA intersected by the crack would be released and converted to $CaCO_3$. This might lead to overestimation of the crack filling that would take place during the healing treatment. In addition, the model underestimates the final crack healing, since it does not consider the duration of the immersion period and the potential autogenous healing that can occur. Therefore, some modifications are needed to obtain more realistic results.

7.3 PROSPECTS

This thesis presented results regarding the development and the efficiency of the of biogenic self-healing agent for cementitious materials and particularly for mortar. Further research can focus on different aspects regarding the testing techniques to be applied for the quantification of self-healing mortar at laboratory scale, on materials that could be considered and on practical concerns related to up-scaling.

- The LWA that were used for the research showed a good compatibility with the cementitious matrix, but also proved to carry efficiently the

biogenic healing agent. However, their incorporation in the cementitious matrix was accompanied by a significant decrease in the compressive strength of the material. It would be therefore quite beneficial to find another type of LWA or of encapsulation technique, which will not only allow a higher amount of healing agent to be accommodated in the LWA, but also to interfere less with the properties of the material.

- In this research, the only type of cement that was used was Portland CEM I. Although type I is widely used in construction for buildings, bridges, pavements etc., it would be quite useful to investigate the compatibility and the efficiency of the biogenic healing agent with the cementitious matrix of another type, that could be applied in diverse environments.
- The setting time of the mortar was significantly affected by the addition of the biogenic healing agent. The use of a setting accelerator in combination with the certain healing agent, which acts as a setting retarder, could be considered and investigated for the future research.
- The addition of fibres can be advantageous for either mortar or concrete. The beneficial effect of fibres that can control and restrict the crack width together with the healing agent action could promote the sealing efficiency of the biogenic self-healing cementitious material.
- Tests that examine the recovery of water-tightness were developed to investigate the resistance of the self-healing mortar to harmful liquids that can affect its durability. However, tests that actually examine the durability of the material have not been conducted yet. Already existing standard methods can be adapted to test the gas-permeability, chloride migration etc. initially on cracked and then on healed specimens.
- The healing treatment that was applied for this research took place exclusively in the laboratory and it included continuous water immersion and wet-dry cycles. Exposure of cracked specimens in external conditions could give a better insight of how the material behaves under real conditions.
- The assessment of healing in cementitious materials is strongly related with the geometrical characteristics of the cracks. Consequently, limiting the diversity of the cracks is of great importance. The crack generation method in combination with the crack shape (parallel walls of through going cracks instead of V-shape cracks) will lead to more

uniform and reproducible results which can decrease the uncertainty and increase the objectivity in the interpretation of the results.

- Impregnation of LWA at laboratory scale can be achieved rather easily and effectively. Large scale impregnation has been achieved so far without the application of vacuum treatment, which is less effective. Among the challenges related with the large-scale application, an efficient impregnation procedure that would result in equal, if not more, healing agent content inside the LWA is one of the most crucial.

Until now, most of the studies which deal with the self-healing technology in cementitious materials have been conducted on mortar samples. The reason for this is that the casting, the healing treatment and the mechanical tests can be easily executed in the laboratory, due to the convenient size of the samples. Fewer studies have focused on using concrete self-healing samples. However, this upscaling is essential for future self-healing structures. Research needs to focus further on the self-healing behaviour of concrete as there are some differences between those two materials that might influence healing efficiency. The differences derive mainly from the larger aggregate size and the lower cement content that is used for the concrete compared to mortar production. The challenges that might occur, due to those differences, have mostly to do with:

- the success of incorporating the healing agent and their capsules in the material,
- the tests to prove self-healing efficiency and
- the self-healing monitoring techniques

In fact, the larger aggregates found in concrete might damage or crush the (often sensitive and brittle) healing agent carriers while mixing or casting. In addition, the reference mortar (in the European standards) has a cement-to-aggregates ratio of 0.28, while the same ratio for concrete is almost the half. This means that the inner surface of a concrete crack is covered by an increased amount of aggregates, compared to mortar, which is translated to a reduced autogenous healing effect. In the case of the biogenic self-healing concrete, the carbon dioxide produced by bacterial respiration further reacts with the portlandite present in the concrete matrix to produce $CaCO_3$. As a result, if the crack area occupied by aggregates is increased, then less amount of portlandite is likely to be found on it. As a result, less healing product will be created inside the cracks. Furthermore, in self-healing mortar research, the most popular shapes of specimens that have been used are the prisms and the cylindrical slabs. For the concrete research, the damage introduction as well as the evaluation tests must be exclusively redesigned for each kind of specimen shape that will be used. Especially, if other shapes than prisms are used then the classical compression and bending tests might not apply. Finally,

the procedure of crack and healing progress monitoring can become more laborious as the specimen size increases. On a concrete slab, for example, the multiple cracking or the fact that a single crack might demonstrate varying crack widths and/or depths can complicate the establishment of a rather objective and reproducible healing assessment method.

In principle, the design of concrete structures along with the budget limitations, target to long lasting structures that will minimize, if not avoid, the need for repair works. The self-healing concrete can exceed the conventional concrete, since it also opts for durable aging structures, where repair can be conducted either automatically or with minimum human intervention, but more importantly the self-repair cost is included in the initial budget. The promising laboratory test results have led to the first full-scale outdoor applications, as mentioned in the second chapter, which will ultimately prove the functionality of the self-healing cementitious materials. Concrete structures could benefit from the implementation of the self-healing technology; particularly the parts of the structures that are not (easily) accessible or frequently inspected, or those that their repair will cause inconvenience to the public. Those could be parts of structures such as tunnels, bridges, parking decks, pipes and irrigation canals. In particular, the biogenic self-healing concrete with the healing agent embedded in LWA, can be applied in a wide variety of structures and structural members where a lightweight structure is needed, or as an external layer on a normal weight structure, provided that oxygen and water will be present.

A

Respiration of active bacteria cells in different organic compounds

Continuous oxygen consumption measurements were conducted on washed bacterial cultures of the three different isolates that were considered for this research. The measurements were conducted in sealed glass flasks and they were used to evaluate the preference of each isolate to a certain organic compound, namely, calcium lactate (CaL), calcium acetate (CaA) and sodium gluconate (NaG). The initial oxygen concentration of each suspension was varying between 200 and 300 μM. Then, the concentration of the oxygen concentration decreased, due to the respiration of the active bacterial cells to a certain organic compound, or it remained almost stable in case that the active cells were not in favour of respiring in the compound. The oxygen concentration of each isolate in the different organic compounds was monitored for approximately 100 minutes. Figures A.1-A.9 show the autogenous respiration curves as well as respiration curves of each isolate pre-grown in one of the three different compounds in carbonate-bicarbonate buffer with different organic carbon sources. Those curves were used for the calculation of the relative respiration rates that are presented in Figure 3.5.

Isolates pre-grown in Lactate

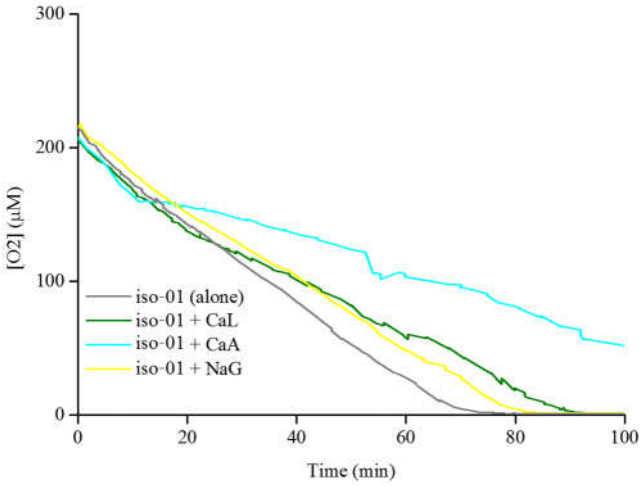

Figure A.1 Autogenous respiration curve and respiration curves of Iso-01 pre-grown in CaL in carbonate-bicarbonate buffer with different organic carbon sources.

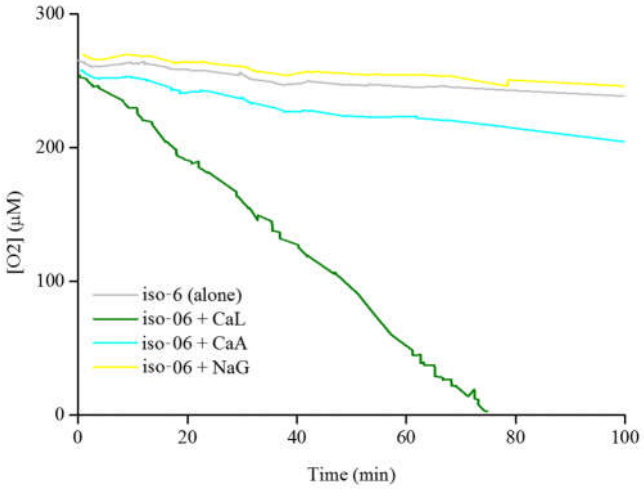

Figure A.2 Autogenous respiration curve and respiration curves of Iso-06 pre-grown in CaL in carbonate-bicarbonate buffer with different organic carbon sources.

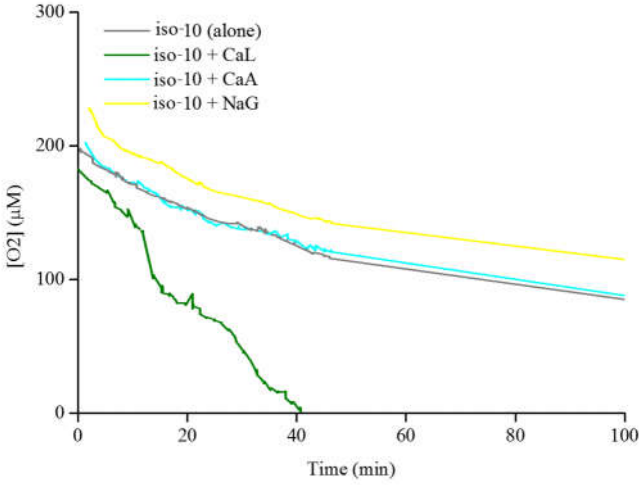

Figure A.3 Autogenous respiration curve and respiration curves of Iso-10 pre-grown in CaL in carbonate-bicarbonate buffer with different organic carbon sources.

Isolates pre-grown in Acetate

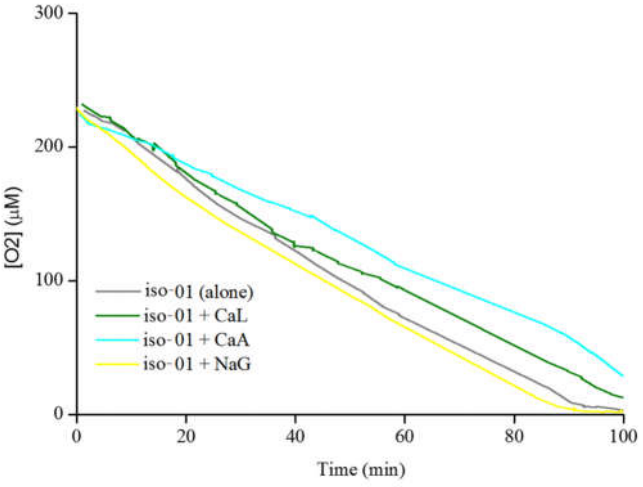

Figure A.4 Autogenous respiration curve and respiration curves of Iso-01 pre-grown in CaA in carbonate-bicarbonate buffer with different organic carbon sources.

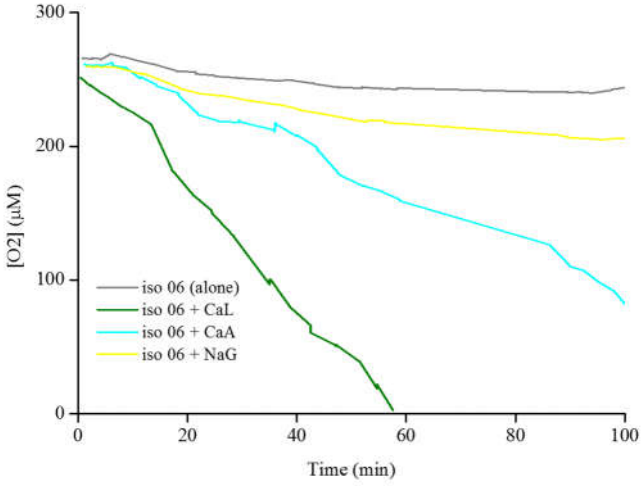

Figure A.5 Autogenous respiration curve and respiration curves of Iso-06 pre-grown in CaA in carbonate-bicarbonate buffer with different organic carbon sources.

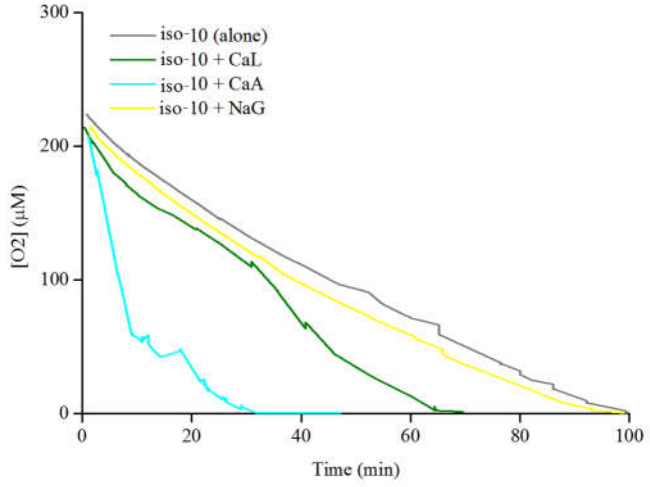

Figure A.6 Autogenous respiration curve and respiration curves of Iso-10 pre-grown in CaA in carbonate-bicarbonate buffer with different organic carbon sources.

Isolates pre-grown in Gluconate

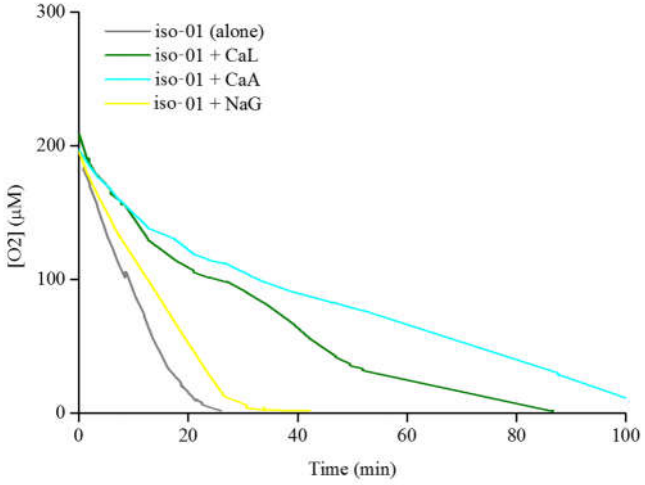

Figure A.7 Autogenous respiration curve and respiration curves of Iso-01 pre-grown in NaG in carbonate-bicarbonate buffer with different organic carbon sources.

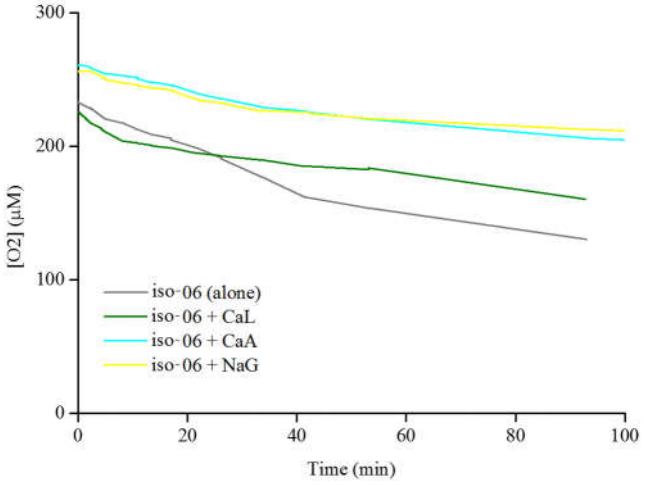

Figure A.8 Autogenous respiration curve and respiration curves of Iso-06 pre-grown in NaG in carbonate-bicarbonate buffer with different organic carbon sources.

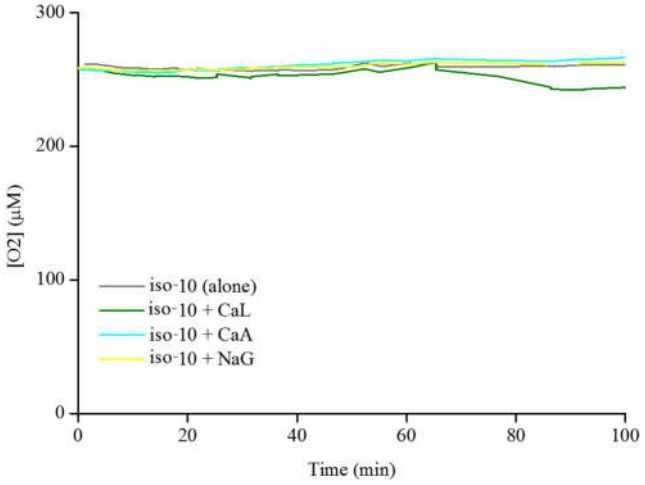

Figure A.9 Autogenous respiration curve and respiration curves of Iso-10 pre-grown in NaG in carbonate-bicarbonate buffer with different organic carbon sources.

B

Mercury intrusion porosimetry on mortar

Mercury intrusion porosimetry was used among other tests to characterize the mortars that were produced during this research. The test aimed to investigate how the addition of the biogenic healing agent into expanded clay particles affected the total porosity of the hardened matrix. The experiment was conducted on 90-days-old specimens. Figures B.1-B.6 present the porosity and differential intrusion in relation to the pore size distribution as obtained by MIP tests on REF, CTRL and BAC specimens.

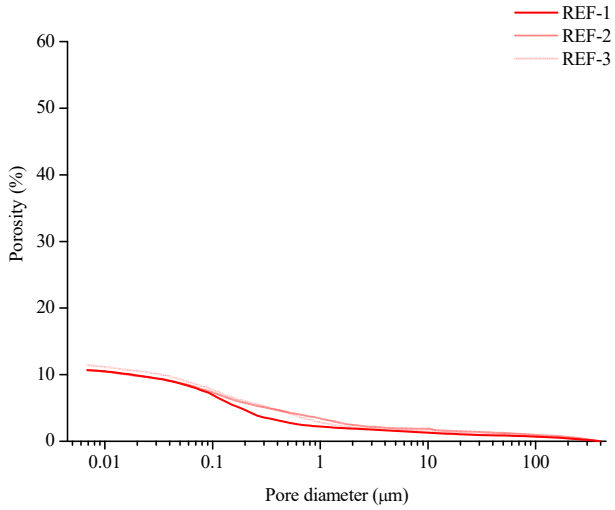

Figure B.1 Pore size - Cumulative intrusion curves on REF specimens measured by MIP.

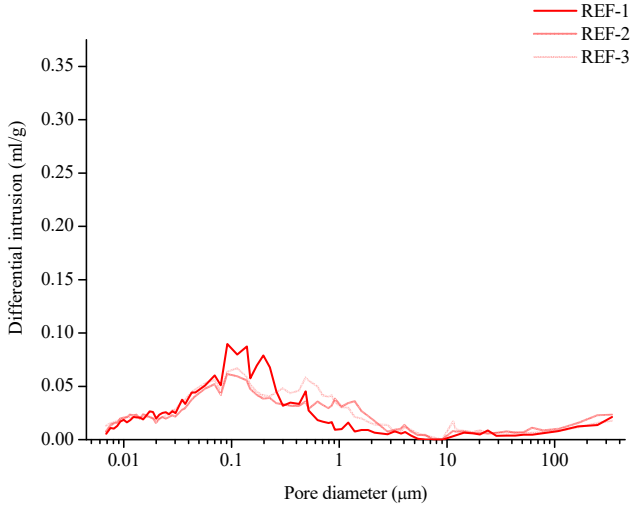

Figure B.2 Pore size distribution curves on REF specimens measured by MIP.

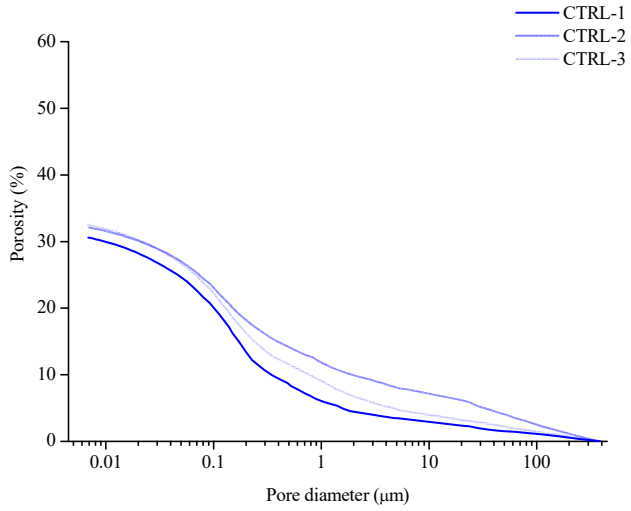

Figure B.3 Pore size - Cumulative intrusion curves on CTRL specimens measured by MIP.

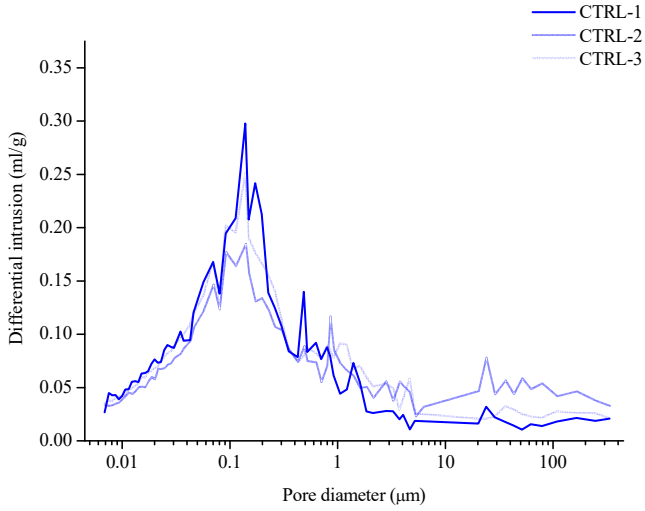

Figure B.4 Pore size distribution curves on CTRL specimens measured by MIP.

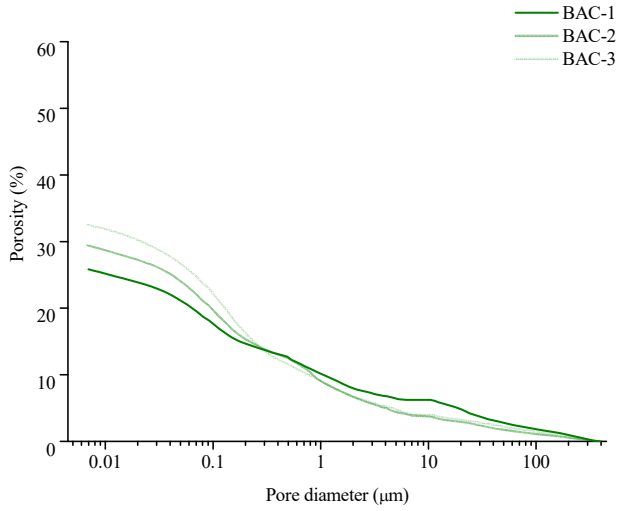

Figure B.5 Pore size - Cumulative intrusion curves on BAC specimens measured by MIP.

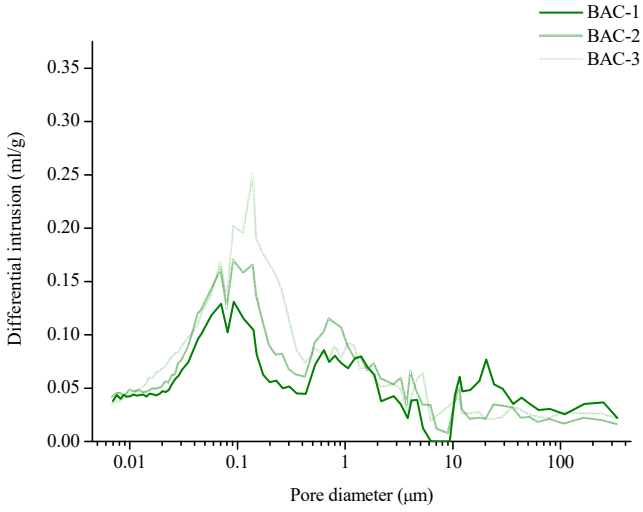

Figure B.6 Pore size distribution curves on BAC specimens measured by MIP.

C

Flexural tests on mortar prisms

Three-point-bending was used during this research as a method of damage introduction on the prismatic specimens. After the completion of the test, a single V-shaped crack was created in the middle of every specimen. The crack introduction was performed on 28-days-old reinforced prismatic specimens. After the healing treatment and for the investigation of the recovery of flexural strength the three-point-bending test was repeated on either 56-days old or 84-days old healed specimens. During testing, the load was applied in the middle of the span of the specimen with a constant pace, resulting in a crack opening increase of 0.5 μm/s. For the first loading-unloading cycle, the specimens were loaded until the crack opening reached a width of approximately 400 μm and then they were slowly unloaded. For the second loading-unloading cycle, the already cracked specimens were loaded until the crack opened approximately 200 μm further and then they were unloaded. Figures C.1-C.15 show the resulting curves from the three-point-bending that was performed on REF, CTRL and BAC specimens. Specimens numbered:

- 7-9 were cracked and subjected to crack permeability via water flow one day after.
- 10-12 were subjected to water submersion for 28 days,
- 13-15 were subjected to water submersion for 56 days,
- 16-18 were subjected to wet-dry cycles for 28 days and
- 19-21 were subjected to water wet-dry cycles for 56 days.

The values obtained during the first, as well as, during the second loading cycles were used for the calculation of R_S as presented in Figure 4.16.

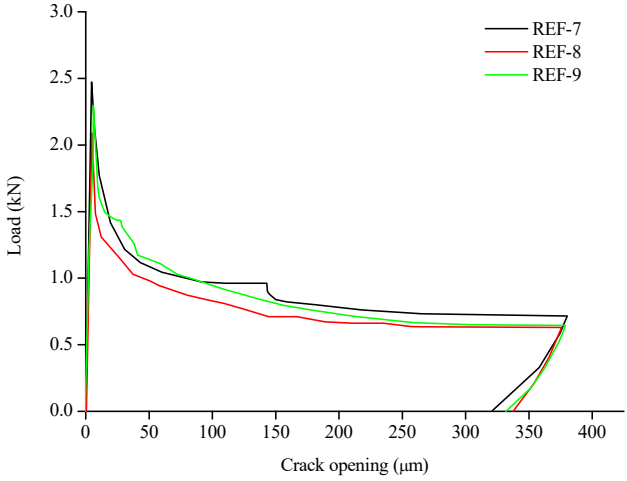

Figure C.1 First cycle of loading-unloading curves on REF specimens (before healing treatment).

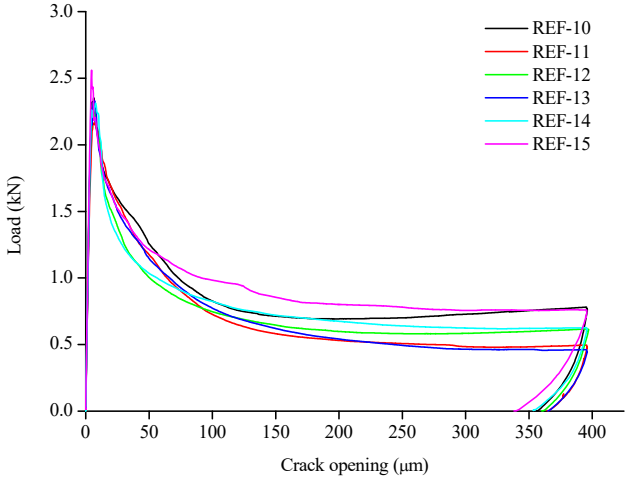

Figure C.2 First cycle of loading-unloading curves on REF specimens (before healing treatment).

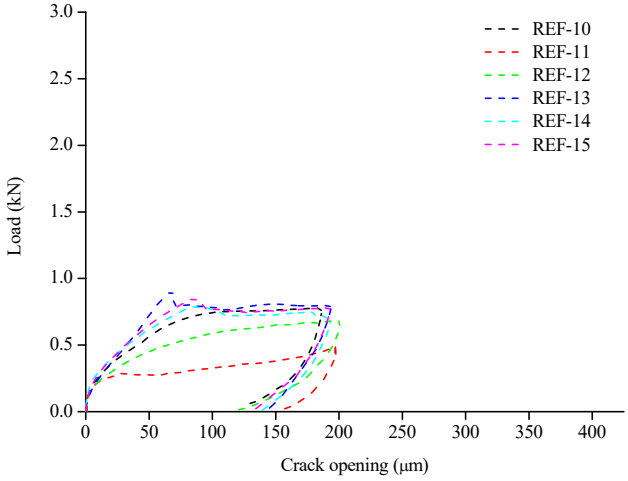

Figure C.3 Second cycle of loading-unloading curves on REF specimens (after water submersion).

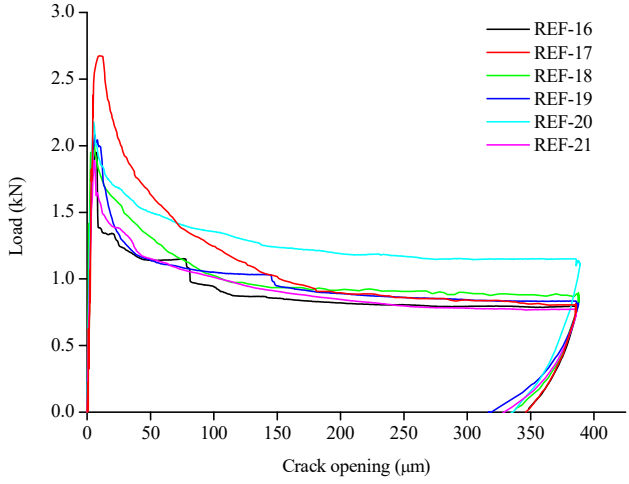

Figure C.4 First cycle of loading-unloading curves on REF specimens (before healing treatment).

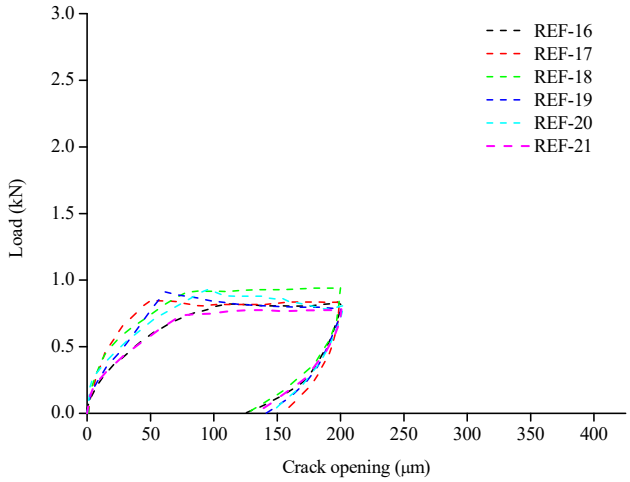

Figure C.5 Second cycle of loading-unloading curves on REF specimens (after wet-dry cycles).

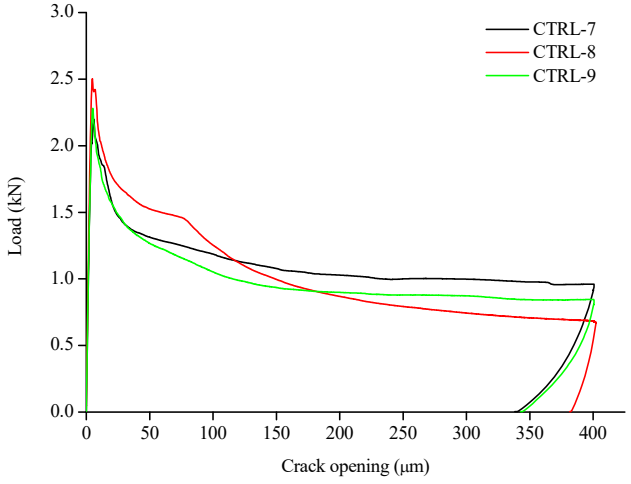

Figure C.6 First cycle of loading-unloading curves on CTRL specimens (before healing treatment).

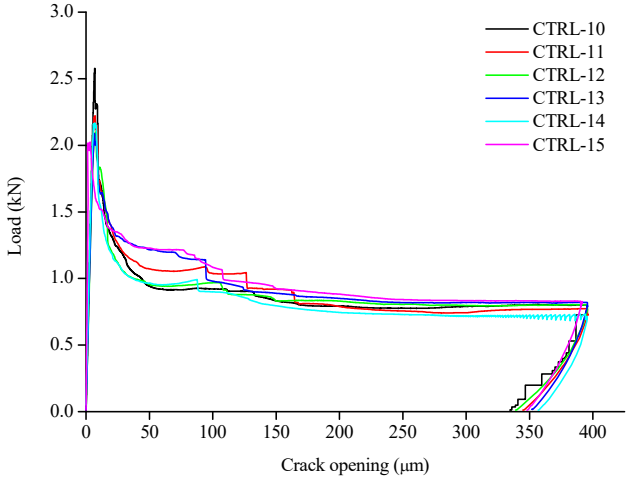

Figure C.7 First cycle of loading-unloading curves on CTRL specimens (before healing treatment).

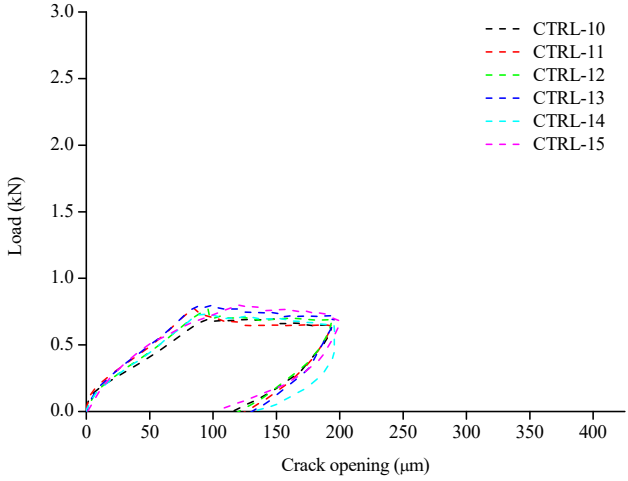

Figure C.8 Second cycle of loading-unloading curves on CTRL specimens (after water submersion).

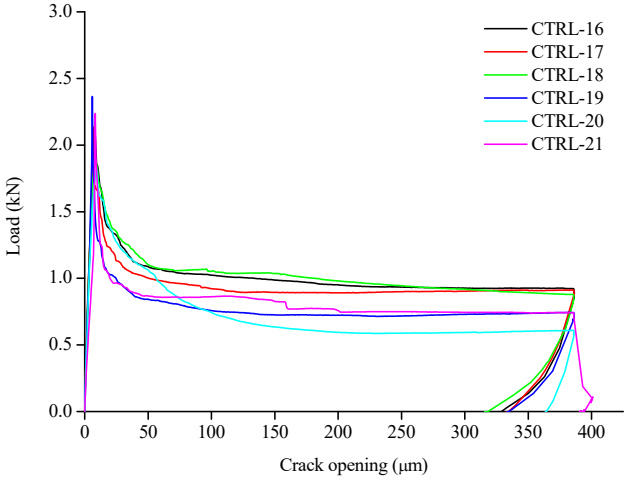

Figure C.9 First cycle of loading-unloading curves on CTRL specimens (before healing treatment).

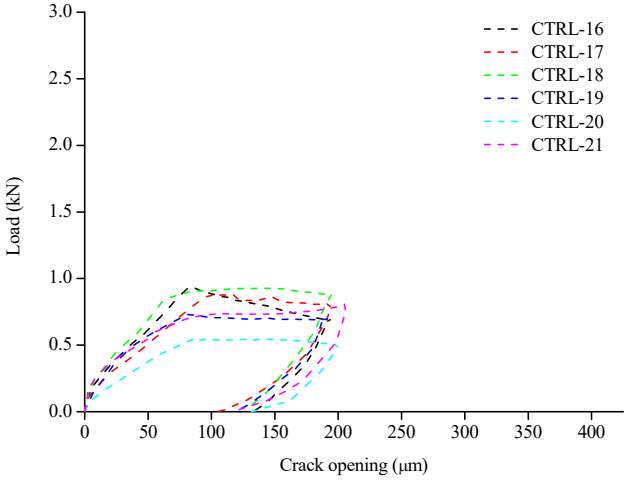

Figure C.10 Second cycle of loading-unloading curves on CTRL specimens (after wet-dry cycles).

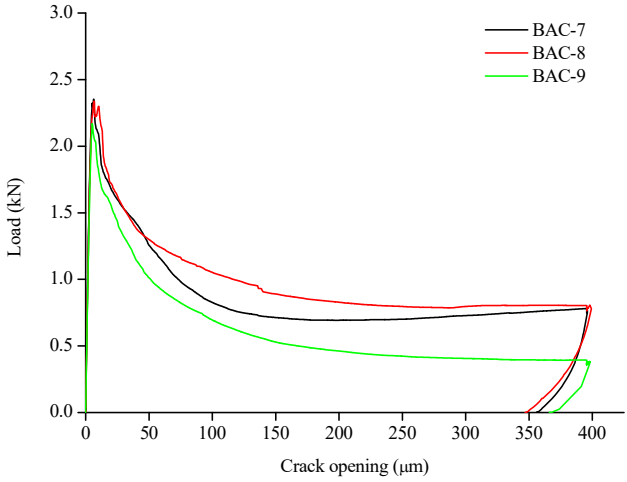

Figure C.11 First cycle of loading-unloading curves on BAC specimens (before healing treatment).

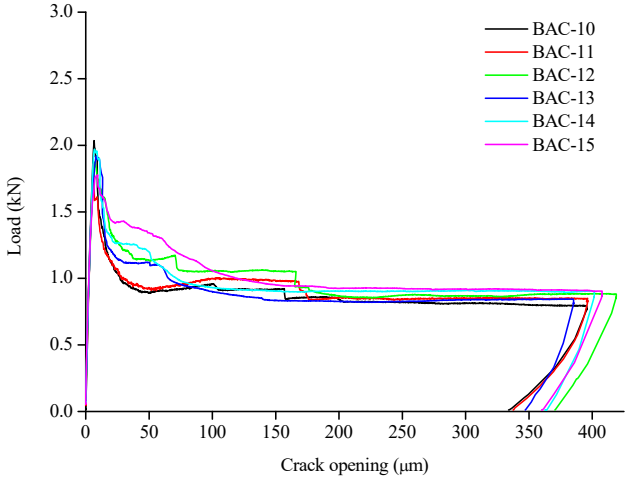

Figure C.12 First cycle of loading-unloading curves on BAC specimens (before healing treatment).

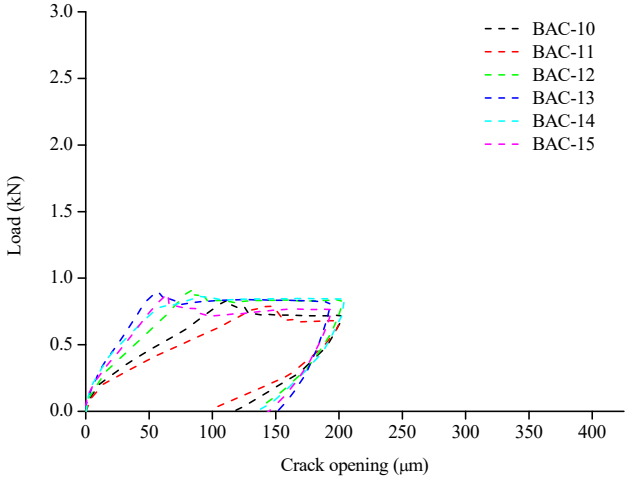

Figure C.13 Second cycle of loading-unloading curves on BAC specimens (after water submersion).

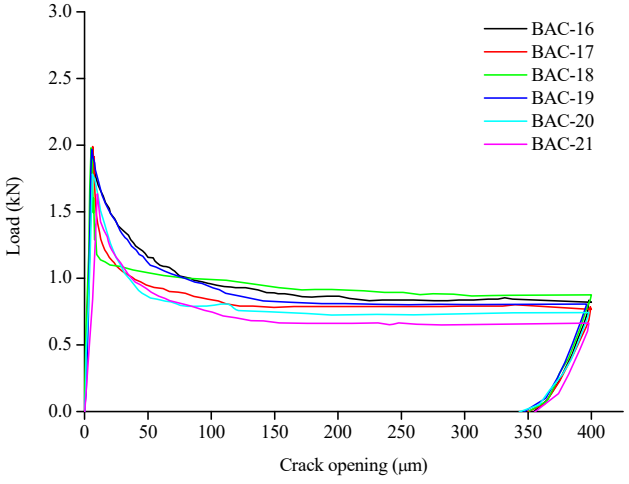

Figure C.14 First cycle of loading-unloading curves on BAC specimens (before healing treatment).

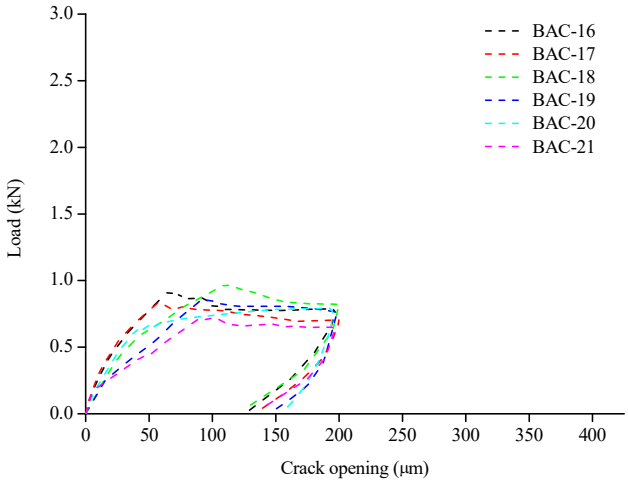

Figure C.15 Second cycle of loading-unloading curves on BAC specimens (after wet-dry cycles).

D

Crack permeability test via water flow on prismatic mortar specimens

Crack permeability test via water flow was used for this research to evaluate the efficiency of the biogenic healing agent embedded in expanded clay particles, which were incorporated in the mortar matrix. The specimens that were used for this test were pre-cracked, reinforced, prismatic specimens, modified with a hole along the whole length of each specimen. The test was performed in triplicates and lasted for approximately 5 minutes. Figures D.1-D.15 show the resulting graphs from the crack permeability test that was performed on REF, CTRL and BAC specimens. Specimens numbered:

- 7-9 were tested one day after cracking without being subjected to the healing treatment,
- 10-12 were tested after water submersion, which lasted for 28 days,
- 13-15 were tested after water submersion, which lasted for 56 days,
- 16-18 were tested after wet-dry cycles, which lasted for 28 days and
- 19-21 were tested after wet-dry cycles, which lasted for 56 days.

The values obtained by those graphs were used for the calculation of the R_{WT} values that are presented in Figure 4. 13..

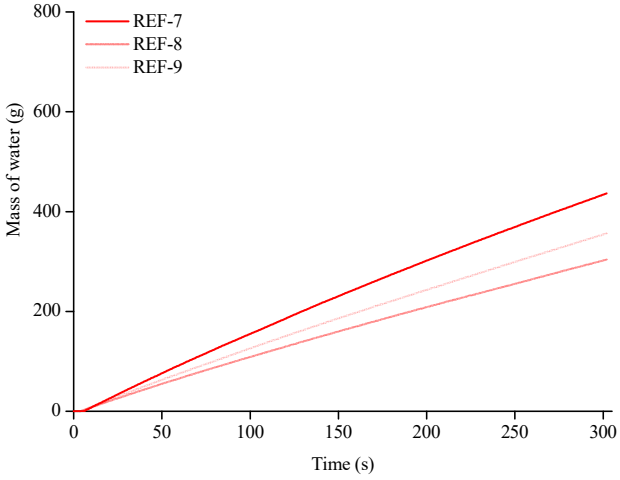

Figure D.1 Water flow curves of REF specimens before healing treatment.

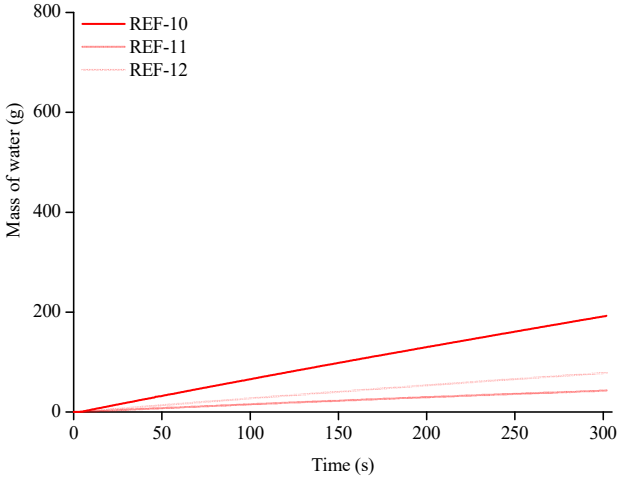

Figure D.2 Water flow curves of REF specimens after 28 days of water submersion.

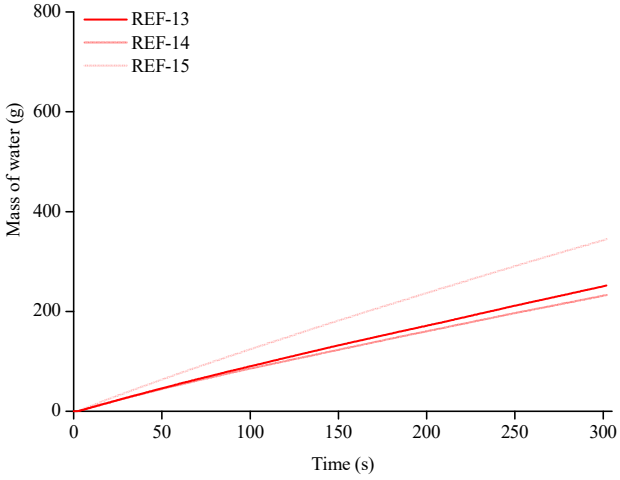

Figure D.3 Water flow curves of REF specimens after 56 days of water submersion.

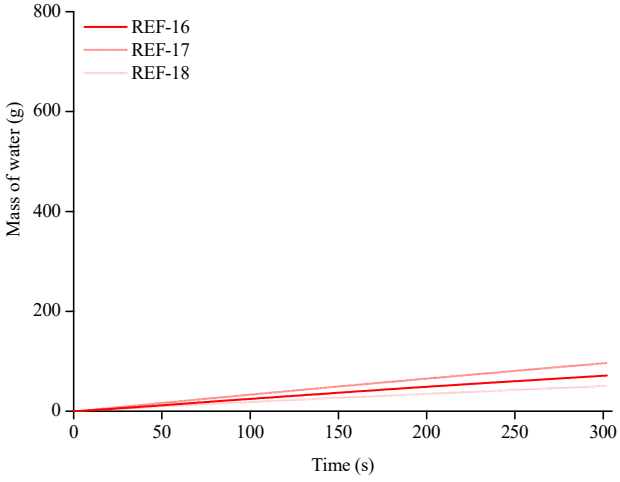

Figure D.4 Water flow curves of REF specimens after 28 days of wet-dry cycles.

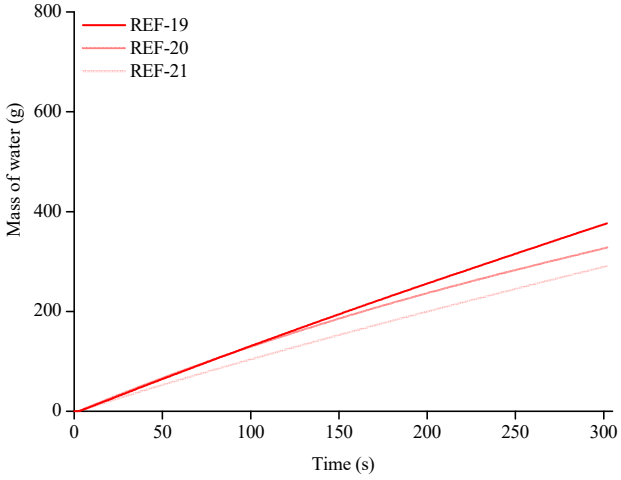

Figure D.5 Water flow curves of REF specimens after 56 days of wet-dry cycles.

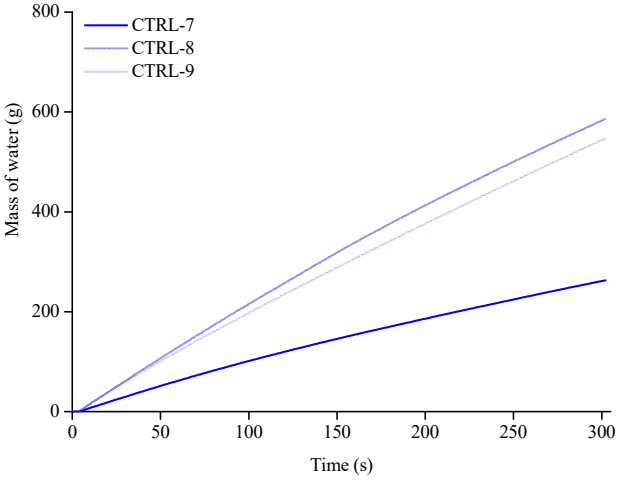

Figure D.6 Water flow curves of CTRL specimens before healing treatment.

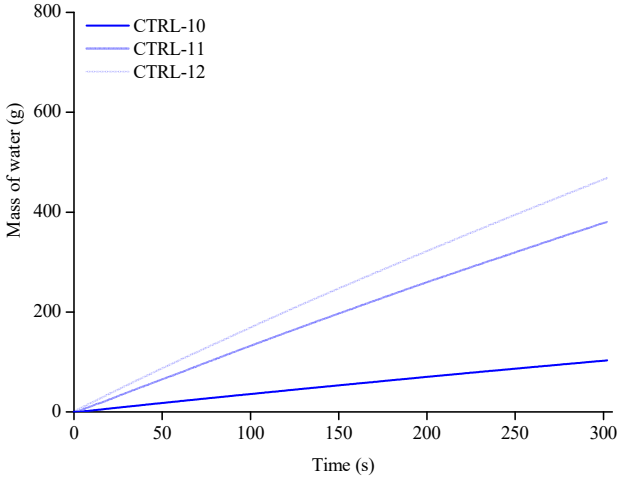

Figure D.7 Water flow curves of CTRL specimens after 28 days of water submersion.

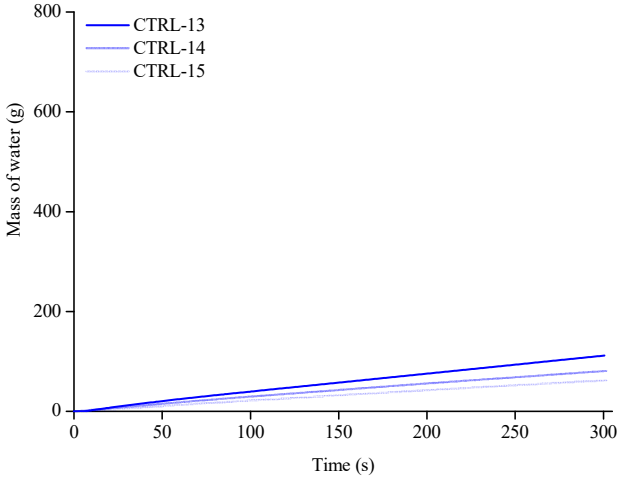

Figure D.8 Water flow curves of CTRL specimens after 56 days of water submersion.

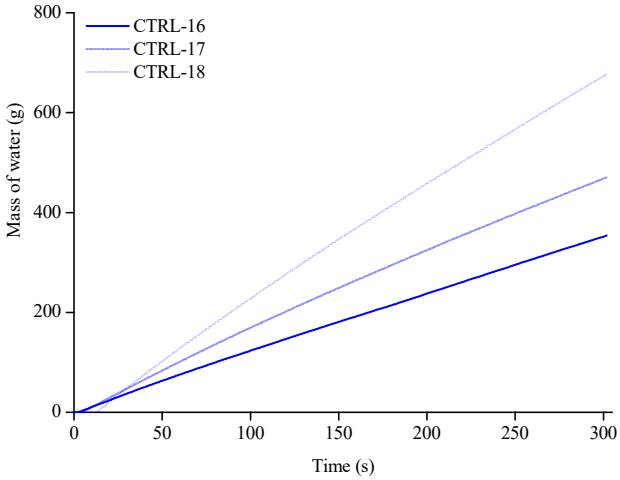

Figure D.9 Water flow curves of CTRL specimens after 28 days of wet-dry cycles.

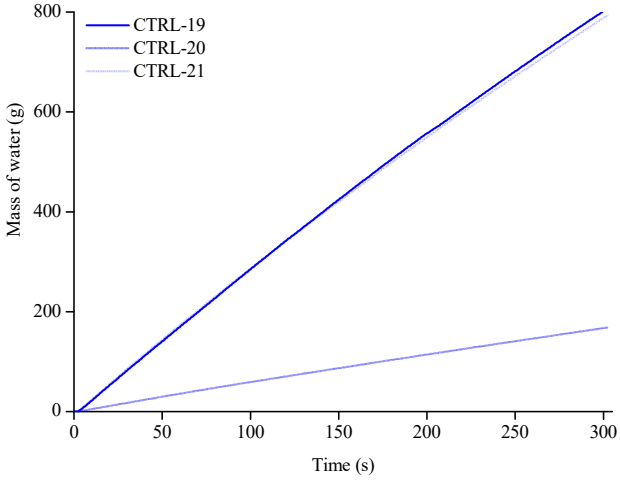

Figure D.10 Water flow curves of CTRL specimens after 56 days of wet-dry cycles.

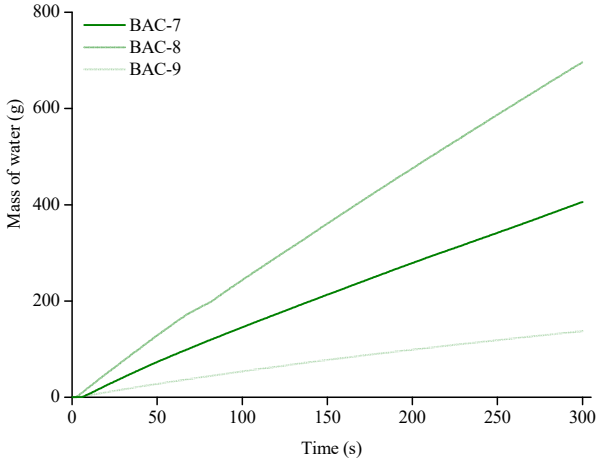

Figure D.11 Water flow curves of BAC specimens before healing treatment.

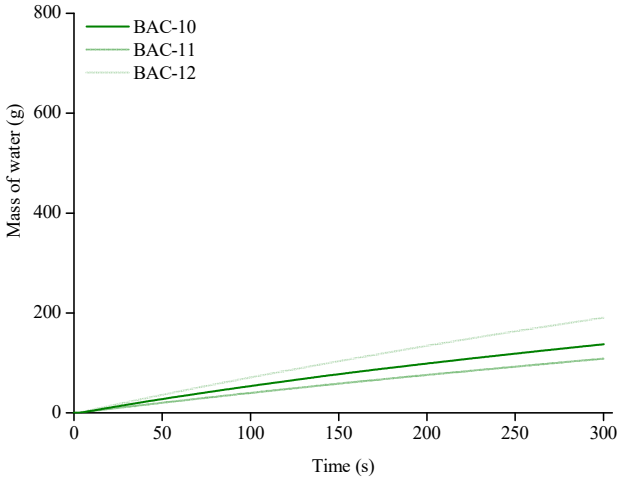

Figure D.12 Water flow curves of BAC specimens after 28 days of water submersion.

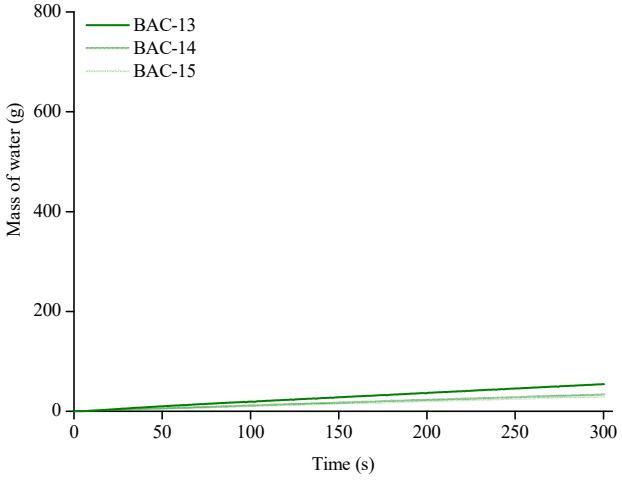

Figure D.13 Water flow curves of BAC specimens after 56 days of water submersion.

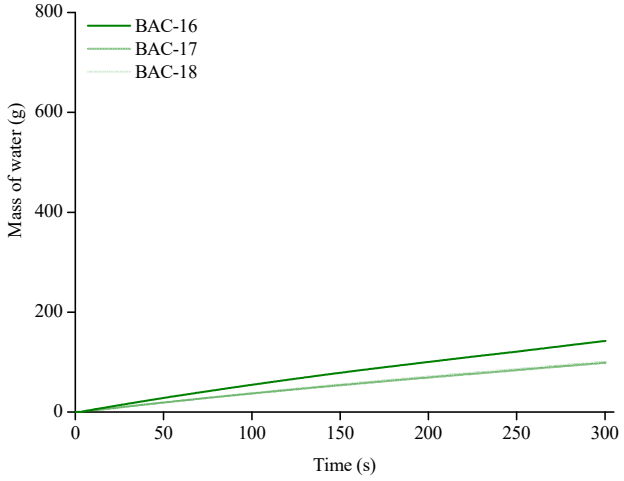

Figure D.14 Water flow curves of BAC specimens after 28 days of wet-dry cycles.

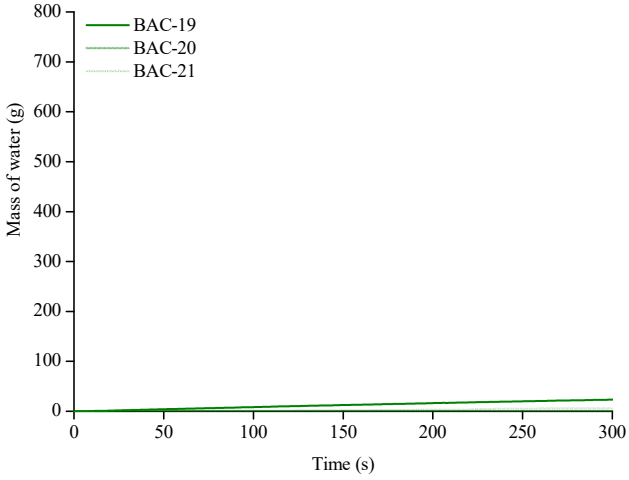

Figure D.15 Water flow curves of BAC specimens after 56 days of wet-dry cycles.

Summary

In concrete structures, it is always a preferable idea to prevent the damage before it happens rather than to repair it afterwards, since it is usually less costly and in some cases the damage detection is impossible. Temperature and humidity fluctuations and/or external loading can trigger micro-cracking on a concrete structure, which in turn can open a pathway for harmful liquids and gasses. Those substances can degrade either the cement matrix or the embedded reinforcement and can cause an extended and irreversible damage. Prevention of damage or instant repair are not always achievable. Therefore, the idea to develop a cementitious material, which can sense the damage and repair it itself in order to mitigate the loss of durability, has gained ground in the last two decades.

Inspired by cut skin and bone fracture healing, numerous researchers worldwide have developed self-healing systems for cementitious materials. The design and development of the self-healing systems consist of two parts; the healing mechanism and the healing material (healing agent). The most commonly used mechanism is the one that releases the (encapsulated) healing agent into the crack after the crack has intersected and split the carrier of healing agent. Scientists have equally focused on optimizing the healing mechanism as well as the healing agent. Simple or more complicated chemical healing agents have been studied extensively. Yet, the biogenic healing agents, which use dormant bacteria spores and their nutrients have become popular over the last decade. Bacterial strains and their nutrients (organic carbon sources) have been carefully selected not only to be compatible with the alkaline cementitious environment, but also to not significantly affect either the fresh- or the hardened-state properties of the material.

The biogenic systems that have been used up to now use different bacterial metabolic pathways; namely, the hydrolysis of urea, the oxidation of organic compounds by using oxygen under aerobic conditions or by using nitrate under anaerobic conditions. This study investigated the oxidation of organic carbon by using oxygen, in order to increase the sealing efficiency of mortar after cracking. In this system, the healing agent is embedded in lightweight aggregates for protection and immobilization. During cracking, the lightweight aggregates break and expose the compounds of the healing agent in the crack. At the same time, moisture and oxygen from the environment are allowed to pass in the crack. Then, the dormant bacterial spores activate, due to favourable conditions (presence of moisture, oxygen and appropriate temperature) and start degrading the nutrients found in the healing agent. The products of the bacterial metabolic activity (calcium carbonate crystals) can then fill the open micro-cracks.

The specific biogenic self-healing system has been also studied previously. The preceding research has showed promising results, regarding the crack filling and the recovery of water-tightness after cracking and healing. Towards optimizing the existing healing agent, in the beginning of the experimental research, different organic precursors were examined to be used as possible bacterial nutrients. In addition, the physical properties of the lightweight aggregates that were used as healing agent carriers, as well as, the effectiveness of the available impregnation methods were investigated.

The fresh- and hardened-state properties of the mortar after the incorporation of the biogenic healing agent were studied. Yet, the focus was set on the investigation of the crack sealing behaviour of the biogenic mortar and on the investigation bacterial activity. On the other hand, experimental results on the recovery of flexural strength and stiffness proved that the healing product cannot provide regain of the mechanical properties.

Two proposed methodologies to assess self-healing at laboratory scale were evaluated through a round robin test. The methodologies ultimately aimed to quantify the crack sealing through water flow and capillary water absorption. However, the outcome of the test series indicated the limitations of the test methodology that are mostly related with the cracking introduction method and can significantly affect the crack sealing results. Therefore, improvements on the experimental procedures are required to enhance the quality of the obtained results.

The results from two experimental methods to evaluate self-healing; namely crack inspection and sealing efficiency test results, were compared with the results of a computer simulation. The comparison revealed that the experimental approaches might overestimate the actual crack closure, while the computer simulations may either over- or underestimate it, depending on the initial hypotheses. Although the currently available methods need some further improvements to mimic a more realistic situation, they can provide us with an insight of the extent healing that takes place inside a micro-crack.

The lightweight biogenic self-healing mortar is a cementitious material, which is designed to exhibit enhanced durability compared to the conventional mortars. Its ability to self-repair can offer protection from aggressive substances that can ingress and damage the material through the open cracks. In fact, experimental results proved that the biogenic mortar exhibits lower compressive strength compared to the same mortar with normal weight sand, improved crack sealing and a very limited or not existent recovery of strength after cracking and healing treatment. Yet, this material could be used where a lightweight structure is needed, or as an external layer on a normal weight structure. Overall, it could be stated that

structures can benefit from the use this material, since the enhanced crack sealing behaviour can prevent durability problems that are related with micro-cracking.

Samenvatting

Bij betonconstructies is het altijd een goed idee om schade te voorkomen voordat deze optreedt, in plaats van deze achteraf te repareren. Meestal is zoiets minder duur en bovendien is soms detectie van schade onmogelijk. Temperatuur- en vochtigheidsschommelingen en/ of externe belasting kunnen microscheuren in een betonconstructie veroorzaken, die vervolgens een pad creëert voor schadelijke vloeistoffen en gassen. Deze stoffen kunnen de cementmatrix of de ingebedde wapening aantasten en uitgebreide en onomkeerbare schade veroorzaken. Voorkoming van schade of onmiddellijke reparatie zijn niet altijd haalbaar. Het idee om een cementgebonden materiaal te ontwikkelen dat de schade kan detecteren en zichzelf kan repareren om het verlies van duurzaamheid te verminderen, heeft de laatste twee decennia terrein gewonnen.

Geïnspireerd door snijwond- en botbreukgenezing hebben talloze onderzoekers over de hele wereld zelfherstellende systemen voor cementachtige materialen ontwikkeld. Het ontwerp en de ontwikkeling van de zelfherstellende systemen bestaat uit twee delen; het genezingsmechanisme en het helende materiaal (genezingsmiddel). Het meest gebruikte mechanisme is datgene dat het (ingekapselde) genezingsmiddel in de scheur vrijgeeft nadat de scheur de drager van het genezingsmiddel heeft doorsneden. Wetenschappers hebben zich in gelijke mate gericht op het optimaliseren van het genezingsmechanisme en het genezende middel. Eenvoudige of meer gecompliceerde chemische genezingsmiddelen zijn uitgebreid bestudeerd. Toch zijn de biogene genezingsmiddelen, die slapende bacteriesporen en hun voedingsstoffen gebruiken, het afgelopen decennium populair geworden. Bacteriestammen en hun voedingsstoffen (organische koolstofbronnen) zijn zorgvuldig geselecteerd, niet alleen om compatibel met de alkalische cementachtige omgeving te zijn, maar ook om de eigenschappen van het materiaal, vloeibaar of verhard, niet significant te beïnvloeden.

De biogene systemen die tot nu toe zijn gebruikt, gebruiken verschillende bacteriële metabole routes; namelijk de hydrolyse van ureum, de oxidatie van organische verbindingen door zuurstof onder aerobe omstandigheden te gebruiken of door nitraat onder anaerobe omstandigheden te gebruiken. Deze studie onderzocht de oxidatie van organische koolstof door gebruik te maken van zuurstof, om de afdichtingsefficiëntie van mortel na scheuren te vergroten. In dit systeem is het genezingsmiddel in lichtgewicht aggregaten ingebed voor bescherming en immobilisatie. Tijdens de scheurvorming breken de lichtgewicht aggregaten en komt het genezingsmiddel in de scheur vrij. Tegelijkertijd kan vocht en zuurstof uit de omgeving in de scheur indringen. Vervolgens activeren de slapende bacteriële sporen, vanwege gunstige omstandigheden (aanwezigheid van

vocht, zuurstof en geschikte temperatuur) en beginnen de in het genezingsmiddel aanwezige voedingsstoffen af te breken. De producten van de bacteriële metabole activiteit (calciumcarbonaatkristallen) kunnen dan de open microscheuren opvullen.

Het specifieke biogene zelfherstellende systeem is ook eerder bestudeerd. Het voorgaande onderzoek heeft veelbelovende resultaten opgeleverd, met betrekking tot het opvullen van scheuren en het herstel van waterdichtheid na scheurvorming en genezing. Op weg naar optimalisatie van het bestaande genezingsmiddel, zijn aan het begin van het experimentele onderzoek verschillende organische voorlopers onderzocht om als mogelijke bacteriële voedingsstoffen te worden gebruikt. Bovendien zijn de fysische eigenschappen van de lichtgewichtaggregaten die werden gebruikt als genezingsmiddeldragers, evenals de effectiviteit van de beschikbare impregnatiemethoden onderzocht.

De eigenschappen van de vloeibare en verharde toestand van de mortel na de opname van het biogene genezingsmiddel zijn bestudeerd. Het belangrijkste aspect van het onderzoek was echter het scheurafdichtingsgedrag van de biogene mortel en de bacteriële activiteit. Aan de andere kant hebben experimentele resultaten op het herstel van buigsterkte en stijfheid bewezen dat het genezende product niet de mechanische eigenschappen kan terugwinnen.

Twee voorgestelde methodologieën om zelfgenezing op laboratoriumschaal te beoordelen, zijn geëvalueerd door middel van een round-robin-test. De methodieken hadden uiteindelijk tot doel de scheurafdichting voor permeabiliteit en capillaire waterabsorptie te kwantificeren. De uitkomst van de testserie gaf echter de beperkingen van de testmethodologie aan die grotendeels aan de methode van het introduceren van scheuren zijn gerelateerd en die de scheurafdichtingsresultaten aanzienlijk kan beïnvloeden. Daarom zijn verbeteringen aan de experimentele procedures vereist om de kwaliteit van de verkregen resultaten te verhogen.

De resultaten van twee experimentele methoden om zelfgenezing te evalueren; namelijk scheurinspectie- en afdichtingsefficiëntietestresultaten, zijn met de resultaten van een computersimulatie vergeleken. De vergelijking liet zien dat de experimentele aanpak de feitelijke scheursluiting zou kunnen overschatten, terwijl de computersimulaties deze kunnen overschatten of onderschatten, afhankelijk van de aanvankelijke hypotheses. Hoewel de momenteel beschikbare methoden nog verdere verbeteringen nodig hebben om een meer realistische situatie na te bootsen, kunnen ze ons inzicht in de mate van genezing die in een microscheur plaatsvindt geven.

De lichtgewicht biogene zelfherstellende mortel is een cementgebonden materiaal dat is ontworpen om een verbeterde duurzaamheid in vergelijking met de conventionele mortels te bieden. Zijn vermogen om zichzelf te repareren kan bescherming tegen agressieve stoffen bieden die het materiaal door de open scheuren kunnen binnendringen en beschadigen. In feite bewezen experimentele resultaten dat de biogene mortel een lagere druksterkte, verbeterde scheurafdichtingen en een zeer beperkt of niet aanwezig herstel van sterkte na scheur- en genezingsbehandeling vertoont vergeleken met dezelfde mortel met zand van normaalgewicht. Toch kan dit materiaal worden gebruikt waar een lichtgewicht structuur nodig is, of als een externe laag op een constructie van normaalgewicht. Over het algemeen kan worden gesteld dat constructies kunnen profiteren van het gebruik van dit materiaal, omdat het verbeterde scheurafdichtingsgedrag duurzaamheidsproblemen kan voorkomen die betrekking tot microscheurvorming hebben.

Curriculum Vitae

Name: Eirini Tziviloglou

Date of Birth: 10 May 1984

Place of Birth: Athens, Greece

Email: e.tziviloglou@tudelft.nl

e.tziviloglou@gmail.com

2013-2017	PhD Candidate in Civil Engineering, Section of Materials and Environment, Microlab, Delft University of Technology, The Netherlands
2010-2013	Independent structural engineer, Athens, Greece
2009-2007	Master of Science (MSc.) in Civil Engineering, Section of Materials and Environment, Microlab, Delft University of Technology, The Netherlands
2002-2007	MEng in Civil Engineering, University of Patras, Greece

List of publications

Conference papers

Tziviloglou, E., Jonkers, H.M., and Schlangen, E. *Bacteria-based self-healing concrete to increase durability of structures*. 2014. In: 1st conference on ageing of materials and structures. Van Breugel, K. and Koenders, E.A.B. Delft, The Netherlands.

Tziviloglou, E., Wiktor, V.A.C., Jonkers, H.M., and Schlangen, E. *Development of bio-based self-healing concrete to increase durability of structures*. 2015. In: CITC-8 (Construction in the 21st Century). Thessaloniki, Greece.

Tziviloglou, E., Wiktor, V.A.C., Jonkers, H.M., and Schlangen, E. *Preparation and optimization of bio-based and light weight aggregate-based healing agent for application in concrete*. 2015. In: 5th international conference on self-healing materials. Durham, North Carolina, USA.

Gruyaert, E., Feiteira, J., Debbaut B., **Tziviloglou, E.**, Jonkers, H.M., and Schlangen, De Belie N. *Evaluation of self-healing effect of mortar containing polymeric healing agents.* In: 5th international conference on self-healing materials. Durham, USA.

Tziviloglou, E., Wiktor, V., Jonkers, H.M., and Schlangen, E. *Performance requirements to ensure the performance of bacteria-based self-healing concrete*. 2016. In: 9th International Conference on Fracture Mechanics of Concrete and Concrete Structures. Berkeley, USA.

Tziviloglou, E., Wiktor, V., Jonkers, H.M., and Schlangen, E. *Bacteria-based self-healing mortar: A comparison of two studies*. 2016. In: Concrete Solutions 2016 (6th International Conference on Concrete Repair). Thessaloniki, Greece.

Tziviloglou, E., Wiktor, V., Wang, J., Paine, K., Alazhari, M., Richardson, A., Gueguen, M., Jonkers, H., Bertron, A., De Belie, N., and Schlangen, E. *Evaluation of experimental methodology to assess the sealing efficiency of bacteria-based self-healing mortar : Round robin test*. 2016. In: RILEM Symposium in Microorganisms-Cementitious Materials Interactions. Delft, The Netherlands.

Gruyaert, E., Feiteira, J., Nele De, B., Malm, F., Nahm, M., Grosse, C.U., and **Tziviloglou, E.** *Non-destructive testing techniques to evaluate the healing efficiency of self-healing concrete at lab-scale*. 2016. In: Emerging Technologies in Non-Destructive Testing VI. Aggelis, D.G., et al. Leiden, The Netherlands.

Journal papers

Tziviloglou, E., Wiktor, V., Jonkers, H.M., and Schlangen, E., *Bacteria-based self-healing concrete to increase liquid tightness of cracks.* Construction and Building Materials, 2016. 122: p. 118-125.

Gruyaert, E., Debbaut, B., Snoeck, D., Díaz, P., Arizo, A., **Tziviloglou, E.**, Schlangen, E., and De Belie, N., Self-healing mortar with pH-sensitive superabsorbent polymers: testing of the sealing efficiency by water flow tests. Smart Materials and Structures, 2016. 25(8).

Tziviloglou, E., Wiktor, V., Jonkers, H.M., and Schlangen, E., *Selection of bacterial nutrient to be used in biogenic healing agent for cementitious materials.*Frontiers in Materials, 2017.

Tziviloglou, E., Pan, Z., Jonkers, H.M., and Schlangen, E., *Bio-based self-healing mortar: An experimental and numerical study.*Journal of Advanced Concrete Technology, 2017. 15:p. 536-543.

Book chapters

Tziviloglou, E., Van Tittelboom, K., Palin, D., Wang, J., Sierra-Beltrán, M.G., Erşan, Y.Ç., Mors, R., Wiktor, V., Jonkers, H.M., Schlangen, E., and De Belie, N., *Bio-Based Self-Healing Concrete: From Research to Field Application*, in *Self-healing Materials*, Eds. Hager, M.D., van der Zwaag, S., and Schubert, U.S. 2016, Springer International Publishing: Cham. p. 345-385.

Jonkers, H.M., Wiktor, V., Sierra Beltran, M.G., Mors, R.M., **Tziviloglou, E.**, and Palin, D., *Limestone-producing bacteria make concrete self healing* in *Self-healing materials*, Eds. Van der Zwaag, S. and Brinkman, E. 2015. p. 137-148.